Miniaturized online comprehensive two-dimensional liquid chromatography

Dissertation

zur Erlangung des akademischen Grades eines

Doktors der Naturwissenschaften

– Dr. rer. nat. –

vorgelegt von

Jakob Haun

geboren in Essen

Fakultät für Chemie

der

Universität Duisburg-Essen

2014

Die vorliegende Arbeit wurde im Zeitraum von April 2009 bis zum März 2014 im Arbeitskreis von Prof. Dr. Torsten C. Schmidt im Fachgebiet Instrumentelle Analytische Chemie (IAC) der Universität Duisburg-Essen durchgeführt.

Tag der Disputation: 23.07.2014

Gutachter: Prof. Dr. Torsten C. Schmidt

Prof. Dr. Oliver J. Schmitz

Vorsitzender: Prof. Dr. Maik Walpuski

Table of contents

Abstract

This thesis deals with the development of a novel multidimensional separation system for the qualitative screening analysis of complex samples that potentially contain hundreds of semi- or nonvolatile analytes. This system is based on a combination of online, comprehensive two-dimensional liquid chromatography and hybrid high-resolution mass spectrometry. A consistent miniaturization of the chromatographic part to nano- and capillary-LC in the first and second dimension, respectively, allowed the mass spectrometer to be hyphenated at full flow rate compatibility, without a flow split after the fast second LC dimension. To facilitate the choice of the conditions for an example application, two studies were included that focused on the applicability of high-temperature LC in the second dimension. First, the influence of high column temperatures on solvent effects observable for ambient temperature reversed-phase second dimensions was investigated by a peak shape study at isocratic elution conditions. Although high temperatures increase solvent compatibility by the reduction of viscosity differences, peak broadening by solvent strength effects cannot be overcome by an increase in temperature. The pre-dominance of these effects at any temperature underline the importance of a sufficiently low transfer volume to the second dimension. Second, eight modern stationary phases were investigated for their long-term high-temperature and pH stability. In this context, a retention factor analysis approach was developed that helps monitoring the status of silica-based reversed-phase columns using not only hydrophobicity losses but also the increase in silanophilic interactions. Accordingly, particles on the basis of the ethylene bridged hybrid (BEH) technology represent the most stable silica-based particles. Nonetheless, for the final implementation of the multidimensional system, sub-3-µm core-shell C18 particle technology was combined with elevated temperature and high pressures to obtain a gradient cycle time of one minute in the second dimension. In the first dimension, a porous graphitic carbon stationary phase was used that allowed implementing a large volume injection. The potential of the multidimensional system was successfully demonstrated by performing a suspected screening with ninety-nine compounds on a wastewater sample. Sixty-five of the suspected analytes were found. An orthogonality of the LC dimensions of 0.6 was calculated via a surface coverage approach referring to the screened compounds. The low solvent consumption makes the novel multidimensional system an environmentally and economically interesting alternative to systems that apply conventionally sized second dimension columns.

Kurzfassung (German abstract)

Diese Dissertation handelt von der Entwicklung eines neuartigen, multidimensionalen Trennsystems zur qualitativen Screeninganalyse komplexer Proben, welche hunderte mittel- bis schwerflüchtige Analyten beinhalten können. Dieses System kombiniert die online-betriebene, umfassend zweidimensionale Flüssigkeitschromatografie mit der hochauflösenden Hybrid-Massenspektrometrie. Eine konsequente Miniaturisierung der Chromatografie zu Nano- und Kapillar-LC in der ersten und zweiten Dimension ermöglichte eine Kopplung des Massenspektrometers unter vollständig kompatiblen Flussratenbedingungen (d. h. ohne einen Split nach der schnellen zweiten Dimension). Um die Wahl der Bedingungen für eine Beispielapplikation zu erleichtern, wurden zwei Studien mit Fokus auf der Verwendbarkeit hoher Ofentemperaturen für die zweite Dimension eingebunden. Zum einen wurde mittels einer Peakformstudie bei isokratischer Elution der Einfluss hoher Ofentemperaturen auf Lösemitteleffekte untersucht, welche auftreten können, wenn Umkehrphasen in der zweiten Dimension verwendet werden. Obwohl hohe Temperaturen die Lösemittelkompatibilität erhöhen, da Viskositätsunterschiede verringert werden, so kann eine durch Lösemittel-stärkeeffekte hervorgerufene Bandenverbreiterung nicht durch eine Temperaturerhöhung kompensiert werden. Die Prädominanz dieser Effekte bei jeglicher Temperatur unterstreicht die Notwendigkeit eines hinreichend kleinen Transfervolumens zur zweiten Dimension. Zum anderen wurden acht moderne stationäre Phasen in Bezug auf ihre Temperatur- und pH-Stabilität untersucht. Eine Vergleichsmethodik mittels Retentionsfaktorenanalyse wurde entwickelt, um den Zustand von silika-basierten Umkehrphasen anhand von Hydrophobi-zitätsverlusten und der Zunahme von silanophilen Wechselwirkungen überwachen zu können. Demnach basieren die stabilsten silika-basierten Partikel auf der BEH-Hybrid-Technologie. Nichtsdestotrotz wurden für das multidimensionalen System teilporöse Partikel (< 3 µm) mit C18-Funktionalisierung in Kombination mit erhöhter Temperatur und hohem Druck in der zweiten Dimension verwendet, um eine Gradienten-Zykluszeit von einer Minute zu realisieren. In der ersten Dimension wurde eine stationäre Phase aus porösem, graphitisiertem Kohlenstoff eingesetzt, welche eine großvolumige Injektion erlaubte. Das Potential des multidimensionalen Systems wurde demonstriert, indem ein 99-Analyten-Suspected-Screening auf eine stark matrixbehaftete Abwasserprobe angewendet wurde. 65 der Zielanalyten wurden gefunden. Bezogen auf die 99 Zielanalyten wurde über einen Surface-Coverage-Ansatz eine Orthogonalität von 0,6 bestimmt. Der geringe Lösemittelverbrauch macht das multidimensionale System zu einer umweltfreundlichen und wirtschaftlichen Alternative zu Techniken, die konventionelle HPLC in der zweiten Dimension nutzen.

Chapter 1 Introduction, concept and goals

This first chapter begins with a general introduction to multidimensional chromatography to clarify the differences to conventional (one-dimensional) chromatographic techniques and to point out the general benefits of such multidimensional approaches. A second section focuses on the fundamentals of the technique of choice which is comprehensive two-dimensional liquid chromatography. In this context, operational aspects are described and frequently occurring problems are described. The third section deals with high-temperature liquid chromatography as a tool for fast LC. A fourth section provides a brief introduction to important aspects of miniaturized LC techniques. The chapter closes with a definition of the goals.

1.1 Introduction to multidimensional chromatography

1.1.1 Multidimensional chromatography in a nutshell

Today's accepted comprehension of the term "multidimensional chromatography" can be traced back to fundamental articles by Giddings published in the 1980ies [1-2]. Back then, he introduced and defined multidimensional separation techniques as a general, promising concept to overcome the inherent peak capacity limitation of common one-dimensional separation techniques. The term "peak capacity" describes the maximum number of consecutive analyte peaks that can be separated with equal resolution within a given separation space [3].

The general concept behind multidimensional chromatographic approaches is to separate the sample mixture (or parts of it) via two or more orthogonal chromatographic separations (dimensions) in a way that the separation gained by the first or any preceding dimension is not lost [4]. In this case, the term orthogonal means that the retention mechanisms of the dimensions ideally differ in such a way that there is no correlation of the obtained retention factors (further information on orthogonality is presented in Section 1.2.4).

1.1.2 From 2-D planar systems to 2-D column chromatography

The first multidimensional chromatographic methods were developed using planar chromatography for bioanalytical separations. In a pioneering work reported by Consden et al. in 1944 [5], two-dimensional (2-D) paper chromatography was introduced for the separation of amino acids. In separate development cycles at perpendicular elution directions, two different mobile phases were applied to the sample on the same paper sheet. For certain mobile phase combinations, this resulted in a substantially increased separation space as the component zones were distributed across an area instead of a line that would be gained from a single dimension separation. When the first reproducibly manufactured thin layer chromatography (TLC) plates became widely available in the early 1960ies in consequence of Stahl's studies [6-8], the 2-D methodology was directly applied to TLC by various authors [9-14]. The success of 2-D planar chromatography also inspired researchers to develop non-chromatographic planar separation techniques such as 2-D gel electrophoresis [15-16] which still represents a contesting technique to 2-D chromatography in proteomics. However, isolation of compound zones and identification of components for the described planar techniques is not a simple task and often takes a lot of time [17]. Moreover, compounds in trace-level concentrations can often not be identified as sensitivity is limited. In contrast,

column chromatographic approaches usually provide higher speed, reproducibility and selectivity. Furthermore, they can easily be automated and hyphenated to mass spectrometry [17]. Therefore, much research work has been devoted to the development of automated column-based 2-D systems starting with the first notable publication on two-dimensional gas chromatography in 1958 [18]. However, spatial 2-D separations cannot be performed on the basis of columns as their walls per se do not permit the use of perpendicular flow directions [19]. The necessary switch to time-based chromatography in which the analytes are eluted from the stationary phase entails the potential risk of re-mixing analytes already separated by the first dimension. Therefore, a major task is to prevent analyte re-mixing within extra-column void volumes and more importantly during the second dimension separation [19]. To avoid the latter situation, a sufficient sampling procedure needs to be introduced that ensures a fraction-wise transfer of the first dimension (D1) eluate to the second dimension (D2) and, thus, a fraction-wise separation in D2 [20-21]. This preventive measure makes the important difference between 2-D column chromatography and approaches that use a simple serial coupling of different stationary phases. The serial combination of strong cation exchange (SCX) and reversed-phase (RP) liquid chromatography represents an often cited exception as it is exploited in multidimensional protein identification technology (MudPIT) approaches [22-25] frequently used in the field of proteomics. There, the mobile phase of one dimension does not significantly elute the analytes on the other dimension, and fractionation is achieved by the step-wise elution from D1.

1.1.3 Heart cutting vs. comprehensive mode

In two-dimensional column chromatography (2-D CC), a fraction-wise transfer to the second dimension is not necessarily needed for the whole D1 eluate; especially not for the chromatographic space where the first dimension separation was already sufficient. Consequently, there are basically two different modes of 2-D CC, the heart cutting (also called heart-cut) and the comprehensive mode [26-27]. In heart cutting 2-D CC, only one (or very few non-consecutive) fraction(s) of the first dimension eluate is/are subjected to the second dimension. The fraction size usually corresponds to the volume occupied by the band or by the chromatographic space that is chosen for further separation. The peak capacity for a heart cutting system (n_{hc}) can be approximated by using Equation 1-1:

$$n_{hc} = n_1 + z \cdot n_2 \qquad \text{Equation 1-1}$$

where n_1 and n_2 are the peak capacities for D1 and D2, respectively, and z is the number of transferred bands.

On the other hand, in comprehensive 2-D CC, the whole D1 eluate is considered for further consecutive separation by D2. Consequently, the comprehensive approach particularly suits for the analysis of very complex samples. Here, a consistent fraction size is predefined and all of the D1 eluate samples are transferred to D2, either in whole or in equal parts [27]. One D1 band is usually cut in multiple fractions. The theoretical peak capacity of a fully orthogonal comprehensive system (n_{c2D}) is still frequently approximated using the product rule by Giddings [1] (see Equation 1-2):

$$n_{c2D} = n_1 \cdot n_2 \qquad \text{Equation 1-2}$$

However, in practice, this equation strongly overestimates n_{c2D}. At least, correction factors which account (1) for the analyte remixing within the collected D1 eluate fractions and (2) for the usually incomplete orthogonality are necessary to obtain more reliable values for n_{c2D} [28]. Nonetheless, the comprehensive mode clearly provides the stronger potential in peak capacity gain in comparison to the heart cutting mode.

With regard to the product rule [1], comprehensive 2-D chromatography techniques are usually abbreviated using the multiplication sign × in between the abbreviations for the respective techniques in the first and second dimension, e.g. GC×GC for approaches that use gas chromatography in both dimensions.

1.1.4 Comprehensive 2-D gas chromatography

The two leading comprehensive 2-D CC techniques are those that apply capillary gas chromatography (GC×GC) [29-32] and liquid chromatography (LC×LC) [26, 28, 33-37] in both dimensions. Further comprehensive 2-D techniques that are not covered by this thesis are for example LC×GC, SFC×GC, SFC×SFC, and SFC×LC [38] where SFC is supercritical fluid chromatography. Although GC×GC is the younger technique compared to LC×LC [39-40], it has reached a significantly higher degree of maturity and is increasingly used in routine laboratories. This success is based on several advantages that GC×GC exhibits over LC×LC:

Although the efficiency of LC separations could recently be improved significantly by the development of new stationary phases and the use of ultrahigh-pressures and/or high temperatures, efficiency of GC separations is still superior [41]. That is because diffusion and inter-phase mass transfer is much faster in GC [26]. Moreover, the flow velocity in GC is not severely limited by pressure as is the case for LC systems [26]. This is the result of the low viscosities of gases. Peak widths in the range of tens of milliseconds can therefore easily be

achieved using the well-known principles of fast GC [26, 42]. Furthermore, the mobile phase, the carrier gas, is chemically inert with respect to the stationary phase, so the same mobile phase can be used for both separation dimensions. The use of a nonpolar and a polar column for D1 and D2, respectively, can already be considered highly orthogonal for many analytes [19]. A big part of the success of GC×GC systems is based on the development of cryo-modulators [43-46]. These thermal sampling devices allow analyte immobilization by freezing them at one or multiple points resulting in an enrichment and refocussing of the analytes. A sudden remobilization by heat results in a fraction-wise focused injection to the second dimension column. These advantages allow a comparably easy automation in GC×GC. A general flow scheme is shown in Figure 1-1.

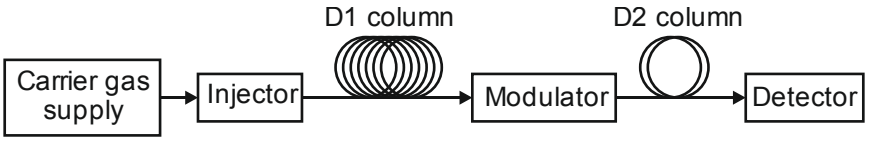

Figure 1-1. General flow scheme of GC×GC.

However, the main limitation of all GC systems is the fact that analytes must provide a sufficient vapor pressure and thermal stability at the GC operating temperature. An increasing number of emerging polar analytes relevant for environmental analysis and large molecules from biochemical analysis need derivatization or are not measurable by GC at all. [47]

1.2 Comprehensive 2-D liquid chromatography

1.2.1 From GC to LC

A broader range of analytes, including thermolabile and nonvolatile substances, can be measured using liquid chromatographic methods [48]. Here, the main limitation is that the analytes must be dissolved by the liquid mobile phase [48]. For the purpose of LC×LC, there is a variety of liquid chromatographic techniques that can potentially be employed and combined as separation dimensions. Among these are reversed-phase (RP), normal-phase (NP), hydrophilic interaction (HILIC), size exclusion (SEC), ion exchange (IEC), and affinity chromatography including the respective subgroups [26].

However, in contrast to gas chromatography, the mobile phase in liquid chromatography is not inert with respect to the stationary phase and the analytes. The mobile phase composition, i.e., the solvents and additives, strongly affects selectivity and elution strength [48]. Moreover, in the worst case, the mobile phase of one liquid chromatographic dimension can

even cause damage to the other stationary phase. A high-pH eluent from a strong anion exchanger (SAX) can for example dissolve (unprotected) silica-based RP particles [49]. Therefore, it is necessary to use adapted solvent systems for each particular stationary phase. As D1 eluate is transferred to the second dimension, the use of two different mobile phases inevitably leads to the mixture of both which can result in solvent incompatibilities [26, 34, 50]. These effects potentially deteriorate the D2 peak shape and can even prevent D2 operation. Further relevant information on solvent effects is provided in Chapter 2.

A second important restriction of liquid chromatography, and therefore of LC×LC, is the pressure limitation of any solvent pump system. In contrast to capillary gas chromatography, an increased flow resistance is given by the application of packed columns [51]. Moreover, mobile phase viscosity is significantly increased for liquids in comparison to gases [52].

The given reasons make it more difficult to automate and speed up LC×LC separations.

1.2.2 Modes of operation

With regard to its limitations, LC×LC is subcategorized in three operation modes on the basis of analysis speed and the degree of automation [34-35, 53]. The main aspects of these modes are summarized below.

Offline mode: In an offline operated system, the D2 run(s) are performed independently from the first dimension run. The fractions are usually collected in a fraction collector, on well plates or on trap columns. This mode provides a maximum flexibility as analysis times can be chosen without limitations. Moreover, the D1 mobile phase can be separated from the analytes by evaporation or by solute trapping [54]. Thus, the risk of solvent effects can be minimized and incompatible solvent systems can be used. The minimum requirement is an HPLC system equipped with a fraction collection device. The offline mode provides highest separation power. Nonetheless, this comes at the price of a disproportionately long analysis time per sample and a limited reproducibility [54].

Stop-flow mode: This mode is also called Stop-and-go mode. It represents an already highly automated LC×LC setup and is, therefore, frequently described as an online approach which is misleading. On the contrary, the similarity to the offline mode is pretty high as the analysis times of the D1 and the D2 runs are independent. The main difference is that the D1 flow is stopped after the collection of each eluate fraction to allow its direct D2 analysis. The fractions are usually collected in a sample loop or on a trap column. In MudPIT approaches [22-25], the D1 fraction is trapped on the D2 stationary phase. For a modern, appropriately set

up system, Kalili and de Villiers [53] reported that the additional D1 band broadening caused by the flow stop does not significantly affect the peak capacity. The latter is comparable to that of offline systems. However, the drawback of a disproportionately long analysis time as well remains. For example, the collection of 50 10-min fractions results in 8.3 h overall D2 run time.

Online mode: In this thesis, online operation means that all D2 runs are performed within the timeframe of the D1 method [35-36]. This requires a maximum LC×LC automation and a very short second dimension cycle time (~ 10 to 120 s). The D1 analysis time which represents the overall analysis time is usually kept below two hours. Fast, online LC×LC applications take only 20 to 30 min per sample [26]. As the maximum peak capacity is obtained at long analysis time [3, 55], online LC×LC cannot compete with stop-flow or offline LC×LC [53]. Nonetheless, the sample throughput is maximized. The fractions are usually collected in multiple, alternating sample loops or less frequently on trap columns as the time needed for trap column elution adds to the limited D2 run time.

The fast GC×GC sampling procedure between the two dimensions is called modulation [27]. This term is often borrowed for the fast sampling in online operated LC×LC. As the words “sampling” and “resampling” can be easily mixed up with sample injection methods, it was decided to use the term modulation predominantly. Accordingly, the device that is used to accomplish modulation will be called modulator.

1.2.3 Operation principles of online LC×LC

A variety of instrumental setups and capillary flow schemes for online LC×LC have been reported as summarized in the reviews of Francois et al. [34, 41]. In the following, the operation principles of an online LC×LC system will be described by using the exemplary flow scheme of Figure 1-2 which has been chosen because of its clarity and due to further advantages to frequently used setups that will be discussed in more detail in Section 4.1.2.

In the presented scheme of Figure 1-2, the modulator consists of two 4-port 2-position valves which ensure that the D1 eluate is alternately filled in one of two sample loops (labelled Loop 1 and 2). Alternation between the loops is obtained by a synchronous switching of both valves. During the filling of one loop, the other loop is flushed to perform the second dimension separation.

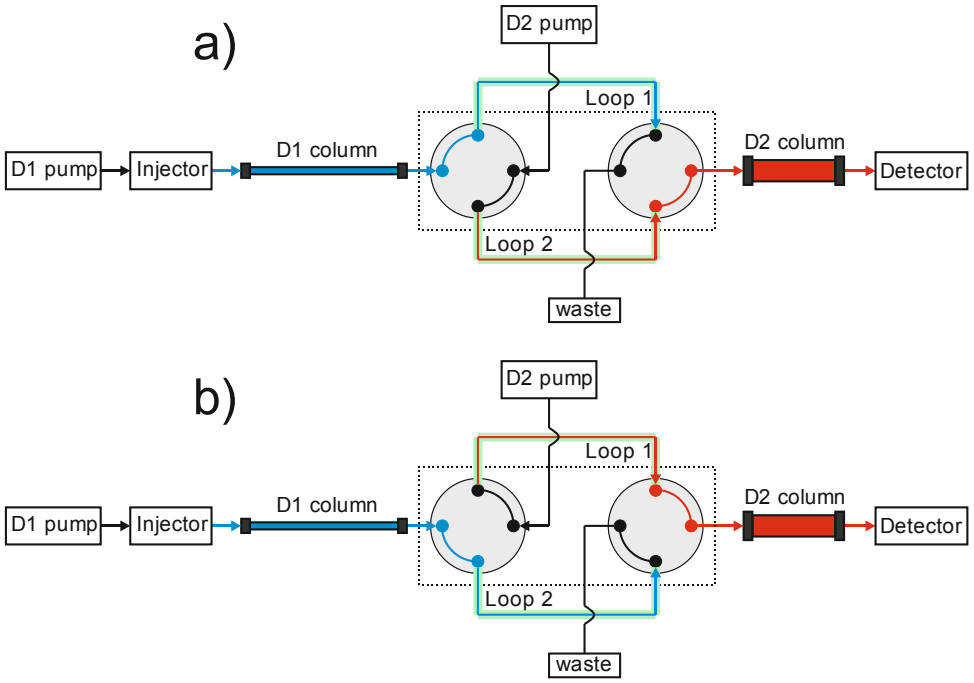

Figure 1-2. Two-loop modulation scheme using two synchronously switched 4-port 2-position valves for both valve positions, (a) and (b). Blue: sample path in first dimension. Red: sample path in second dimension. Green: modulation (sample) loops.

The setup of Figure 1-2 can easily be adapted to a two-trap modulation by replacing the loops by two trapping columns. Counterflow flushing of the traps/loops can be obtained by interchanging the positions of the D2 pump and the D2 column/detector combination at the connection ports of the modulation valves.

The inherent D2 runtime limitation of online LC×LC can be visualized using Figure 1-2. The time for a complete D2 analysis cycle has to be equal to or smaller than the modulation loop filling time. In case of a too slow D2 separation, the delayed switching of the valves would result in a diversion of D1 eluate to the waste bottle.

A frequently used strategy to cope with the runtime limitation is to use a narrow-bore column at a low flow rate in D1 and a wide, but short analytical-bore column at a high flow rate (up to 5 mL min^{-1}) in the second dimension [56-57]. This is also indicated in Figure 1-2.

Online LC×LC usually is performed without first dimension detection [26] (compare Figure 1-2). Information from the D1 separation is indirectly conserved by the modulation if at least 3-4 samples per D1 peak (width: 8 standard deviations) are collected [20]. In other words, the hypothetical D1 chromatogram is scanned by a fraction-wise analysis of the D1 eluate (Figure 1-3).

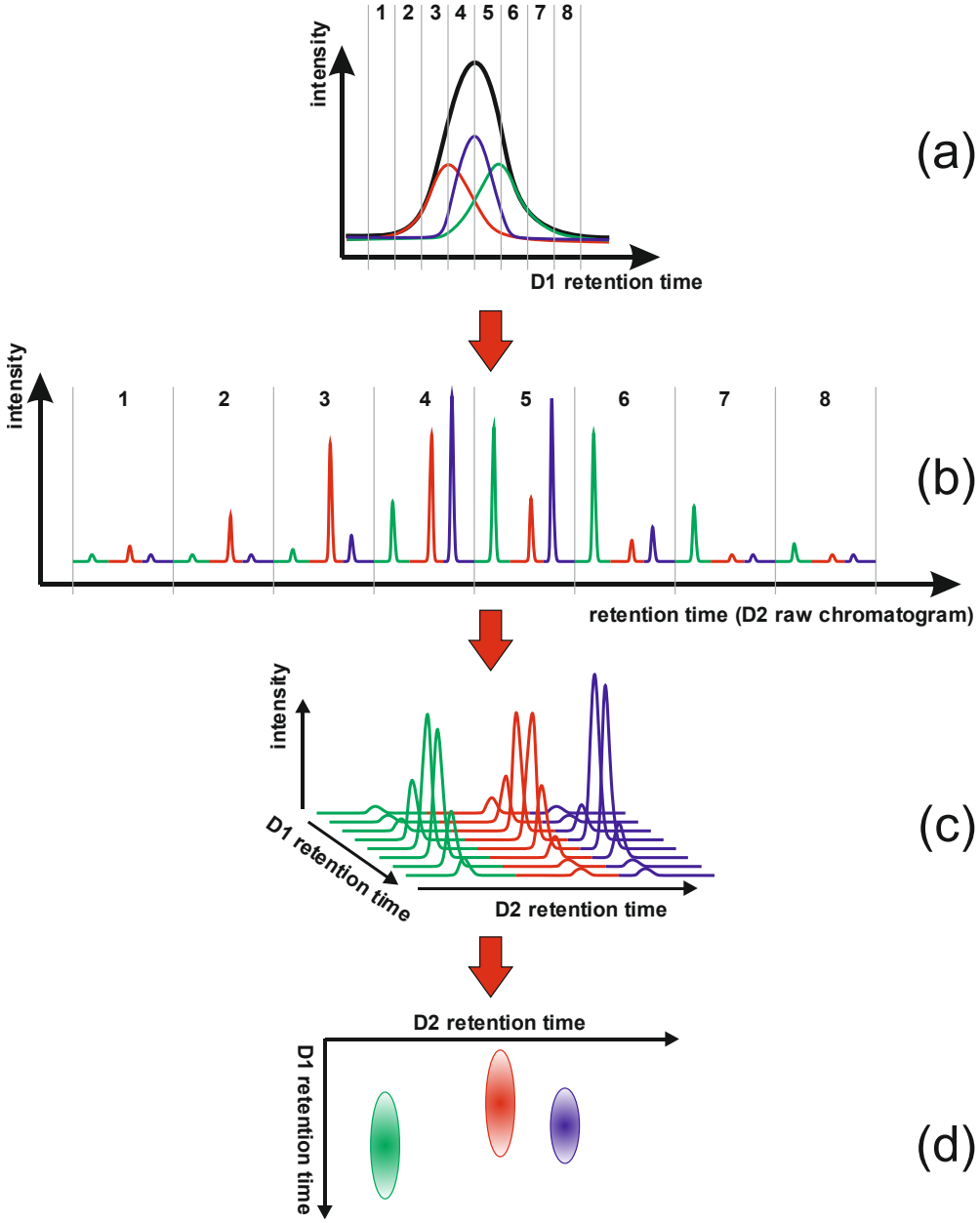

Figure 1-3. Schematic view of the steps of chromatogram evolution in comprehensive 2-D column chromatography. (a) The eluate of the D1 band (black) that consists of co-eluting signals (red, blue, green) is fractionated. (b) Data of fraction-wise separation in D2 is acquired consecutively by the detector. (c) Rearrangement of the single D2 chromatograms to a matrix. (d) Visualization (exemplarily as a 2-D plot). Self-created on the basis of scheme 1 in [58].

The modulation procedure results in a fractionation of the D1 eluate (Figure 1-3a) and in a direct transfer of the collected fractions to the second dimension. The detector positioned after the D2 column is then used to consecutively acquire D2 data for each D1 eluate fraction. In case of continuous acquisition, information of the single D2 runs is collected in one raw chromatogram (Figure 1-3b). If the D2 gradient cycle is sufficiently shorter than the fraction collection time (modulation time), it is possible to write in single-run D2 chromatogram files.

In either case, the chromatogram raw data of the D2 runs have to be rearranged to a side-by-side matrix as visually indicated in Figure 1-3c. In this step, D1 time stamps are assigned to each D2 chromatogram on the basis of the modulation time interval to create the missing D1 retention time axis. In the final step, the raw data matrix is used to create a chromatogram plot (Figure 1-3d). For print applications, two-dimensional plots as for example color maps or contour (line) plots are frequently used as they provide component zones similar to developed 2-D TLC plates [59]. 3-D visualizations are better suited for on-screen presentations as they need to be freely rotatable to view all information.

1.2.4 Orthogonality

Orthogonality, the basic requirement for any multidimensional chromatographic separation, describes the ideal case in which the retention factors obtained for the sample solutes are statistically independent (uncorrelated) between the combined separation systems [27]. As a result, the peaks are distributed evenly and randomly across the whole rectangular separation area which is described by the first and second dimension peak capacities as the respective side lengths [60]. The main practical limitation of orthogonality is given by the limited dimensionality of the sample, this means, by the number of independent analyte properties (sample dimensions) that allow the entity of sample compounds to be separated via the used separation systems [61]. Accordingly, in practice, the effective area in which the peaks are situated always is smaller than the theoretically available area.

Line formation of compound zones, i.e. strong positive or negative correlations of the retention times, can be caused by similar or correlated separation mechanisms in both dimensions or by one-dimensional samples [61]. An example for the latter is for example a homologous series of n-alkanes. The sample constituents differ in size just as in hydrophobicity. As both properties are correlated for the n-alkanes, only one independent solute parameter is available for the separation. Cluster formation of the analyte spots can occur due to similarities in the chemical structure or properties of the analytes. Although both phenomena, line and cluster formation, decrease the effective utilization of the separation space and thus overall orthogonality [60], multiple lines and clusters can be helpful for the interpretation of 2-D chromatograms of complex samples as the solutes can be grouped according to the correlations. This, for example, is usually exploited in case of combinations of normal-phase and reversed-phase liquid chromatography [36].

It can be concluded that orthogonality has to be evaluated for every kind of sample separately. The term orthogonality includes different aspects to that can be used as a measure

for comparisons: "[…] (1) independence of [the] dimensions […,] (2) spatial spreading of [the] peaks […,] (3) peak capacity […, and] (4) the part [of the separation space] occupied by peaks […]" [62]. Accordingly, many comparison methods have been published so far as is apparent from reviews [26, 34-35, 60, 63] and recent contributions such as [62, 64-65]. However, each of the methods provides its advantages and disadvantages, and there is an ongoing discussion and search for the "ideal" approach.

The approach chosen for this thesis is adapted from that of Dück et al. [65] and determines the surface coverage by calculating the convex hull, however, on the basis of the apex plot (peak maxima plot). Details are described in Sections 5.3.1 and 5.6.3. The advantages of the applied method include (1) its independence from the correctness of any peak capacity determination while it still can be used as a correction factor for n_{c2D}, (2) its direct use of measured retention time pairs without the need to include all signals to the calculation, (3) its comparably low dependence on analyte number variations, and (4) the simple calculation that can be performed without dedicated software other than a spreadsheet program. Nonetheless, the main disadvantages as for all convex hull methods are (1) the missing consideration of the exact peak distribution within the convex hull and (2) the sensitivity toward single outlier points that are uncharacteristic components with regard to the sample entity [60]. Both points can lead to an overestimation of the orthogonality.

Previous reviews [26, 33, 56-57] provide tables and lists that contain stationary phase combinations that have already been tested in LCxLC for the separation of certain sample types to help finding a starting point for own orthogonality evaluations. Stoll et al. summarized that combinations of different types of liquid chromatography as for example SEC×RP, IEC×RP, IEC×NP, HILIC×RP and NP×RP often yield high orthogonality [26]. However, there are restrictions to these combinations such as a limited efficiency and reproducibility, as well as solvent incompatibilities – especially in case of hyphenations of RP and NP [26]. All of these restrictions are pronounced for online LC×LC. A further, more general difficulty is given by the divergence of the sets of analytes that can be separated by the different chromatography types. Therefore, in the last years, RP×RP was promoted by Stoll et al. as an alternative that allows broader applicability [26, 36]. Although separation by hydrophobic interaction is a retention mechanism that all RP phases have in common and, therefore, full orthogonality cannot be obtained, it is wrong to assume that RP×RP generally results in strong correlations [26]. The use of RP chromatography allows choosing between hundreds of stationary phases that can provide substantially different selectivity. This is caused by the varying proportions of secondary retention mechanisms as for example steric

exclusion, hydrogen bonding-, π-π-, dipole-dipole-, and ionic interactions [66]. Moreover, the choice of the mobile phase and temperature conditions can also further influence selectivity [48] and, thus, the orthogonality of an RP×RP system. The loss in orthogonality is compensated by high speed, efficiency and reproducibility which can be additionally boosted by the use of gradient elution in both dimensions. This results in high peak capacity production rates above 30 min^{-1} for small molecules and short cycle times [26]. Nonetheless, although the solvent systems of both dimensions are usually miscible, RP×RP is still susceptible to solvent effects caused by elution strength [67] or viscosity mismatches [68]. These can lead to peak distortions, to a decrease in efficiency or even to an interruption of the system operation. A more detailed introduction to solvent effects is presented in Section 2.1.

In consequence of the described advantages, it was decided to apply RP chromatography in both dimensions of the online LC×LC system. Details on the exact stationary phase choice are discussed in Sections 4.3.2 and 4.3.3.

1.3 Fast LC and the benefits of high temperatures

As described in Section 1.2.2, the application of online LC×LC requires the adherence to very short cycle time limits in the second dimension (< 2 min). Accordingly, the separation in D2 has to be performed fast to avoid so-called wrap-arounds [27].

These are situations in which a compound cannot be eluted from the D2 column during the cycle in which the corresponding D1 eluate sample was injected [27]. Instead, it would elute in one of the following D2 cycles, i.e., after injection of the next D1 fraction. Wrapped-around bands disturb a clear assignment of the separated compounds to certain D1 fractions in the chromatogram. Moreover, they potentially lead to serious problems during data analysis, for example, due to broadening of wrapped-around bands, unwanted coelution, and/or D2 retention time shifts between consecutive D1 fractions of a wrapped-around band [34]. The severity of these effects depends on the exact mobile phase programs of both dimensions.

The following strategies to enhance the speed in liquid chromatography assume that the selectivity of the system is given or has already been optimized. Thus, the analysis time and resolution mainly depend on the separation efficiency and the applied mobile phase velocity [48]. Good efficiency is necessary to keep the compounds separated; however, high values potentially lead to long analysis times. A high mobile phase velocity is necessary for a fast transport of the analytes through the column; nonetheless, a too high velocity beyond the van-Deemter optimum potentially results in a loss in separation efficiency [69].

In general, short columns are preferred for fast LC [48, 69]. This results in shorter migration times of solvents and analytes through the column. However, the overall efficiency is decreased proportionally to the column length [69] and, consequently, columns cannot be shortened arbitrarily.

The following approaches allow a significant increase in mobile phase velocity without a significant loss in efficiency:

- Ultrahigh-performance chromatography (UHPLC): The use of small particles and pressures above 400 bars.
- Special stationary phase technology: Monoliths or columns packed with core-shell particles.
- High-temperature liquid chromatography (HT-LC): According to the definition of Teutenberg [70], this term relates to techniques that employ column oven temperatures between 60 °C and that of the critical point of the mobile phase.

All of these strategies have already been applied to online LC×LC. In their review, Stoll et al. extensively described the benefits of high-temperature to fast LC and online LC×LC. [26]

An increase in temperature basically has two important effects that influence the speed of a separation. On the one hand, the static permittivity of the water is reduced [71]. That means that water acts more like an organic solvent and can even be used to replace organic solvents in reversed-phase LC. Accordingly, the elution strength increases and most analytes are forced to leave the column earlier. Secondly, the viscosity and viscosity differences of RP solvents and their binary mixtures are decreased [72].

As can be seen from the fundamental Equation 1-3 that is derived from the Darcy law [69], a decrease in mobile phase viscosity (η) reduces the pressure drop along the column (ΔP).

$$\Delta P = \frac{\varphi_D \, \eta \, l_c \, u}{d_p^2} \qquad \text{Equation 1-3}$$

where φ_D is the flow resistance factor based on the Darcy law, l_c is the column length, u is the average linear mobile phase velocity and d_p is the particle diameter of the stationary phase.

For a pressure limited system such as any LC system, this decrease in backpressure allows increasing u which is directly proportional to the volumetric flow rate (see Equation 1-4, [73]).

$$u = \frac{4\,F}{d_c^2\,\pi\,\varepsilon_T} \qquad \text{Equation 1-4}$$

where F is the volumetric flow rate, d_c is the inner diameter of the column and ε_T is the total porosity of the packing.

Apart from the pressure drop of the column, the extra-column contribution to the system backpressure is as well decreased as is shown exemplarily for cylindrical extra-column volumes such as those of capillaries. According to the Hagen-Poiseuille law, the pressure drop across a capillary or another cylindrical volume can be approximated by Equation 1-5 [70]:

$$\Delta P = \frac{128\,\eta\,l_{cap}\,F}{d_{cap}^4\,\pi} \qquad \text{Equation 1-5}$$

where l_{cap} is the length of a capillary and d_{cap} is the inner diameter of the capillary.

For any system that works at its pressure limit, it follows that the flow rate can be increased when higher temperatures are applied as a decreasing mobile phase viscosity reduces the backpressure caused by the column (Equation 1-3) and the capillary system (Equation 1-5).

At the same time, temperature influences the efficiency of the separation system as shall be indicated exemplarily by using an extended van-Deemter equation derived by Antia and Horvath [74] (Equation 1-6) .

$$H = A \cdot d_p + B \cdot \frac{D_m}{u} + C \cdot \frac{d_p^2}{D_m} \cdot u + D \cdot \frac{d_p^{5/3}}{D_m^{2/3}} \cdot u^{2/3} + \frac{2 \cdot k \cdot u}{(1+k)^2 \cdot k_d} \qquad \text{Equation 1-6}$$

where H is the plate height; A, B, C, and D are dimensionless constants that are usually assumed not to change with temperature; k_d is the desorption rate constant; k is the retention factor of the analyte; and D_m is the solute diffusion coefficient in the mobile phase.

The diffusion coefficient D_m increases with temperature [70] and is part of three terms. These are related to longitudinal molecular diffusion, the resistances to intra-particle and extra-particle stagnant film mass transfer [74]. Although the maximum efficiency at the optimum mobile phase velocity is not increased by temperature (constant A term, related to "eddy diffusion"), the changes of the other terms result in a shift of the optimum mobile phase velocity to higher values without a significant loss in overall efficiency [74] (compare Figure 1-4). Moreover, an increase in temperature flattens the progression of the van-Deemter curve at mobile phase velocities above the optimum. For a more detailed discussion, refer to Teutenberg [70].

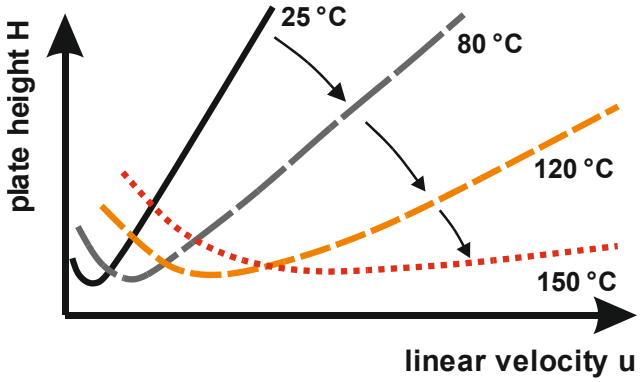

Figure 1-4. Rough sketch describing the change of the van-Deemter curve progression for increasing oven temperature. Conditions: 3 µm fully porous reversed phase particles, rapid sorption kinetics. Self-created on the basis of Fig. 1 in [75].

A unique feature of fast LC approaches based on HT-LC is that viscosity-driven solvent effects are potentially reduced, as the viscosity mismatch between the D1 and D2 mobile phases is potentially diminished (compare Chapter 2).

1.4 Miniaturized LC techniques

1.4.1 Motives and definition

Common motives to miniaturize a liquid chromatographic system are the reduction of solvent consumption (toward a greener and less costly chromatography), the availability of only very small sample volumes (biochemical analysis) and last but not least the increased theoretical sensitivity with regard to the injected absolute mass of the solutes. The gain in sensitivity is caused by the reduced analyte dilution in small columns. In the case of mass spectrometric detection, sensitivity is additionally increased by the decrease of the solvent load to the ion source, especially where low-flow ion sources such as nanoelectrospray ionization (nanoESI) can be used. However, the sensitivity gain is delimited by the injection volume that has to be decreased in accordance with the reduction of the column volume. [76-77]

Typically, the initial step of the miniaturization of LC systems is the reduction of the inner diameter (i.d.) of the column. In literature, there is still no standardization of the nomenclature of miniaturized LC systems [76-77]. However, it is widely accepted to categorize the systems according to the i.d. of the analytical column instead of using flow rates. Table 1-1 shows the categorization of the systems that was chosen for this thesis.

Table 1-1. Categorization of miniaturized LC systems on the basis of the column i.d. in comparison to conventional (U)HPLC.

Category	Column i.d. in µm
NanoLC	25* – 100
CapillaryLC (capLC)	100 – 500
MicroLC	500 – 1000
Conventional (U)HPLC	1000 – 4600

*for packed-bed nanoLC. Even smaller diameters are used in open-tubular nanoLC.

NanoLC is usually performed using flow rates in the range of 1-1000 nL min^{-1}. Capillary- and microLC normally share the range of 1-300 µL min^{-1}. The particle diameters of the packings are more or less the same compared to conventional (U)HPLC [76-77]. As in case of the conventional techniques, a trend to the application of smaller particles (1-3 µm) is apparent. However, the increased pressure drop that is due to the reduction of the column i.d. does not permit the use of even smaller particles at practicable flow rates. This is underlined by the fact that miniaturized LC systems do usually not provide the full pressure range of modern UHPLC systems.

1.4.2 Importance of extra-column volumes

Besides the reduction of the column i.d., it is of utmost importance to reduce all extra-column volumes [76-77]. Otherwise, unnecessarily prolonged analysis times and significantly increased extra-column band broadening result. A similar discussion has recently emerged with regard to the introduction of UHPLC systems which also can be seen as miniaturized HPLC due to the reduction of the column i.d. from 4.6 to 2.1 mm, or even 1 mm [78-79].

The relevance of the extra-column band broadening can be demonstrated by a general formula for extra-column band broadening [79]. The variance of a peak (σ^2) which is also the second central moment is a measure for the spread of the peak distribution. The total variance of an observed peak in liquid chromatography (σ_T^2) is given by the sum of the single variance contributions that arise from the system parts through which the analytes are transported (see Equation 1-7 adapted from [79]).

$$\sigma_T^2 = \sigma_{col}^2 + \sigma_{ec}^2 = \sigma_{col}^2 + \sigma_{cap}^2 + \sigma_{inj}^2 + \sigma_{det}^2 + \sigma_{tc}^2 + \sigma_{fil}^2 + \sigma_{con}^2 + \ldots$$

Equation 1-7

where σ_{col}^2 is the variance contribution of the column, σ_{ec}^2 is the extra-column variance contribution, σ_{cap}^2 is the variance contribution of the capillaries, σ_{inj}^2 is that of caused by the injector, σ_{det}^2 is that of the detector, σ_{tc}^2 is that caused by the acquisition time constant / acquisition frequency, σ_{fil}^2 is that of optional inline filters or unions, and σ_{con}^2 is that arising from potential void volumes that occur at the capillary connections. The periods indicate that any potential further contribution also adds to the observed variance.

In the ideal case, the peak variance is small and mainly caused by the contribution of the column. An acceptable σ_{ec}^2 should at least be smaller than ten percent of σ_{col}^2 [78]. Besides the acquisition time constant and the column, several extra-column void volumes contribute to the overall band broadening (see Equation 1-7). The dispersion and diffusion processes that occur within these volumes and that cause the band broadening are sometimes difficult to predict as they depend on the exact geometry of the void volume. However, a variance contribution usually increases with the size of the corresponding extra-column void volume as was for example shown by Fountain et al. [80] for capillaries of different inner diameters. This underlines the necessity to reduce all extra-column volumes. This is as well true for the flow cell of a UV detector. Here, the decrease in cell diameter results in a shortened measuring path length if the light beam is applied perpendicularly to the flow stream. Thus, the cell geometry usually needs to be adapted to longitudinal or extended light path flow cells [81].

However, the diameters of the extra-column volumes can often not be reduced to the same extent as compared to the diameter of the column because of the increasing back pressure and the risk of clogging [78, 81]. Therefore, it is also important to shorten the length of the extra-column flow path.

1.5 Scope of the thesis

The aim of this thesis was to develop a novel multidimensional separation system for a comprehensive qualitative assessment of complex environmental samples that contain emerging, semi- and non-volatile analytes within a molecular mass range of ~ 50 – 1000 Da. For this purpose, online comprehensive two-dimensional liquid chromatography should be hyphenated to hybrid high-resolution mass spectrometry. The high resolving power of the mass spectrometer allows for a highly accurate monoisotopic mass determination and, thus,

for a proposal of the molecular formula of the analyte. A hybrid-type mass spectrometer provides the additional advantage that selective fragmentation experiments can be performed to obtain structural information on the analytes [82].

The hyphenation should be established without using any flow split but at full flow rate compatibility between the second LC dimension and the mass spectrometer. This way, unnecessary analyte losses should be avoided while preserving a sensitive detection without a too high solvent load to the ion source of the mass spectrometer. The core strategy to implement this hyphenation should be the consistent miniaturization of the online LC×LC part of the system to online nanoLC×capillaryLC. The retention mechanisms should be based on the use of reversed-phase chromatography columns in either dimension. The potential of the final system should be evaluated by applying a suspected screening to a wastewater sample.

For the online LC×LC part of the system, a modulation time of one minute should be established. In this context, it should be evaluated whether high-temperature liquid chromatography could be employed to speed up the second dimension of the multidimensional system.

Accordingly, this thesis is structured as follows:

The compatibility of the solvent systems used in both separation dimensions dictates the success and the operation conditions of any two-dimensional separation [34]. **Chapter 2** addresses the presence and importance of solvent effects in a high-temperature reversed-phase second dimension. In this context, it contains a peak shape study performed using isocratic elution conditions and ZirChrom-PBD columns of different size that are heated isothermally. Special attention is given to the influence of the oven temperature.

A prerequisite for any heated liquid chromatographic dimension is a sufficient temperature stability of the stationary phase and its column hardware [70]. Therefore, in **Chapter 3**, the long-term high-temperature and pH stability of eight modern commercially available stationary phases are evaluated and compared to existing data. This should provide a more recent overview on the available stationary phase technologies that allow the successful operation of a high-temperature liquid chromatographic separation dimension.

Chapter 4 introduces the instrumentation, i.e., the development platform, used for the implementation of the multidimensional system and covers preliminary theoretical considerations on the capillary system setup, stationary phase choice, column dimensions, solvent sytems, elution mode and the heating concept. In this context, the results of Chapter 2

and Chapter 3 are picked up and discussed together with current literature and preliminary laboratory work to find the optimum conditions for the operation of the multidimensional system.

Chapter 5 deals with the final implementation of the multidimensional system and its evaluation using a suspected screening method that was applied on wastewater as the model matrix.

Finally, the thesis closes with general conclusions and an outlook in **Chapter 6**.

1.6 References

[1] Giddings, J. C. *TWO-DIMENSIONAL SEPARATIONS: CONCEPT AND PROMISE*. Anal. Chem. 1984, ***56***, 1258A-1270A.

[2] Giddings, J. C. *Concepts and Comparisons in Multidimensional Separation*. J. High Resolut. Chromatogr. Chromatogr. Commun. 1987, ***10***, 319-323.

[3] Neue, U. D. *Peak capacity in unidimensional chromatography*. J. Chromatogr. A 2008, ***1184***, 107-130.

[4] Giddings, J. C. In *Multidimensional Chromatography - Techniques and Applications*; Cortes, H. J., Editor; Chromatographic Science Series Vol. 50; Marcel Dekker, Inc.: New York and Basel, 1990; pp. 1-28.

[5] Consden, R.; Gordon, A. H.; Martin, A. J. P. *Qualitative Analysis of Proteins: a Partition Chromatographic Method Using Paper*. Biochem. J. 1944, ***38***, 224-232.

[6] Stahl, E. *Dünnschicht-Chromatographie - IV. Mitteilung: Einsatzschema, Randeffekt, "saure und basische" Schichten, Stufentechnik*. Arch. Pharm. (Weinheim, Ger.) 1959, ***292/64***, 411-416.

[7] Stahl, E. *Dünnschicht-Chromatographie - II. Mitteilung: Standardisierung, Sichtbarmachung, Dokumentation und Anwendung.* Chem.-Ztg. 1958, ***82***, 323-329.

[8] Stahl, E. *Dünnschicht-Chromatographie - Methode, Einflussfaktoren und einige Anwendungsbeispiele.* Pharmazie 1956, ***11***, 633-637.

[9] Skidmore, W. D.; Entenman, C. *Two-dimensional thin-layer chromatography of rat liver phosphatides*. J. Lipid Res. 1962, ***3***, 471-475.

[10] Yasuda, S. K. *IDENTIFICATION OF N-NITROSO- AND NITRODIPHENYLAMINES BY TWO-DIMENSIONAL THIN-LAYER CHROMATOGRAPHY*. J. Chromatogr. 1964, ***13***, 65-70.

[11] Wagener, H.; Frosch, B. *Zweidimensionale dünnschichtchromatographische Trennung von Gallensäuren*. Klin. Wochenschr. 1963, ***41***, 1094-1095.

[12] Stahl, E.; Kaldewey, H. *Spurenanalyse physiologisch aktiver, einfacher Indolderivate*. Hoppe-Seyler's Z. Physiol. Chem. 1961, ***323***, 182-191.

[13] Stahl, E. *Neue Anwendungsgebiete der Dünnschicht-Chromatographie*. Angew. Chem. 1961, ***73***, 646-654.

[14] Lepage, M. *THE SEPARATION AND IDENTIFICATION OF PLANT PHOSPHOLIPIDS AND GLYCOLIPIDS BY TWO-DIMENSIONAL THIN-LAYER CHROMATOGRAPHY*. J. Chromatogr. 1964, ***13***, 99-103.

[15] O'Farrell, P. H. *High-Resolution Two-Dimensional Electrophoresis of Proteins*. J. Biol. Chem. 1975, ***250***, 4007-4021.

[16] Klose, J. *Protein Mapping by Combined Isoelectric Focusing and Electrophoresis of Mouse Tissues - A Novel Approach to Testing for Induced Point Mutations in Mammals*. Humangenetik 1975, ***26***, 231-243.

[17] Schure, M. R.; Cohen, S. A. In *MULTIDIMENSIONAL LIQUID CHROMATOGRAPHY - Theory and Applications in Industrial Chemistry and the Life Sciences*; Cohen, S. A.; Schure, M. R., Editors; Jon Wiley & Sons: Hoboken, NJ, USA, 2008; pp. 1-7.

[18] Simmons, M. C.; Snyder, L. R. *Two-Stage Gas-Liquid Chromatography*. Anal. Chem. 1958, ***30***, 32-35.

[19] Mostafa, A.; Gorecki, T.; Tranchida, P. Q.; Mondello, L. In *Comprehensive Chromatography in Combination with Mass Spectrometry*; Mondello, L., Editor; Wiley Series on Mass Spectrometry; Wiley: Hoboken, NJ, USA, 2011; pp. 93-144.

[20] Murphy, R. E.; Schure, M. R.; Foley, J. P. *Effect of Sampling Rate on Resolution in Comprehensive Two-Dimensional Liquid Chromatography*. Anal. Chem. 1998, ***70***, 1585-1594.

[21] Seeley, J. V. *Theoretical study of incomplete sampling of the first dimension in comprehensive two-dimensional chromatography*. J. Chromatogr. A 2002, ***962***, 21-27.

[22] Washburn, M. P.; Wolters, D.; Yates, J. R. *Large-scale analysis of the yeast proteome by multidimensional protein identification technology*. Nat. Biotechnol. 2001, ***19***, 242-247.

[23] Wolters, D. A.; Washburn, M. P.; Yates, J. R. *An Automated Multidimensional Protein Identification Technology for Shotgun Proteomics*. Anal. Chem. 2001, ***73***, 5683-5690.

[24] McDonald, W. H.; Ohi, R.; Miyamoto, D. T.; Mitchison, T. J.; Yates, J. R. *Comparison of three directly coupled HPLC MS/MS strategies for identification of proteins from complex mixtures: single-dimension LC-MS/MS, 2-phase MudPIT, and 3-phase MudPIT*. Int. J. Mass Spectrom. 2002, ***219***, 245-251.

[25] Motoyama, A.; Xu, T.; Ruse, C. I.; Wohlschlegel, J. A.; Yates, J. R. *Anion and Cation Mixed-Bed Ion Exchange for Enhanced Multidimensional Separations of Peptides and Phosphopeptides*. Anal. Chem. 2007, ***79***, 3623-3634.

[26] Stoll, D. R.; Li, X. P.; Wang, X. O.; Carr, P. W.; Porter, S. E. G.; Rutan, S. C. *Fast, comprehensive two-dimensional liquid chromatography*. J. Chromatogr. A 2007, ***1168***, 3-43.

[27] Marriott, P. J.; Schoenmakers, P.; Wu, Z. Y. *Nomenclature and Conventions in Comprehensive Multidimensional Chromatography - An Update*. LC GC Eur. 2012, ***25***, 266-275.

[28] Carr, P. W.; Davis, J. M.; Rutan, S. C.; Stoll, D. R. In *Advances in Chromatography, Vol. 50*; Grushka, E.; Grinberg, N., Editors; CRC Press - Taylor & Francis Group: London, UK, 2012; pp. 139-235.

[29] Edwards, M.; Mostafa, A.; Gorecki, T. *Modulation in comprehensive two-dimensional gas chromatography: 20 years of innovation*. Anal. Bioanal. Chem. 2011, ***401***, 2335-2349.

[30] Marriott, P. J.; Chin, S. T.; Maikhunthod, B.; Schmarr, H. G.; Bieri, S. *Multidimensional gas chromatography*. Trends Anal. Chem. 2012, ***34***, 1-21.

[31] Murray, J. A. *Qualitative and quantitative approaches in comprehensive two-dimensional gas chromatography*. J. Chromatogr. A 2012, ***1261***, 58-68.

[32] Seeley, J. V. *Recent advances in flow-controlled multidimensional gas chromatography*. J. Chromatogr. A 2012, ***1255***, 24-37.

[33] Dugo, P.; Cacciola, F.; Kumm, T.; Dugo, G.; Mondello, L. *Comprehensive multidimensional liquid chromatography: Theory and applications*. J. Chromatogr. A 2008, ***1184***, 353-368.

[34] Francois, I.; Sandra, K.; Sandra, P. *Comprehensive liquid chromatography: Fundamental aspects and practical considerations-A review*. Anal. Chim. Acta 2009, ***641***, 14-31.

[35] Guiochon, G.; Marchetti, N.; Mriziq, K.; Shalliker, R. A. *Implementations of two-dimensional liquid chromatography*. J. Chromatogr. A 2008, ***1189***, 109-168.

[36] Stoll, D. R. *Recent progress in online, comprehensive two-dimensional high-performance liquid chromatography for non-proteomic applications*. Anal. Bioanal. Chem. 2010, ***397***, 979-986.

[37] Jandera, P. *Comprehensive two-dimensional liquid chromatography - practical impacts of theoretical considerations. A review*. Cent. Eur. J. Chem 2012, ***10***, 844-875.

[38] Francois, I.; Sandra, P.; Sciarrone, D.; Mondello, L. In *Comprehensive Chromatography in Combination with Mass Spectrometry*; Mondello, L., Editor; Wiley Series on Mass Spectrometry; Wiley: Hoboken, NJ, USA, 2011; pp. 429-448.

[39] Erni, F.; Frei, R. W. *TWO-DIMENSIONAL COLUMN LIQUID-CHROMATOGRAPHIC TECHNIQUE FOR RESOLUTION OF COMPLEX-MIXTURES*. J. Chromatogr. 1978, ***149***, 561-569.

[40] Liu, Z. Y.; Phillips, J. B. *Comprehensive Two-Dimensional Gas Chromatography using an On-Column Thermal Modulator Interface*. J. Chromatogr. Sci. 1991, ***29***, 227-231.

[41] Francois, I.; Sandra, K.; Sandra, P. In *Comprehensive Chromatography in Combination with Mass Spectrometry*; Mondello, L., Editor; Wiley Series on Mass Spectrometry; Wiley: Hoboken, NJ, USA, 2011; pp. 281-330.

[42] Grall, A.; Leonard, C.; Sacks, R. *Peak Capacity, Peak-Capacity Production Rate, and Boiling Point Resolution for Temperature-Programmed GC with Very High Programming Rates*. Anal. Chem. 2000, ***72***, 591-598.

[43] Marriott, P. J.; Kinghorn, R. M. *Longitudinally Modulated Cryogenic System. A Generally Applicable Approach to Solute Trapping and Mobilization in Gas Chromatography*. Anal. Chem. 1997, ***69***, 2582-2588.

[44] Ledford, E. B.; Billesbach, C. *Jet-Cooled Thermal Modulator for Comprehensive Multidimensional Gas Chromatography*. J. High Resolut. Chromatogr. 2000, ***23***, 202-204.

[45] Beens, J.; Adahchour, M.; Vreuls, R. J. J.; van Altena, K.; Brinkman, U. A. T. *Simple, non-moving modulation interface for comprehensive two-dimensional gas chromatography*. J. Chromatogr. A 2001, ***919***, 127-132.

[46] Harynuk, J.; Gorecki, T. *New liquid nitrogen cryogenic modulator for comprehensive two-dimensional gas chromatography*. J. Chromatogr. A 2003, ***1019***, 53-63.

[47] Grob, R. L. In *Modern Practice of Gas Chromatography*, 4th edition; Grob, R. L.; Barry, E. F., Editors; John Wiley & Sons: Hoboken, NJ, USA, 2004; pp. 25-64.

[48] Snyder, L. R.; Kirkland, J. J.; Dolan, J. W. *Introduction to Modern Liquid Chromatography*. 3rd edition; John Wiley & Sons: Hoboken, NJ, USA, 2010.

[49] Delahunty, C. M.; Yates, J. R. *MudPIT: multidimensional protein identification technology*. Biotechniques 2007, ***43***, 563-569.

[50] Jandera, P. *Programmed elution in comprehensive two-dimensional liquid chromatography*. J. Chromatogr. A 2012, ***1255***, 112-129.

[51] Guiochon, G. *Comparison of the Theoretical Limits of Separating Speed in Liquid and Gas-Chromatography*. Anal. Chem. 1980, ***52***, 2002-2008.

[52] Giddings, J. C. *Comparison of Theoretical Limit of Separating Speed in Gas and Liquid Chromatography*. Anal. Chem. 1965, ***37***, 60-63.

[53] Kalili, K. M.; de Villiers, A. *Systematic optimisation and evaluation of on-line, off-line and stop-flow comprehensive hydrophilic interaction chromatography x reversed phase liquid chromatographic analysis of procyanidins, Part I: Theoretical considerations*. J. Chromatogr. A 2013, ***1289***, 58-68.

[54] Majors, R. E. *Multidimensional and comprehensive liquid chromatography*. LC GC N. Am. 2005, ***23***, 1074-1084.

[55] Wang, X. L.; Barber, W. E.; Carr, P. W. *A practical approach to maximizing peak capacity by using long columns packed with pellicular stationary phases for proteomic research*. J. Chromatogr. A 2006, ***1107***, 139-151.

[56] Dugo, P.; Mondello, L.; Cacciola, F.; Donato, P. In *Comprehensive Chromatography in Combination with Mass Spectrometry*; Mondello, L., Editor; Wiley Series on Mass Spectrometry; Wiley: Hoboken, NJ, USA, 2011; pp. 331-390.

[57] Dugo, P.; Mondello, L.; Cacciola, F.; Donato, P. In *Comprehensive Chromatography in Combination with Mass Spectrometry*; Mondello, L., Editor; Wiley Series on Mass Spectrometry; Wiley: Hoboken, NJ, USA, 2011; pp. 391-427.

[58] Adahchour, M.; Beens, J.; Vreuls, R. J. J.; Brinkman, U. A. T. *Recent developments in comprehensive two-dimensional gas chromatography (GC × GC) I. Introduction and instrumental set-up*. Trends Anal. Chem. 2006, ***25***, 438-454.

[59] Shalliker, R. A.; Gray, M. J. In *Advances in Chromatography, Vol. 44*; Grushka, E.; Grinberg, N., Editors; CRC Press - Taylor & Francis Group: Boca Raton, FL, USA, 2006; pp. 177-236.

[60] Gilar, M.; Fridrich, J.; Schure, M. R.; Jaworski, A. *Comparison of Orthogonality Estimation Methods for the Two-Dimensional Separations of Peptides*. Anal. Chem. 2012, ***84***, 8722-8732.

[61] Giddings, J. C. *Sample dimensionality: a predictor of order-disorder in component peak distribution in multidimensional separation*. J. Chromatogr. A 1995, ***703***, 3-15.

[62] Nowik, W.; Heron, S.; Bonose, M.; Nowik, M.; Tchapla, A. *Assessment of Two-Dimensional Separative Systems Using Nearest-Neighbor Distances Approach. Part 1: Orthogonality Aspects*. Anal. Chem. 2013, ***85***, 9449-9458.

[63] Al Bakain, R.; Rivals, I.; Sassiat, P.; Thiebaut, D.; Hennion, M. C.; Euvrard, G.; Vial, J. *Comparison of different statistical approaches to evaluate the orthogonality of chromatographic separations: Application to reverse phase systems*. J. Chromatogr. A 2011, ***1218***, 2963-2975.

[64] Zeng, Z. D.; Hugel, H. M.; Marriott, P. J. *A Modeling Approach for Orthogonality of Comprehensive Two-Dimensional Separations*. Anal. Chem. 2013, ***85***, 6356-6363.

[65] Dück, R.; Sonderfeld, H.; Schmitz, O. J. *A simple method for the determination of peak distribution in comprehensive two-dimensional liquid chromatography*. J. Chromatogr. A 2012, ***1246***, 69-75.

[66] Snyder, L. R.; Dolan, J. W.; Carr, P. W. *A New Look at the Selectivity of RPC Columns. The hydrophobic subtraction model evaluates the selectivity of HPLC reversed-phased columns so that researchers can choose a suitable substitute or a sufficiently orthogonal second column*. Anal. Chem. 2007, ***79***, 3254-3262.

[67] Layne, J.; Farcas, T.; Rustamov, I.; Ahmed, F. *Volume-load capacity in fast-gradient liquid chromatography - Effect of sample solvent composition and injection volume on chromatographic performance*. J. Chromatogr. A 2001, ***913***, 233-242.

[68] Shalliker, R. A.; Guiochon, G. *Solvent viscosity mismatch between the solute plug and the mobile phase: Considerations in the applications of two-dimensional HPLC*. Analyst 2010, ***135***, 222-229.

[69] Fekete, S.; Kohler, I.; Rudaz, S.; Guillarme, D. *Importance of instrumentation for fast liquid chromatography in pharmaceutical analysis*. J. Pharm. Biomed. Anal. 2014, ***87***, 105-119.

[70] Teutenberg, T. *High-Temperature Liquid Chromatography - A User's Guide for Method Development*. Royal Society of Chemistry: Cambridge, UK, 2010.

[71] Teutenberg, T.; Wiese, S.; Wagner, P.; Gmehling, J. *High-temperature liquid chromatography. Part III: Determination of the static permittivities of pure solvents*

and binary solvent mixtures—Implications for liquid chromatographic separations. J. Chromatogr. A 2009, ***1216***, 8480-8487.

[72] Teutenberg, T.; Wiese, S.; Wagner, P.; Gmehling, J. *High-temperature liquid chromatography. Part II: Determination of the viscosities of binary solvent mixtures—Implications for liquid chromatographic separations*. J. Chromatogr. A 2009, ***1216***, 8470-8479.

[73] Nguyen, D. T. T.; Guillarme, D.; Rudaz, S.; Veuthey, J. L. *Chromatographic behaviour and comparison of column packed with sub-2 µm stationary phases in liquid chromatography*. J. Chromatogr. A 2006, ***1128***, 105-113.

[74] Antia, F. D.; Horvath, C. *HIGH-PERFORMANCE LIQUID-CHROMATOGRAPHY AT ELEVATED-TEMPERATURES - EXAMINATION OF CONDITIONS FOR THE RAPID SEPARATION OF LARGE MOLECULES*. J. Chromatogr. 1988, ***435***, 1-15.

[75] Vanhoenacker, G.; Sandra, P. *High temperature and temperature programmed HPLC: possibilities and limitations*. Anal. Bioanal. Chem. 2008, ***390***, 245-248.

[76] Fanali, C.; Dugo, L.; Dugo, P.; Mondello, L. *Capillary-liquid chromatography (CLC) and nano-LC in food analysis*. Trends Anal. Chem. 2013, ***52***, 226-238.

[77] Gama, M. R.; Collins, C. H.; Bottoli, C. B. G. *Nano-Liquid Chromatography in Pharmaceutical and Biomedical Research*. J. Chromatogr. Sci. 2013, ***51***, 694-703.

[78] Wu, N. J.; Bradley, A. C.; Welch, C. J.; Zhang, L. *Effect of extra-column volume on practical chromatographic parameters of sub-2-µm particle-packed columns in ultra-high pressure liquid chromatography*. J. Sep. Sci. 2012, ***35***, 2018-2025.

[79] Gritti, F.; Guiochon, G. *On the minimization of the band-broadening contributions of a modern, very high pressure liquid chromatograph*. J. Chromatogr. A 2011, ***1218***, 4632-4648.

[80] Fountain, K. J.; Neue, U. D.; Grumbach, E. S.; Diehl, D. M. *Effects of extra-column band spreading, liquid chromatography system operating pressure, and column temperature on the performance of sub-2-mu m porous particles*. J. Chromatogr. A 2009, ***1216***, 5979-5988.

[81] Prüß, A.; Kempter, C.; Gysler, J.; Jira, T. *Extracolumn band broadening in capillary liquid chromatography*. J. Chromatogr. A 2003, ***1016***, 129-141.

[82] Krauss, M.; Singer, H.; Hollender, J. *LC-high resolution MS in environmental analysis: from target screening to the identification of unknowns*. Anal. Bioanal. Chem. 2010, ***397***, 943-951.

Chapter 2 Solvent effects in a heated reversed-phase second dimension

Redrafted and extended from "J. Haun, T. Teutenberg, T. C. Schmidt, Influence of temperature on peak shape and solvent compatibility: Implications for two-dimensional liquid chromatography, Journal of Separation Science, 2012, 35 (14), 1723-1730, DOI: 10.1002/jssc.201101092"

As an extension to the original publication, description, results, and discussion of capillaryLC experiments were added.

Solvent compatibility is a limiting factor for the success of two-dimensional liquid chromatography (2-D LC). In the second dimension, solvent effects can result in overpressures as well as in peak broadening or even distortion. A peak shape study was performed on a one-dimensional high-performance liquid chromatography (HPLC) system to simulate the impact of peak distorting solvent effects on a reversed-phase second dimension separation operated at high temperatures. This study includes changes in injection volume, solute concentration, column inner diameter, eluent composition and oven temperature. Special attention was given to the influence of high temperatures on the solvent effects. High-temperature HPLC (HT-HPLC) is known to enhance second dimension separations in terms of speed, selectivity, and solvent compatibility. The ability to minimize the viscosity contrast between the mobile phases of both dimensions makes HT-HPLC a promising tool to avoid viscosity mismatch effects like (pre-)viscous fingering. In case of our study, viscosity mismatch effects could not be observed. However, our results clearly show that the enhancement in solvent compatibility provided by the application of high temperatures does not include the elimination of solvent strength effects. The additional peak broadening and distortion caused by this effect is a potential error source for data processing in 2-D LC.

2.1 Introduction

2.1.1 Relevance of solvent compatibility in 2-D LC

In two-dimensional liquid chromatography (2-D LC), the sample (or parts of it) is subjected to two independent liquid chromatographic systems in row [1-5]. This combination adds the necessity of a second injection in-between the two separation dimensions. This means that sample originating from the fractionation of the first dimension's eluate is injected to the second dimension. The solvent composition of the sample is dictated by the mobile phase used for the first dimension separation. Moreover, the sample volume is typically significantly larger than a conventional sample load to a high-performance liquid chromatography (HPLC) column operated in one-dimensional mode [6]. Therefore, the practitioner has to keep an eye on the physicochemical properties and the compatibility of both dimensions' mobile phases. Otherwise, the injection of incompatible solvents to the second dimension could induce overpressures due to a higher viscosity of the solvent mixture. Even if there are no significant overpressures, the injection could give rise to several solvent effects that negatively affect the retention behavior of analytes [6], resulting in peak broadening and even distortion.

2.1.2 Main consequences of peak broadening/distortions in 2-D LC

Peak broadening/distortion can have a huge impact on qualitative and quantitative data processing in one- and two-dimensional liquid chromatography, regardless of the specific technique or mode. First of all, it becomes very difficult to decide where a peak starts and where it ends. The fact that sample composition in 2-D LC is often very complex (hundreds or thousands of compounds) intensifies this problem because distorted peaks overlap with a higher probability. Especially in cases where no mass spectrometric detector is available, peak splitting in terms of two peak maxima will lead to the assumption that there are two or even more co-eluting substances. In comprehensive 2-D LC, peak distortions may have an even larger impact on data processing compared to heart-cut techniques due to the third dimension of the peaks. Up to now it is difficult to choose a mathematical model for a correct qualitative and quantitative interpretation of comprehensive 2-D LC data [7]. Gaussian peak shapes are often assumed for both dimensions. Moreover, peak broadening/distortion will reduce peak capacity [8-9] and could even entail a prolongation of the runtime in the second dimension.

2.1.3 Most prominent peak distorting solvent effects

Unfortunately, the way to an optimum of orthogonality between the two separation systems often leads to the necessity to combine two solvent systems of typically different nature. A well-known example is the combination of normal- and reversed-phase chromatography yielding a very high degree of orthogonality in theory [1]. In this case, solvent immiscibility is reported to severely limit the success of such 2-D LC combinations [10]. However, if the use of water-immiscible solvents can be avoided and common reversed-phase solvents are used, the miscibility of all solvents is given, except for a miscibility gap of the system water/tetrahydrofuran between 70 and 140 °C [11].

Besides immiscibility effects, solvation effects can occur if certain analytes do not remain soluble in one of the solvent systems [12]. Furthermore, it is known since the first applications of 2-D LC [13] that solvent strength effects can have a severe impact on peak shape. Too strong solvents transferred from the first dimension can disturb the band focusing abilities of the second dimension column and entail peak broadening or breakthrough of the solutes [14-15].

2.1.4 Effects caused by viscosity mismatch

Peak distorting effects arising from viscosity differences are often overlooked as highlighted recently by Shalliker and Guiochon [6]. Unavoidable bed heterogeneity and wall effects are assumed to additionally promote the destabilization of the interface between two solvents of sufficiently different viscosities inside the HPLC column. For high viscosity discrepancies, this destabilization can result in the formation of solvent fingers of the less viscous solvent penetrating the preceding more viscous solvent (viscous fingering, VF). This effect was first observed by Hill in 1952 [16] and named by Saffman and Taylor in 1958 [17]. In general, the peak distorting effects due to viscous fingering are most severe for those solutes travelling the longest time in the influence of the sample solvent plug. For most applications and reversed-phase solvents, these are the solutes eluting at or near the dead time.

The formation of fingers, however, is not a necessity. It is reported that even relatively low viscosity differences can give rise to interface instabilities (pre-VF) that result in peak distortion [18]. Mayfield et al. observed viscosity mismatch effects even for the combination of the two often used solvent systems water/acetonitrile and water/methanol [19].

2.1.5 Strategies to avoid solvent effects

In the following, "solvent effects" is used as a collective term for the solvent effects mentioned in Sections 2.1.3 and 2.1.4 that entail additional peak broadening or distortion. In order to bypass the problems that can arise due to the combination of two different solvents, several reports [6, 20-22] advice to evaporate the first dimension solvent prior to the second dimension, but most of these techniques are time-consuming. Tian et al. [20-21] even developed a special on-line vacuum evaporation interface as a tool to combine normal-phase with reversed-phase chromatography, in which the sample solvent is evaporated by high temperatures and vacuum. The main disadvantage of this interface is a poor recovery of the analytes, which is below 60% even for nonvolatile compounds [3].

Another strategy to minimize solvent effects in 2-D LC is the dilution of the sample which is transferred to the second dimension. Several authors [23-27] used an additional pump to add a dilution solvent via a T-fitting to the eluate of the first dimension prior to second dimension analysis. An alternate dilution method is to create a sufficiently large difference in column diameters of the first dimension compared to the second dimension. For example, Dugo et al. [10] successfully avoided immiscibility effects for a comprehensive normal-/ reversed-phase method by the application of a microbore column and low flow rates in the first dimension. However, all dilution methods work on the expense of sensitivity.

Shalliker and Guiochon [6] recommend five criteria to be adopted to minimize viscosity mismatch effects in two-dimensional HPLC. Besides the minimization of the solvents' viscosity contrast – the most straightforward method – the reduction of the sample volume transferred to the second dimension is the most promising rule [6] because dispersion is a limiting factor for viscosity contrast effects [28]. Other criteria – like "the less viscous solvent should be used in the first dimension" or "viscosity contrast should be maintained such that it never changes sign" [6] – are not that easy to adopt.

2.1.6 High-temperature HPLC

A known way to minimize the viscosity contrast of solvent mixtures is the application of high-temperature HPLC (HT-HPLC) [29]. The advantages and disadvantages of this technique have been comprehensively reviewed by Teutenberg [11]. By using high temperatures (above 60 °C and below the critical point), the practitioner can exert influence on certain physicochemical properties of the mobile phase. For example, solvent viscosities, viscosity maxima of binary solvent mixtures and viscosity differences between different solvents are reduced with increasing temperature [29]. Moreover, the static permittivity of

water and its solvent mixtures is lowered and the elution strength of these mixtures is increased with increasing temperature [30]. HT-HPLC was already applied by Stoll et al. mainly to enhance the speed of second dimension separations in 2-D LC [1, 31-33]. To date, however, little is known about the influence of the column temperature on the solvent effects that could occur in 2-D LC.

2.1.7 Goals

In this work, a peak shape study was carried out in order to study solvent effects occurring in a reversed-phase second dimension column operated at high temperatures. The experimental conditions reflect a typical critical situation in which a first dimension gradient is close to its end (high organic content) and the second dimension gradient is at its beginning (low organic content). The solvent systems water–methanol (first dimension) and water–acetonitrile (second dimension) are miscible in any proportion. HT-HPLC was applied as an approach to minimize the viscosity contrast between these solvent mixtures. Comparably low sample volumes were selected to keep solvent strength effects low. The main goal was to find out which solvent effects occur under the chosen conditions with special attention on the influence of the column temperature. Additionally, the experiments were adapted to a capillary LC system. This was done to evaluate whether the same effects occur under the conditions of this upcoming method providing better compatibility to mass spectrometric detectors.

2.2 Material and methods

2.2.1 Liquid chromatographic system

2.2.1.1 General remarks

The high-temperature reversed-phase second dimension separation was simulated by a conventional one-dimensional HPLC system in combination with a high-temperature oven. The autosampler acted as a substitute for the modulation interface.

2.2.1.2 High-temperature HPLC system

Conventional HPLC experiments were carried out using a modular Shimadzu HPLC system (Duisburg, Germany) consisting of an SCL-10A_{SP} system controller, two LC-10AD_{VP} pumps, a DGU-14 A degassing unit, an SIL-10AD_{VP} auto injector and an SPD-10A_{VP} diode array detector. Data were processed using the LCsolution software package (version 1.21 SP1, Shimadzu Corporation, Kyoto, Japan) and a conventional IBM-type personal computer. A

commercially available SIM HT-HPLC 200 block-heating column oven (SIM – Scientific Instruments Manufacturer, Oberhausen, Germany) was used to establish the desired high-temperature conditions for the stationary and mobile phase. The eluent was preheated 5 °C above the respective column temperature and cooled behind the column to 60 °C. Two interchangeable zirconia-based reversed-phase columns of the type ZirChrom-PBD (ZirChrom Separations Inc., Anoka, MN, USA) were used as stationary phase. Both 150 mm columns packed with 3 µm particles differed only in inner diameter of 2.1 and 3 mm. A 500 psi back-pressure regulator (Upchurch Scientific, IDEX Health & Science, Oak Harbor, WA, USA) was connected to the outlet of the diode array detector to avoid a phase transition of the eluent in the low-pressure region of the heated system. The detection unit was set to measure ultraviolet (UV) absorption at 254 nm. Flow rate was adjusted to 0.5 mL min^{-1} for all experiments.

2.2.1.3 The capillaryLC system

For the capillaryLC experiments, one of the two binary pumps of a NanoLC-Ultra 2D pump system (Eksigent Technologies (AB Sciex), Dublin, CA, USA) was used. Samples were injected by time-controlled valve switching at 1 µL min^{-1} injection flow rate using an HTS PAL autosampler (CTC Analytics AG, Zwingen, Switzerland). A capillaryLC column (0.3 x 100 mm) was packed by G&T Septech AS (Trollåsen, Norway) with 3 µm ZirChrom-PBD material to ensure comparability to the columns of the HT-HPLC experiments. The air-based column oven, part of the aforementioned Eksigent NanoLC-Ultra 2D pump system, was set to 60 °C for all measurements. A fixed-wavelength detector (UV Detector 200, Wissenschaftliche Gerätebau Dr. Ing. Herbert Knauer GmbH, Berlin, Germany) fit up with a 75 µm i.d. capillary flow cell (SunChrom Wissenschaftliche Geräte GmbH, Friedrichsdorf, Germany) with a volume of 44 nL delivered UV absorption data measured at a wavelength of 254 nm. Flow rate was adjusted to 10 µL min^{-1}.

2.2.1.4 Column choice

ZirChrom-PBD stationary phase material was selected because of its known high thermal stability (up to 150 °C) [34] and because of its unique selectivity compared to other reversed-phase materials [35], making it an interesting option for the combination of two reversed-phase dimensions. We decided to use these comparably long columns to keep the results of the study compatible to heart cutting and/or offline 2-D LC techniques. Columns used in online comprehensive 2-D LC are usually much shorter. However, peak distorting solvent effects generally depend on the sample volume to column volume ratio. Therefore, solvent

effects that are observed on long columns will very likely occur on shorter columns with increased severity.

2.2.2 Chemicals

2.2.2.1 Solvents used in high-temperature HPLC

Ultrapure water was produced using an Elix-10/Milli-Q Plus combination (Millipore GmbH, Schwalbach, Germany). Both, methanol and acetonitrile were Optigrade – HPLC gradient grade purchased from Promochem (LGC Standards GmbH, Wesel, Germany).

2.2.2.2 Solvents used in elevated temperature capillaryLC

ULC/MS grade water was received from Biosolve b. v. (Valkenswaard, the Netherlands). Acetonitrile and methanol were Optigrade for LC/MS (Promochem, LGC Standards GmbH, Wesel, Germany). All capillaryLC eluents were acidified by adding 0.1% formic acid by volume (puriss. p.a., ~ 98%, Sigma-Aldrich Corporation, Schnelldorf, Germany) in order to prevent capillary clogging.

2.2.2.3 Solvent effect test mix (SE-mix)

For all solvent effect experiments, a test mix and its dilutions composed of uracil, 19-nortestosterone and epitestosterone (all three purchased from Sigma-Aldrich Corporation, Schnelldorf, Germany) dissolved in water/methanol 20:80 (v/v) were used. The solutes' purities were ≥ 99.0% (puriss., HPCE), ≥ 99.0% (puriss., HPLC) and ≥ 98.0% (HPLC), respectively. Mass concentrations and absolute masses of the three solutes in the injected test mixtures are listed in Table 2-1 and Table 2-2. All samples were filtered through a 0.45 µm membrane filter before usage in capillaryLC.

Table 2-1. Mass concentrations and absolute masses of the solutes in the high-temperature HPLC solvent effect test mixes.

			Uracil	19-Nortestosterone	Epitestosterone
Standard solution	Mass conc. in µg mL^{-1}		100	200	200
	Abs. mass in µg	*1 µL sample*	0.1	0.2	0.2
1:10 dilution	Mass conc. in µg mL^{-1}		10	20	20
	Abs. mass in µg	*1 µL sample*	0.01	0.02	0.02
		10 µL sample	0.1	0.2	0.2

Table 2-2. Mass concentrations and absolute masses of the solutes in the capillaryLC solvent effect test mixes.

			Uracil	19-Nortestosterone	Epitestosterone
Standard solution	Mass conc. in µg mL^{-1}		100	200	200
	Abs. mass in ng	*50 nL sample*	5	10	10
1:5 dilution	Mass conc. in µg mL^{-1}		20	40	40
	Abs. mass in ng	*250 nL sample*	5	10	10

2.2.2.4 Column stability test mix

Column stability was monitored by applying a test mixture containing naphthalene, acenaphthene (≥ 99.0% (puriss., GC) and ≥ 99.0% (purum, HPLC), Sigma-Aldrich Corporation, Schnelldorf, Germany) and uracil.

2.2.3 Test procedures

All measurements which are described in the following were repeated at least three times to ensure that the observed effects could be reproduced. Moreover, additional replicates of the experiments were acquired by a second operator at a different time to confirm the results. Column stability was monitored by the described test mix under isocratic conditions at 30 °C in order to rule out a significant influence of the column quality on peak shape. Although a certain loss of the plate numbers was measured over the whole time of experimental work, all peak shape parameters of the test solutes were constant.

2.2.3.1 Basic experiments (HT-HPLC)

One microliter of the undiluted SE-mix (Table 2-1) was subjected to an HPLC separation using pure water as mobile phase and the 2.1 × 150 mm ZirChrom-PBD column as stationary phase. The column temperature was set to 90 °C (isothermal) to allow the elution of the two non-polar steroids. Moreover, 10 µL of a 1:10 dilution of the SE-mix were measured to observe peak shape changes due to increased sample volume at constant absolute solute masses compared to the first injection. Furthermore, only 1 µL of the 1:10 dilution was analyzed the same way in order to evaluate possible mass overload effects of the first injection.

2.2.3.2 Mobile phase experiments (HT-HPLC)

In a first set of comparative experiments, in the following called mobile phase experiments, the influence of an addition of acetonitrile as an organic modifier to the mobile phase was investigated for all three SE-mix injections by increasing the modifier ratio in steps

of 5-20% in separate isocratic runs. The same experiments – extended by additional runs with an organic modifier ratio of 25% – were later repeated using methanol instead of acetonitrile to study the differences.

2.2.3.3 Temperature experiments (HT-HPLC)

During a second set of comparative experiments, later named temperature experiments, the isothermal column temperature was changed in consecutive runs to 120, 130, 140, 150 and 160 °C, respectively. All other parameters were chosen corresponding to the basic experiments (refer to Section 2.2.3.1).

2.2.3.4 Column diameter comparison (HT-HPLC)

Additionally, the three basic experiments were repeated using a 3.0 × 150 mm column instead of the 2.1 × 150 mm column in order to investigate the influence of the column inner diameter on the observed effects. In this case, the column temperature was set to 120 °C to avoid too long retention times of the steroid solutes.

2.2.3.5 CapillaryLC methods

The methods of the mobile phase experiments with acetonitrile described in Section 2.2.3.2 were transferred to capillaryLC. Because of limitations by the polymeric material used for parts of the column hardware and capillary sleeves, high-temperature conditions were not established to prevent the equipment from damage. However, in case of the smaller 0.3 x 100 mm column, the steroid solutes eluted already at 60 °C using water as the mobile phase. Thus, it was not necessary to use higher temperatures. The injection volumes had to be adjusted to the smaller column dimensions. Therefore, 50 nL of the undiluted SE-mix and 250 nL of a 1:5 dilution of the SE-mix were applied to the system, respectively, to reach the desired parity of the solutes' absolute masses (see Table 2-2).

2.3 Results and discussion

2.3.1 Mobile phase experiments (HT-HPLC)

At first, the changes of peak shape for the three SE-mix solutes over the set of mobile phase experiments described in Section 2.2.3.2 compared to the basic measurements (refer to Section 2.2.3.1) shall be discussed. In this respect and starting with acetonitrile as additive to the mobile phase, Figure 2-1 shows overlays for each solute at two different injection volumes separately, but at constant absolute masses of the solutes.

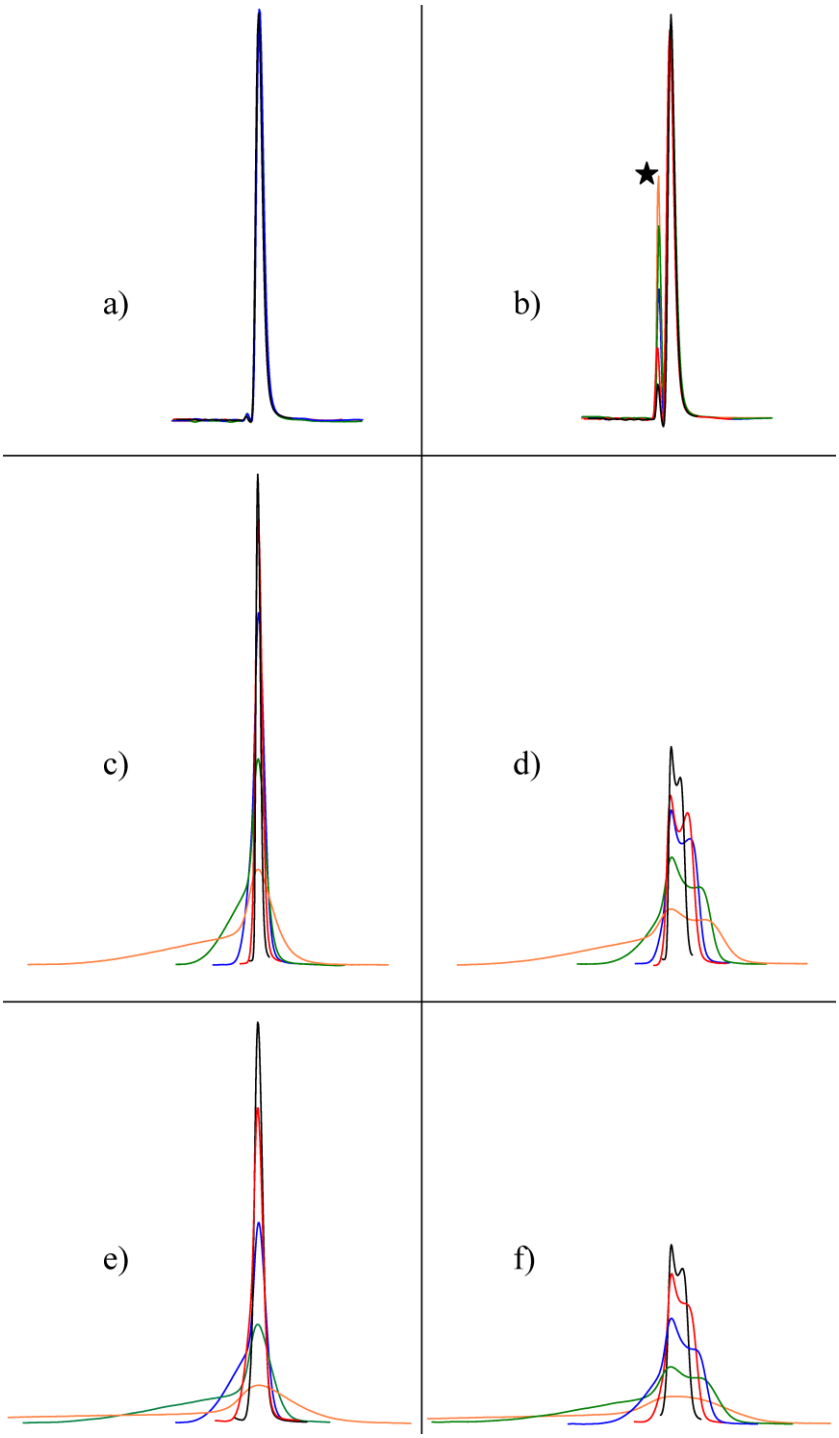

Figure 2-1. Impact of a change in % B on peak shapes of uracil (a and b), 19-nortestosterone (c and d) and epitestosterone (e and f) for two injection volumes (a, c, and e: 1 µL and b, d, and f: 10 µL). Absolute mass of each solute is constant. Chromatographic conditions: stationary phase: 2.1 × 150 mm ZirChrom-PBD, 3 µm particles; mobile phase composition (water/acetonitrile (v/v)) is given by the color code: orange - 100:0, green - 95:5, blue - 90:10, red - 85:15 and black - 80:20; isocratic mode at 0.5 mL min^{-1}; temperature: isothermal at 90 °C; sample solvent: water/methanol 20:80 (v/v); detection: UV at 254 nm. Black star: peak by sample solvent. Area-normalized overlay view. For a better visualization, the fronting of the orange peaks is cut to size.

Although this type of illustration perfectly suits to monitor the peak shape changes, it may give the misleading impression that the peaks of each overlay never differ in retention. Therefore, the original chromatogram view is added as SI-Figure 2-1. In Table 2-3, tailing factors are given only for the 1 µL injections because of the strong distortions in case of the 10 µL injections.

Table 2-3. Tailing factors at 5% height for the peaks presented in the left column of Figure 2-1 (1 µL injections).

Mobile phase H_2O/ACN (v/v)	Tailing factor (uracil)	Tailing factor (19-nortestosterone)	Tailing factor (epitestosterone)
100:0	1.62	0.66	0.61
95:5	1.64	0.70	0.62
90:10	1.65	0.93	0.69
85:15	1.64	1.29	0.89
80:20	1.66	1.55	1.19

For the 1 µL injections of the undiluted SE-mix, uracil shows a sharp band with only a slight tailing. As can be seen, peak shape does not change when increasing the acetonitrile concentration in the mobile phase. In contrast to uracil, peak broadening in terms of a remarkably broad fronting is visible for the steroid solutes when the concentration of acetonitrile in the mobile phase (% B) is below 15%. Although the sample volume is very small and dilution in mobile phase at the column head should be fast, the extent to which the peaks are broadened allows the assumption that the solvent strength difference contributes to the peak shape, even at this low sample volume. However, as can be seen in Figure 2-1 and SI-Figure 2-1, the observed peak broadening for 1 µL injections can be overcome by increasing the acetonitrile concentration in the mobile phase (% B), so even a possible contribution of the solvent strength effect is not critical here. The observed peaks approach a sharp and more symmetrical shape at higher % B and peak shoulders disappear.

For 10 µL injections at constant analyte concentrations, overall peak broadening is much more pronounced and accompanied by severe peak splitting for the steroids. As can be seen from Figure 2-1 and SI-Figure 2-1, peaks can lose more than one half of their original height due to the splitting. On first sight, the uracil peak seems also to be split, but the first peak is due to methanol or an impurity in it, because of increasing background absorption at higher acetonitrile concentrations in the mobile phase. This was confirmed by injecting different volumes of the sample solvent (water/methanol 20:80 (v/v)) as blanks. Those results are provided as supporting information (see SI-Figure 2-2). Although the peak widths of the

steroid compounds decrease with higher organic content in the mobile phase (Figure 2-1 and SI-Figure 2-1), it is not possible to overcome the peak splitting in case of the 10 µL injections.

The chromatograms which were obtained by the same experiments with 1 µL of the 1:10 dilution of the SE-mix corresponding to ten times smaller absolute masses for each solute (see SI-Figure 2-3) show very similar peak shapes compared to the 1 µL injection of the undiluted mix (Figure 2-1). Therefore, it can be concluded that peak broadening as shown in Figure 2-1 is no mass overload effect and also no dilution effect.

As described in Section 2.2.3.2, the experiments were repeated using methanol instead of acetonitrile as organic modifier (% B) in the mobile phase (see SI-Figure 2-4, SI-Figure 2-5 and SI-Table 2-1). The results for methanol differ in one important point: The type of the steroids' peak broadening changes from fronting (acetonitrile) to tailing (methanol). Therefore, the choice of the organic solvent in the mobile phase seems to have an influence on the retention mechanism. The main observations are, however, the same as for acetonitrile: For 1 µL injections of the undiluted SE-mix, a trend to sharp and more symmetrical peak shapes is visible for increasing % B in the mobile phase. In comparison to an addition of acetonitrile to the mobile phase, the addition of the same volume of methanol results in slightly worse peak shapes. This can be explained by the higher solvent strength of acetonitrile which reduces the solvent strength mismatch to a larger extent and also forces a faster elution. The additional peak broadening resulting from the higher injection volume (10 µL injections) cannot be overcome by the increase of organic modifier in the mobile phase. So, the solvent strength effect may not be avoided by using the same solvents for both mobile phases in 2-D LC if there is still a sufficient difference in solvent strength between the mixtures.

The results presented in Figure 2-1 and SI-Figure 2-4 comply with findings of Layne et al. who showed data on the effects of sample solvent composition and injection volume in fast gradient one-dimensional HPLC [36]. Although their measurement conditions differed in important points (gradient elution, acetonitrile as sample solvent, silica-based C18 column, ambient temperature, etc.), Layne et al. observed a similar relationship between the 1 and 10 µL sample volumes if a high solvent strength mobile phase is injected: The excessive band broadening due to bad band focusing at the column head. Comparing our results to those of Layne et al. [36], one can also deduce that a fast gradient elution instead of the isocratic elution would at most overcome the excess in band broadening for late eluting compounds.

Besides the solvent strength effect, no further peak distorting effects are visible in our results of the solvent experiments. The fact that peak broadening is larger for compounds eluting at long retention times indicates that the viscosity difference has no significant effect on the peak shape. The authors suppose that the used sample volumes are too small to cause a viscosity mismatch effect. This also complies with findings obtained by Layne et al. [36], who changed the viscosity by the addition of PEG-600.

Our presented results also comply with those of Jandera et al. [15] who focused a study on solvent effects and the use of short core-shell stationary phases in combination with fast gradient elution in comprehensive 2-D LC. Like Layne et al. [36], these authors [15] found a predominant solvent strength effect at temperatures used in conventional HPLC.

2.3.2 Temperature experiments (HT-HPLC)

In Figure 2-2, the results of the temperature experiments are presented (see Section 2.2.3.3). Again, SI-Figure 2-6 provides an alternative chromatogram view on the changes of the peak shapes. In Table 2-4, tailing factors for all peaks of the 1 µL injections are given.

Table 2-4. Tailing factors at 5% height for the peaks presented in the left column of Figure 2-2 (1 µL injections).

Temperature in °C	Tailing factor (uracil)	Tailing factor (19-nortestosterone)	Tailing factor (epitestosterone)
120	1.56	0.64	0.60
130	1.58	0.69	0.62
140	1.55	0.78	0.65
150	1.52	0.89	0.72
160	1.44	1.03	0.80

On first sight, the increase of the isothermal column temperature tends to result in the same peak shape effects compared to those of the increasing organic modifier concentration. For 1 µL injections of the undiluted SE-mix, peaks become sharper and more symmetrical as the temperature is increased. This behavior can be explained by the increasing elution strength of water at higher temperature [30]. The additional peak broadening/splitting originating from the ten times higher injection volume can also not be overcome by increasing the column temperature. In contrast to the mobile phase experiments, the methanol peak measured shortly before the uracil peak (black star, Figure 2-2) remains visible (compare to Figure 2-1). This can be explained by the facts that the temperature is held constant for the detection (60 °C) and that the mobile phase composition does not change.

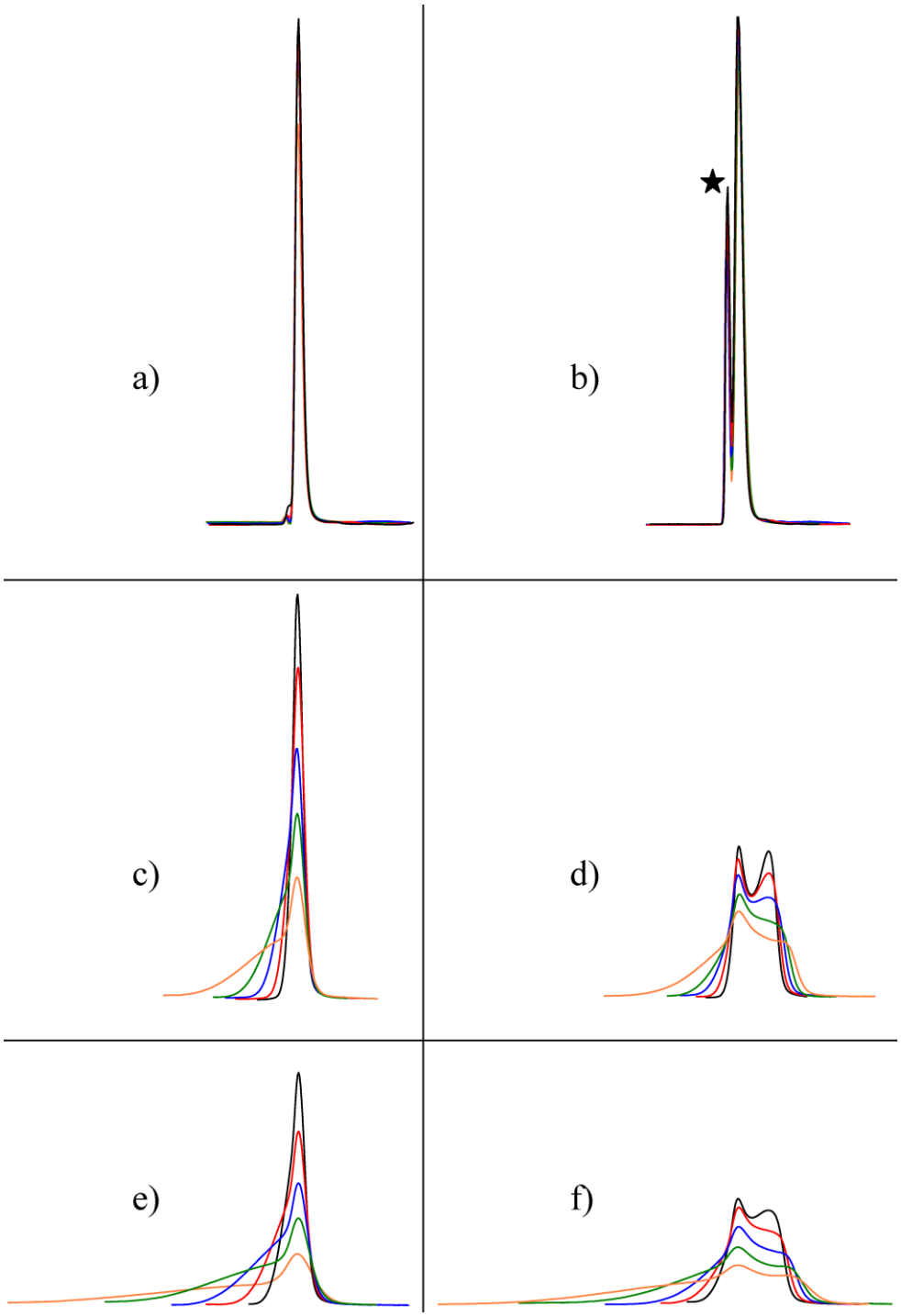

Figure 2-2. Impact of a change in column temperature on peak shapes of uracil (a and b), 19-nortestosterone (c and d) and epitestosterone (e and f) for two injection volumes (a, c, and e: 1 µL and b, d, and f: 10 µL). Absolute mass of each solute is constant. Chromatographic conditions: stationary phase: 2.1 × 150 mm ZirChrom-PBD, 3 µm particles; mobile phase: water; isocratic mode at 0.5 mL min^{-1}; temperature mode: isothermal; column temperature (°C) is given by the color code: orange - 120, green - 130, blue - 140, red - 150 and black - 160; sample solvent: water/methanol 20:80 (v/v); detection: UV at 254 nm. Black star: peak by sample solvent. Area-normalized overlay view. For a better visualization, the fronting of the orange peaks is cut to size.

The additional monitoring of the injections of 1 µL of the 1:10 diluted SE-mix during the temperature experiments proves again that the peak shapes are not influenced by mass overload effects (see SI-Figure 2-7).

The peak broadening and splitting observed for the HT-HPLC experiments might lead to the assumption that stationary phase degradation has caused a dead volume at the top of the column. However, column test chromatograms before and after the experiments, as well as the 1 µL injections prove that Gaussian peak shapes are still obtained. This would not be observed if there was a dead volume.

As can be seen in Figure 2-2, peaks become more symmetrical as the temperature is increased. An opposite behavior would have been expected if mobile phase preheating had been insufficient [37-38]. Therefore, insufficient mobile phase preheating can be excluded as a reason for any peak distortions.

2.3.3 Column diameter comparison (HT-HPLC)

As described in Section 2.2.3.4, the experiments were carried out on a column of the same type, but with an inner diameter of 3.0 mm instead of 2.1 mm. The results for two injections with equal absolute solute masses are presented in Figure 2-3.

By using the 3.0 mm inner diameter column, the peak broadening can be reduced drastically. Unlike the results presented in Figure 2-1 and Figure 2-2, no pronounced fronting is observed for the steroid solutes at 1 µL sample volume. For 10 µL sample volume, the expected additional peak broadening originating from increased volume load turned out to be very small. Only a slight fronting is observed for the steroids.

Sample volume can be described as a percentage of the effective column volume. A sample volume below an approximate limit of 1% of the effective column volume is considered to be a good guideline to prevent volume overload effects in one-dimensional HPLC. In Table 2-5, the percentage of the effective column volume taken by the sample is provided for the different sample plugs and columns used for our work. In order to account for the fact that the columns are filled with a porous medium, the cylindrical volume of the stainless steel tube was corrected assuming a total porosity value of 0.7 [39].

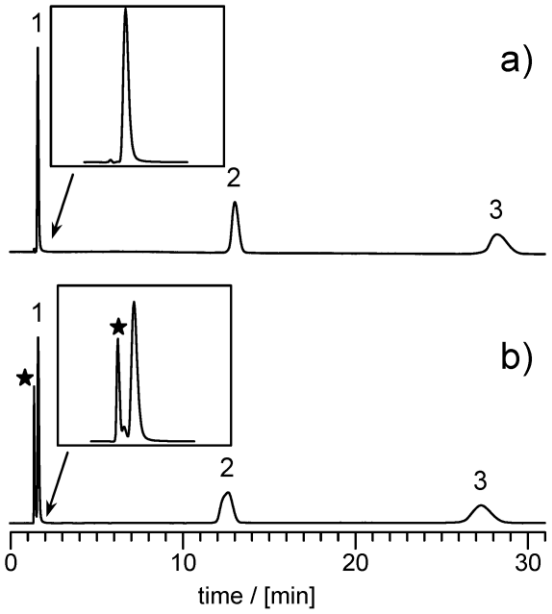

Figure 2-3. Separation of uracil (1), 19-nortestosterone (2) and epitestosterone (3) for two injection volumes: (A) 1 µL and (B) 10 µL. Absolute mass of each solute is constant. Chromatographic conditions: stationary phase: 3 × 150 mm ZirChrom-PBD, 3 µm particles; mobile phase: A: water; isocratic mode at 0.5 mL min^{-1}; temperature: isothermal at 120 °C; sample solvent: water/methanol 20:80 (v/v); detection: UV at 254 nm. Black star: effect by sample solvent.

Table 2-5. Comparison of sample and column volume for defined injection volumes and columns.

Column	Effective column volume	Sample volume	Volume ratio (sample / column)
3.0 x 150 mm	742 µL	1 µL	0.13%
		10 µL	1.35%
2.1 x 150 mm	364 µL	1 µL	0.27%
		10 µL	2.75%

As can be seen from Table 2-5, the sample volume of 10 µL injected onto a 2.1 × 150 mm column significantly exceeds 1% of the effective column volume. In this case, the solvent strength effect is pronounced (compare Figure 2-1 and Figure 2-2). For all injections with a volume of less than 1% of the effective column volume, this effect is not observed.

As can be seen from Table 2-5, an increase in column inner diameter is beneficial if solvent strength effects are considered. Unfortunately, the increase in the inner diameter of the second dimension column results in an additional dilution of the solutes that raises the limits of detection.

2.3.4 CapillaryLC observations

In Figure 2-4, the results of the adapted mobile phase experiments for capillaryLC dimensions are shown.

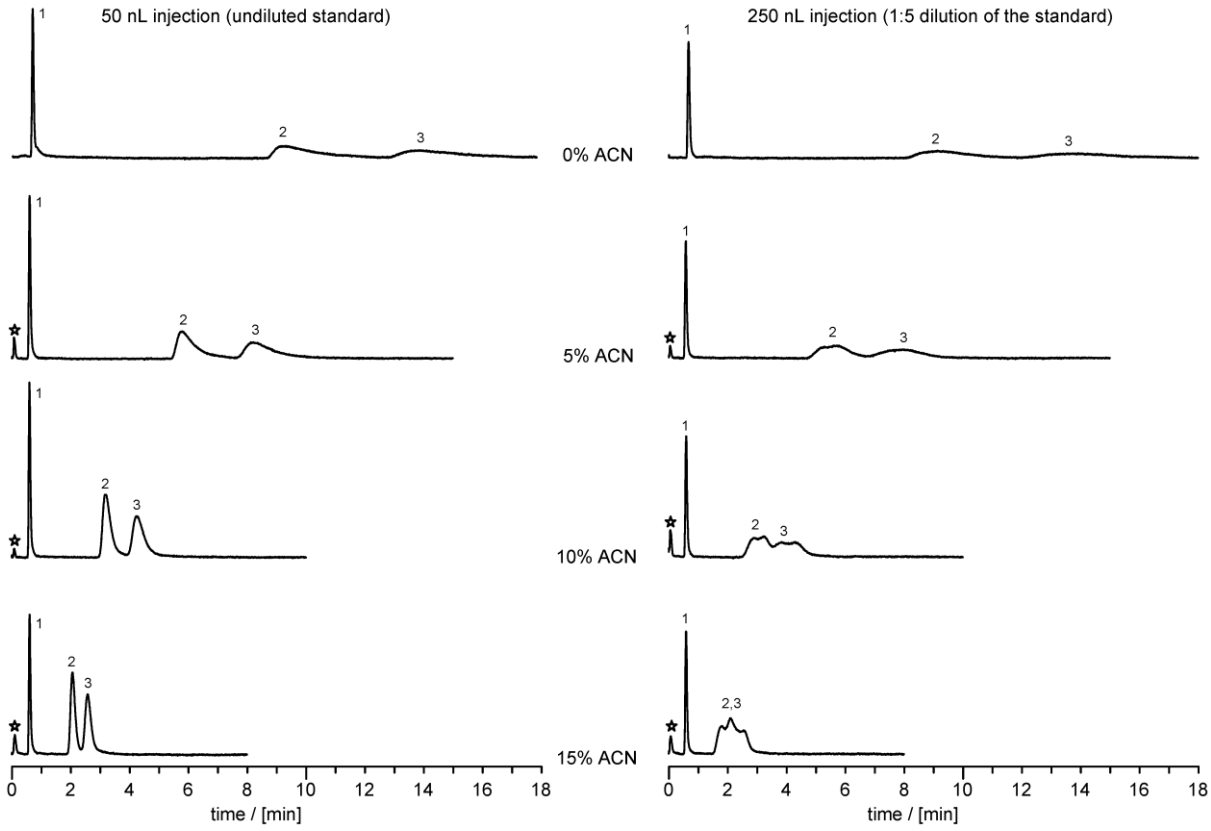

Figure 2-4. Impact of a change in % B on a reversed-phase capillaryLC separation of uracil (1), 19-nortestosterone (2) and epitestosterone (3) for two injection volumes. Absolute mass of each analyte is constant. Chromatographic conditions: stationary phase: 0.3 x 100 mm ZirChrom-PBD, 3 µm particles; mobile phase: A: water, B: acetonitrile (ACN), eluents A and B acidified by 0.1% formic acid; isocratic mode at 10 µL min^{-1}; temperature: isothermal at 60 °C; sample solvent: water/methanol 20:80 (v/v) + 0.1% formic acid; detection: UV at 254 nm.

The corresponding tailing factors for the 50 nL injections can be found in Table 2-6. In Figure 2-4, the peaks marked by stars are irreproducible effects measured before dead-time. A possible explanation is the flow rate (and pressure) change due to the injection at reduced flow rate.

Table 2-6. Tailing factors at five percent height for the peaks in the left column of Figure 2-4 (50 nL injections).

Mobile phase H_2O/ACN (v/v)	Tailing factor (uracil)	Tailing factor (19-nortestosterone)	Tailing factor (epitestosterone)
100:0	1.55	3.03	n.a.
95:5	1.54	2.75	2.20
90:10	1.55	1.95	1.52
85:15	1.55	1.41	1.24

In general, the peak fronting peak shape observed for the steroids when separated on the conventional HPLC system (compare SI-Figure 2-1) is replaced by a tailing for the capillaryLC separation. Among possible reasons are different properties of the packing of the capillaryLC column compared to the conventional diameter columns that were packed by a different manufacturer, as well as the use of formic acid. Moreover, extra-column void volumes within the miniaturized capillary system are known to cause peak broadening in terms of a tailing [40]. However, the relevant main observation is similar: the solvent strength effect caused by a too large injection of sample dissolved in a strong solvent. It leads to additional peak broadening that cannot be overcome by increasing the solvent strength of the mobile phase. From this it follows that solvent strength effects can also occur on miniaturized liquid chromatographic systems as those used for the multidimensional system (Chapter 5).

As the effective column volume was ~4.95 µL assuming a total porosity of 0.7, a 50 nL injection corresponded to ~1% of the column volume and 250 nL to ~5% (compare Table 2-5). Thus, the rule of thumb known from conventional HPLC that only 1% of the effective column volume should be injected seems applicable in capillaryLC as well.

2.4 Concluding remarks

The application of HT-HPLC has become a valuable tool to enhance reversed-phase second dimension separations of two-dimensional LC systems regarding speed, selectivity and solvent compatibility [1, 31-33]. However, our results show that the enhancement in solvent compatibility does not include the elimination of solvent strength effects that occur as well in capillaryLC second dimensions. Peak distortions caused by these solvent strength effects disturb a correct qualitative and quantitative data processing and may prolong runtimes and reduce peak capacities. Thus, it remains of utmost importance to keep the solvent strength of the first dimension mobile phase low if sample volumes produced by the first dimension fractionation cannot be minimized. Therefore, the results underline the recommendation

originally given by Stoll et al. [1] that a slight temperature gradient in the first dimension is a promising tool to reduce the solvent fraction in the eluate transferred to the second dimension. This would lower the elution strength in the second dimension toward a better band focusing. Dilution of the first dimension's eluate is an easy option. However, the practitioner has to keep in mind that a dilution always works at the expense of sensitivity. Furthermore, our results also clearly show that viscosity mismatch effects like (pre-)viscous fingering were not observed under the chosen conditions.

Acknowledgements

The authors would like to thank for financial support from the German Federal Ministry of Economics and Technology within the agenda for the promotion of industrial cooperative research and development (IGF) based on a decision of the German Bundestag. The access was organized by the AiF, Arbeitsgemeinschaft industrieller Forschungsvereinigungen, Cologne, Germany (IGF-Project No. 15928 N).

2.5 References

[1] Stoll, D. R.; Li, X. P.; Wang, X. O.; Carr, P. W.; Porter, S. E. G.; Rutan, S. C. *Fast, comprehensive two-dimensional liquid chromatography*. J. Chromatogr. A 2007, ***1168***, 3-43.

[2] Guiochon, G.; Marchetti, N.; Mriziq, K.; Shalliker, R. A. *Implementations of two-dimensional liquid chromatography*. J. Chromatogr. A 2008, ***1189***, 109-168.

[3] Francois, I.; Sandra, K.; Sandra, P. *Comprehensive liquid chromatography: Fundamental aspects and practical considerations-A review*. Anal. Chim. Acta 2009, ***641***, 14-31.

[4] Dugo, P.; Cacciola, F.; Kumm, T.; Dugo, G.; Mondello, L. *Comprehensive multidimensional liquid chromatography: Theory and applications*. J. Chromatogr. A 2008, ***1184***, 353-368.

[5] Shalliker, R. A.; Gray, M. J. In *Advances in Chromatography, Vol. 44*; Grushka, E.; Grinberg, N., Editors; CRC Press - Taylor & Francis Group: Boca Raton, FL, USA, 2006; pp. 177-236.

[6] Shalliker, R. A.; Guiochon, G. *Solvent viscosity mismatch between the solute plug and the mobile phase: Considerations in the applications of two-dimensional HPLC*. Analyst 2010, ***135***, 222-229.

[7] Thekkudan, D. F.; Rutan, S. C.; Carr, P. W. *A study of the precision and accuracy of peak quantification in comprehensive two-dimensional liquid chromatography in time*. J. Chromatogr. A 2010, ***1217***, 4313-4327.

[8] Neue, U. D.; Mazzeo, J. R. *A theoretical study of the optimization of gradients at elevated temperature*. J. Sep. Sci. 2001, ***24***, 921-929.

[9] Neue, U. D. *Theory of peak capacity in gradient elution*. J. Chromatogr. A 2005, ***1079***, 153-161.

[10] Dugo, P.; Favoino, O.; Luppino, R.; Dugo, G.; Mondello, L. *Comprehensive Two-Dimensional Normal-Phase (Adsorption) - Reversed-Phase Liquid Chromatography*. Anal. Chem. 2004, ***76***, 2525-2530.

[11] Teutenberg, T. *High-Temperature Liquid Chromatography - A User's Guide for Method Development*. Royal Society of Chemistry: Cambridge, UK, 2010.

[12] Snyder, L. R.; Kirkland, J. J.; Dolan, J. W. *Introduction to Modern Liquid Chromatography*. 3rd edition; John Wiley & Sons: Hoboken, NJ, USA, 2010.

[13] Erni, F.; Frei, R. W. *TWO-DIMENSIONAL COLUMN LIQUID-CHROMATOGRAPHIC TECHNIQUE FOR RESOLUTION OF COMPLEX-MIXTURES*. J. Chromatogr. 1978, ***149***, 561-569.

[14] Hoffman, N. E.; Pan, S. L.; Rustum, A. M. *INJECTION OF ELUITES IN SOLVENTS STRONGER THAN THE MOBILE PHASE IN REVERSED-PHASE LIQUID-CHROMATOGRAPHY*. J. Chromatogr. A 1989, ***465***, 189-200.

[15] Jandera, P.; Hajek, T.; Cesla, P. *Effects of the gradient profile, sample volume and solvent on the separation in very fast gradients, with special attention to the second-dimension gradient in comprehensive two-dimensional liquid chromatography*. J. Chromatogr. A 2011, ***1218***, 1995-2006.

[16] Hill, S. *CHANNELLING IN PACKED COLUMNS*. Chem. Eng. Sci. 1952, ***1***, 247-253.

[17] Saffman, P. G.; Taylor, G. *THE PENETRATION OF A FLUID INTO A POROUS MEDIUM OR HELE-SHAW CELL CONTAINING A MORE VISCOUS LIQUID*. Proc. R. Soc. London Ser. A 1958, ***245***, 312-329.

[18] Catchpoole, H. J.; Shalliker, R. A.; Dennis, G. R.; Guiochon, G. *Visualising the onset of viscous fingering in chromatography columns*. J. Chromatogr. A 2006, ***1117***, 137-145.

[19] Mayfield, K. J.; Shalliker, R. A.; Catchpoole, H. J.; Sweeney, A. P.; Wong, V.; Guiochon, G. *Viscous fingering induced flow instability in multidimensional liquid chromatography*. J. Chromatogr. A 2005, ***1080***, 124-131.

[20] Tian, H. Z.; Xu, J.; Guan, Y. F. *Comprehensive two-dimensional liquid chromatography (NPLC x RPLC) with vacuum-evaporation interface*. J. Sep. Sci. 2008, ***31***, 1677-1685.

[21] Tian, H. Z.; Xu, J.; Xu, Y.; Guan, Y. F. *Multidimensional liquid chromatography system with an innovative solvent evaporation interface*. J. Chromatogr. A 2006, ***1137***, 42-48.

[22] Freeman, D. H. *Review: Ultraselectivity through Column Switching and Mode Sequencing in Liquid Chromatography*. Anal. Chem. 1981, ***53***, 2-5.

[23] Moore, A. W.; Jorgenson, J. W. *Comprehensive Three-Dimensional Separation of Peptides Using Size Exclusion Chromatography/ Reversed Phase Liquid Chromatography/Optically Gated Capillary Zone Electrophoresis*. Anal. Chem. 1995, ***67***, 3456-3463.

[24] Trathnigg, B.; Rappel, C.; Raml, R.; Gorbunov, A. *Liquid exclusion-adsorption chromatography: a new technique for isocratic separation of non-ionic surfactants - V. Two-dimensional separation of fatty acid polyglycol ethers*. J. Chromatogr. A 2002, ***953***, 89-99.

[25] Veigl, E.; Posch, W.; Lindner, W.; Tritthart, P. *Selective and Sensitive Analysis of 1-Nitropyrene in Diesel Exhaust Particulate Extract by Multidimensional HPLC*. Chromatographia 1994, ***38***, 199-206.

[26] Haefliger, O. P. *Universal Two-Dimensional HPLC Technique for the Chemical Analysis of Complex Surfactant Mixtures*. Anal. Chem. 2003, ***75***, 371-378.

[27] Murahashi, T. *Comprehensive two-dimensional high-performance liquid chromatography for the separation of polycyclic aromatic hydrocarbons*. Analyst 2003, ***128***, 611-615.

[28] Rousseaux, G.; De Wit, A.; Martin, M. *Viscous fingering in packed chromatographic columns: Linear stability analysis*. J. Chromatogr. A 2007, ***1149***, 254-273.

[29] Teutenberg, T.; Wiese, S.; Wagner, P.; Gmehling, J. *High-temperature liquid chromatography. Part II: Determination of the viscosities of binary solvent mixtures—Implications for liquid chromatographic separations*. J. Chromatogr. A 2009, ***1216***, 8470-8479.

[30] Teutenberg, T.; Wiese, S.; Wagner, P.; Gmehling, J. *High-temperature liquid chromatography. Part III: Determination of the static permittivities of pure solvents and binary solvent mixtures—Implications for liquid chromatographic separations*. J. Chromatogr. A 2009, ***1216***, 8480-8487.

[31] Stoll, D. R.; Carr, P. W. *Fast, Comprehensive Two-Dimensional HPLC Separation of Tryptic Peptides Based on High-Temperature HPLC*. J. Am. Chem. Soc. 2005, ***127***, 5034-5035.

[32] Stoll, D. R.; Cohen, J. D.; Carr, P. W. *Fast, comprehensive online two-dimensional high performance liquid chromatography through the use of high temperature ultra-fast gradient elution reversed-phase liquid chromatography*. J. Chromatogr. A 2006, ***1122***, 123-137.

[33] Stoll, D. R.; Wang, X.; Carr, P. W. *Comparison of the Practical Resolving Power of One- and Two-Dimensional High-Performance Liquid Chromatography Analysis of Metabolomic Samples*. Anal. Chem. 2008, ***80***, 268-278.

[34] Teutenberg, T.; Hollebekkers, K.; Wiese, S.; Boergers, A. *Temperature and pH-stability of commercial stationary phases*. J. Sep. Sci. 2009, ***32***, 1262-1274.

[35] Neue, U.; Van Tran, K.; Iraneta, P. C.; Alden, B. A. *Characterization of HPLC packings*. J. Sep. Sci. 2003, ***26***, 174-186.

[36] Layne, J.; Farcas, T.; Rustamov, I.; Ahmed, F. *Volume-load capacity in fast-gradient liquid chromatography - Effect of sample solvent composition and injection volume on chromatographic performance*. J. Chromatogr. A 2001, ***913***, 233-242.

[37] Fields, S. M.; Ye, C. Q.; Zhang, D. D.; Branch, B. R.; Zhang, X. J.; Okafo, N. *Superheated water as eluent in high-temperature high-performance liquid chromatographic separations of steroids on a polymer-coated zirconia column*. J. Chromatogr. A 2001, ***913***, 197-204.

[38] Guillarme, D.; Heinisch, S.; Rocca, J. L. *Effect of temperature in reversed phase liquid chromatography*. J. Chromatogr. A 2004, ***1052***, 39-51.

[39] Meyer, V. R. *Practical High-Performance Liquid Chromatography*. 5th edition; John Wiley & Sons: Chichester, UK, 2010.

[40] Gritti, F.; Guiochon, G. *Kinetic performance of narrow-bore columns on a micro-system for high performance liquid chromatography*. J. Chromatogr. A 2012, ***1236***, 105-114.

2.6 Chapter appendix

2.6.1 Figures

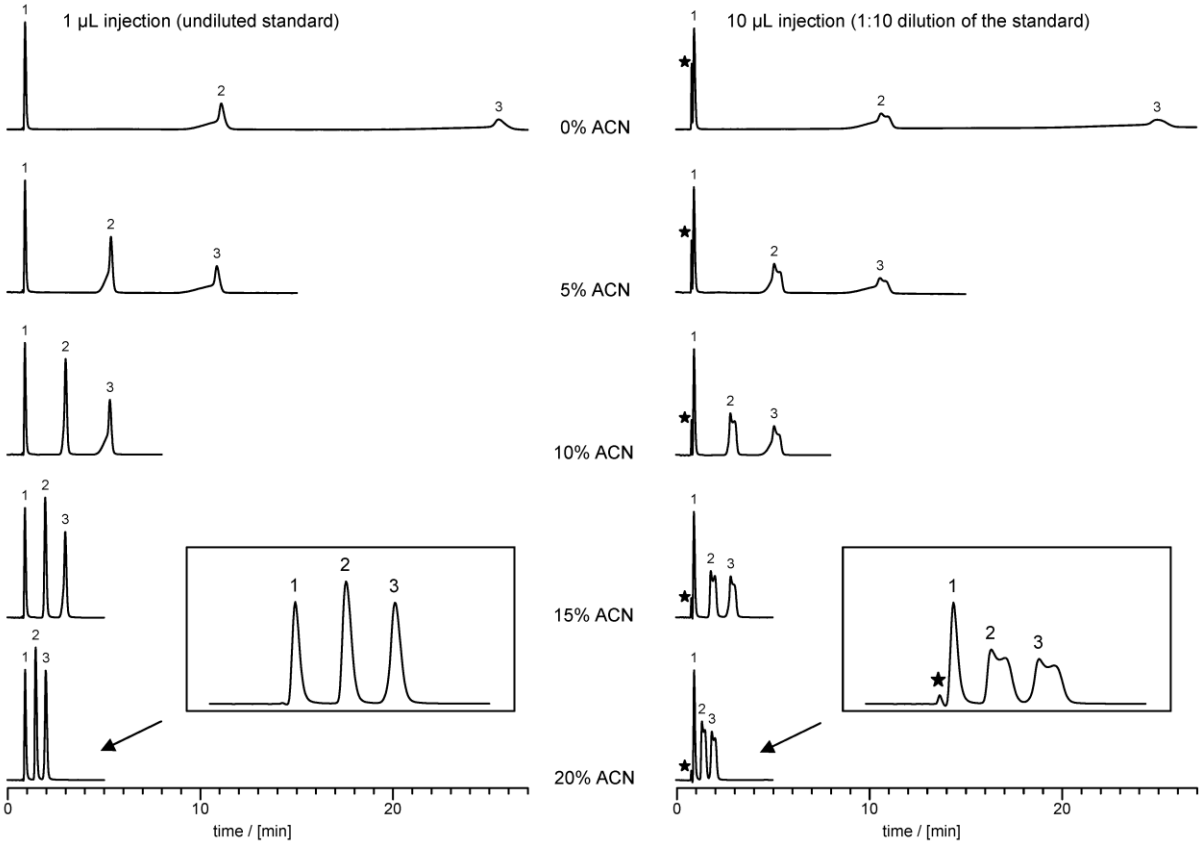

SI-Figure 2-1. Original chromatogram view of the peaks in Figure 2-1. Impact of a change in % B on a reversed-phase separation of uracil (1), 19-nortestosterone (2) and epitestosterone (3) for two injection volumes. Absolute mass of each solute is constant. Chromatographic conditions: stationary phase: 2.1 x 150 mm ZirChrom-PBD, 3 µm particles; mobile phase: A: water, B: acetonitrile; isocratic mode at 0.5 mL min^{-1}; temperature: isothermal at 90 °C; sample solvent: water/methanol 20:80 (v/v); detection: UV at 254 nm. Black star: peak by sample solvent.

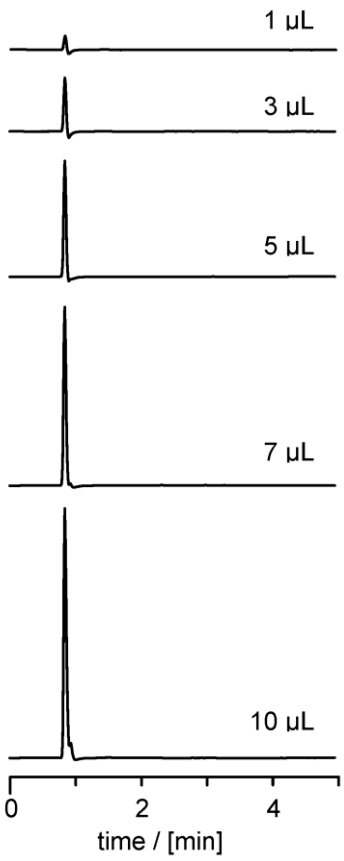

SI-Figure 2-2. Chromatograms of blank injections for different sample volumes, showing the effect produced by the sample solvent (water/methanol 20:80 (v/v)). Chromatographic conditions: stationary phase: 2.1 x 150 mm ZirChrom-PBD, 3 µm particles; mobile phase: water; isocratic mode at 0.5 mL min^{-1}; temperature: isothermal at 90 °C; detection: UV at 254 nm.

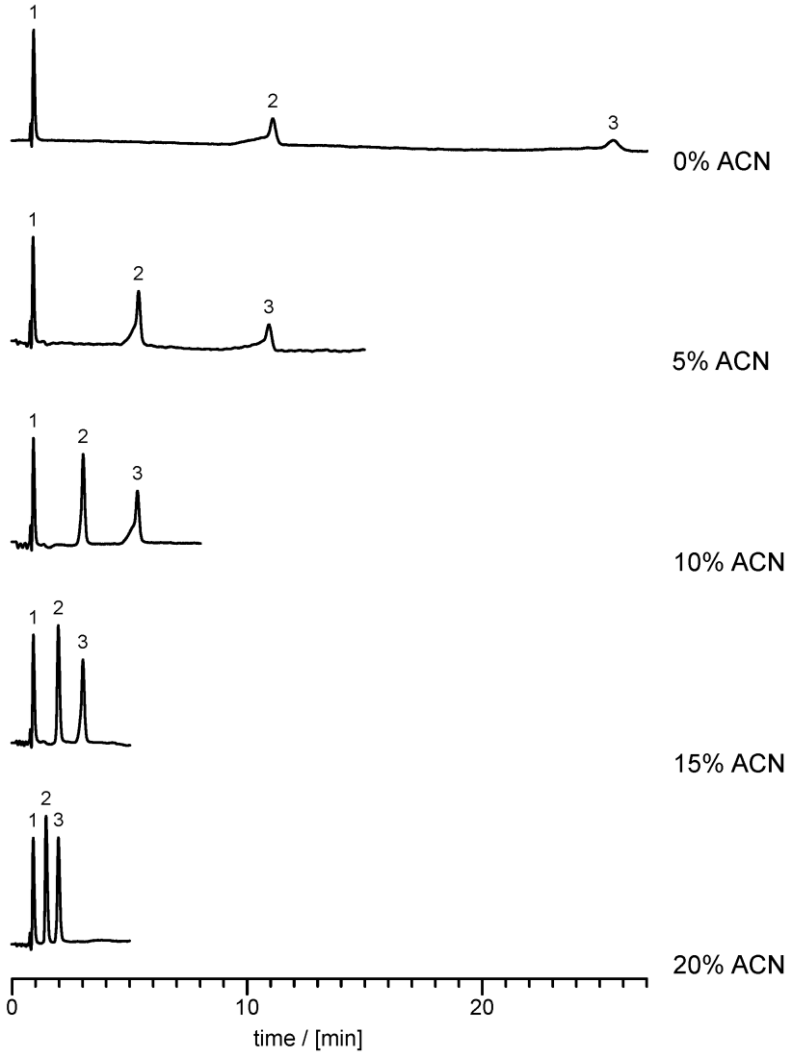

SI-Figure 2-3. Impact of a change in % B on a reversed-phase separation of uracil (1), 19-nortestosterone (2) and epitestosterone (3) (injection volume: 1 µL, 1:10 dilution). Absolute mass of each solute is one tenth compared to Figure 2-1. Chromatographic conditions: stationary phase: 2.1 x 150 mm ZirChrom-PBD, 3 µm particles; mobile phase: A: water, B: acetonitrile; isocratic mode at 0.5 mL min^{-1}; temperature: isothermal at 90 °C; sample solvent: water/methanol 20:80 (v/v); detection: UV at 254 nm.

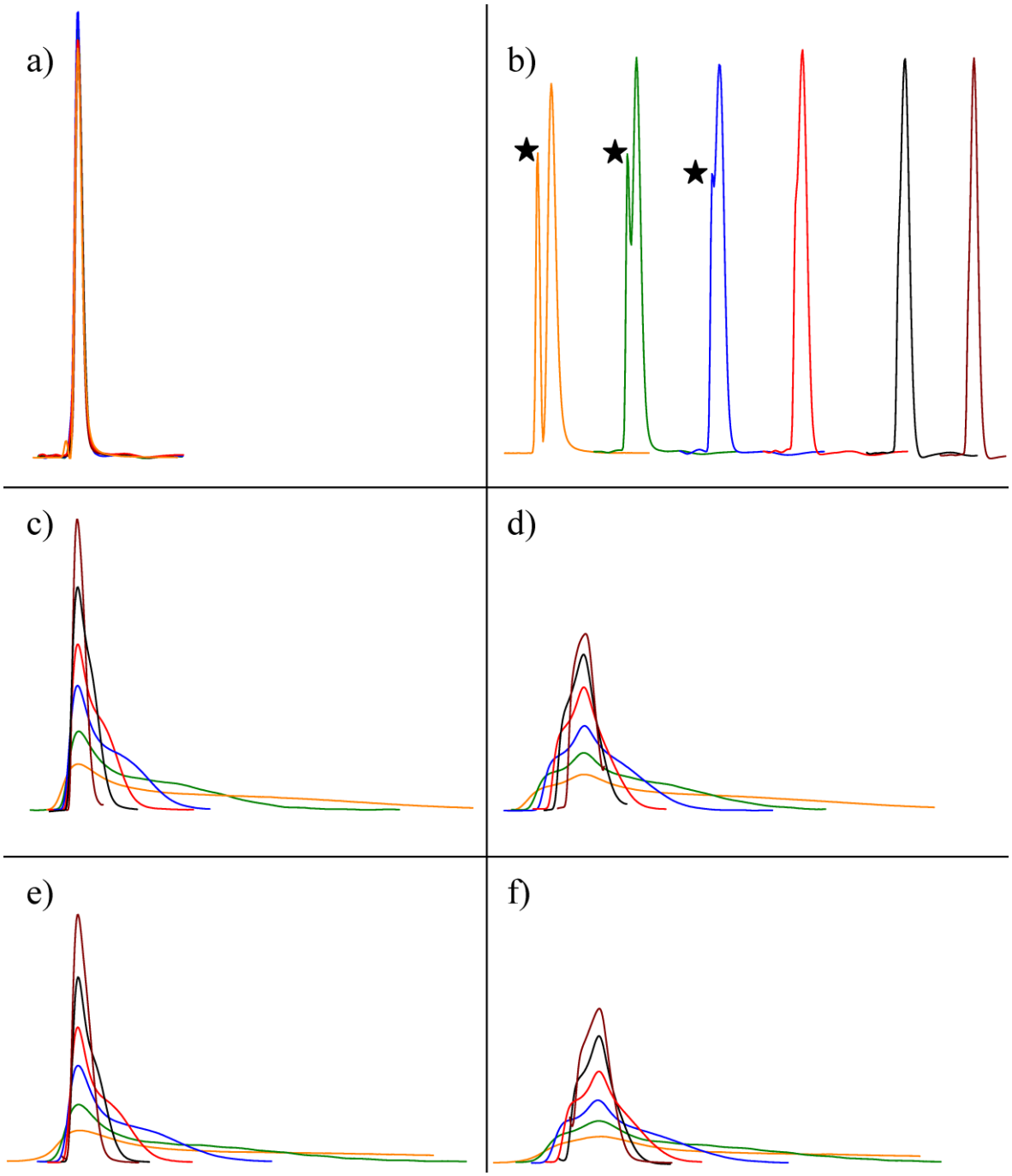

SI-Figure 2-4. Impact of a change in % B on peak shapes of uracil (a,b), 19-nortestosterone (c,d) and epitestosterone (e,f) for two injection volumes (a,c,e: 1 µL, b,d,f: 10 µL). Absolute mass of each solute is constant. Chromatographic conditions: stationary phase: 2.1 x 150 mm ZirChrom-PBD, 3 µm particles; mobile phase composition (water/methanol (v/v)) is given by the color code: orange – 100:0, green – 95:5, blue - 90:10, red – 85:15, black – 80:20, brown - 75:25; isocratic mode at 0.5 mL min^{-1}; temperature: isothermal at 90 °C; sample solvent: water/methanol 20:80 (v/v); detection: UV at 254 nm. Black star: peak by sample solvent. Area-normalized overlay view. For a better visualization, the fronting of the orange peaks is cut to size.

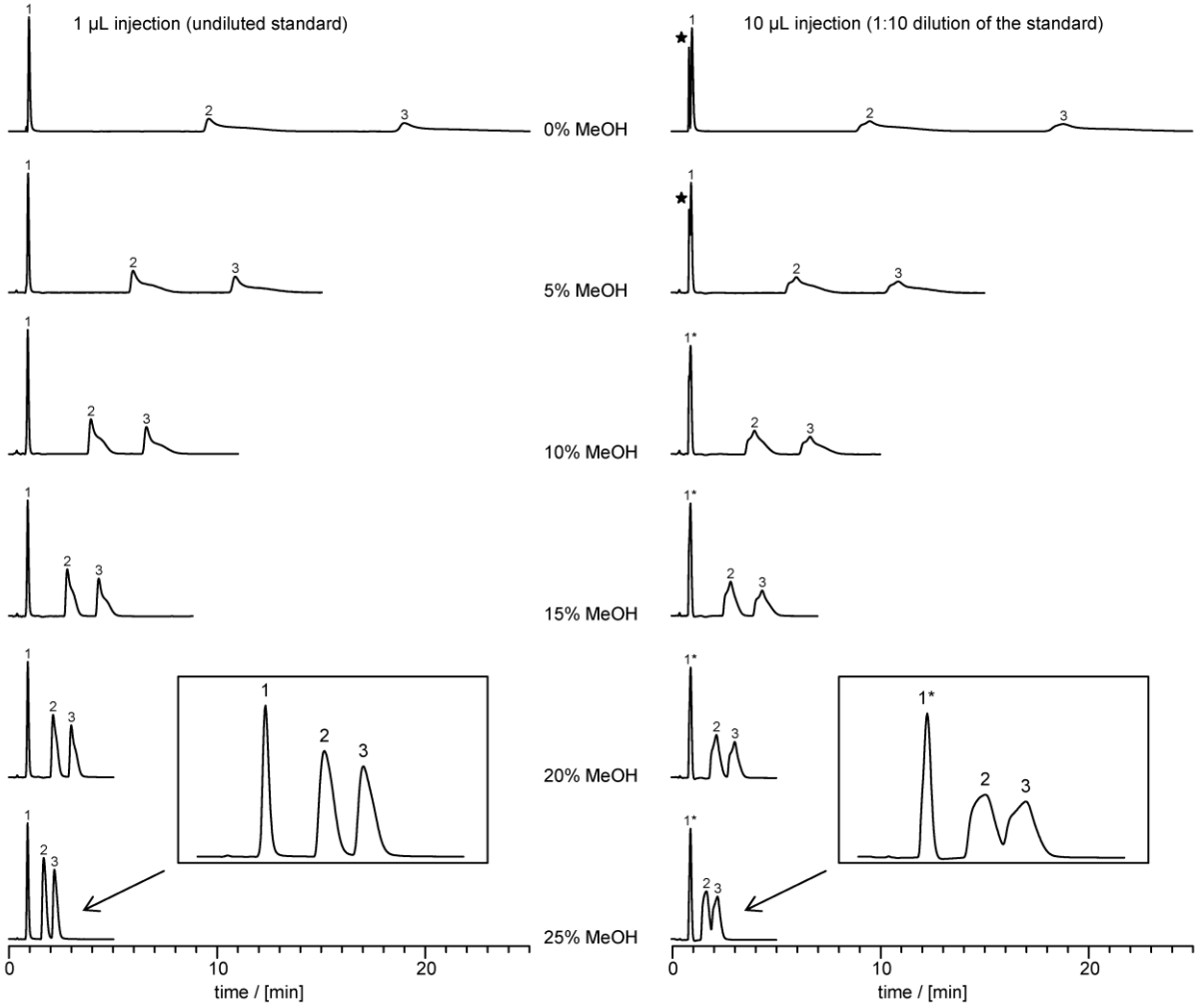

SI-Figure 2-5. Original chromatogram view of the peaks in SI-Figure 2-4. Impact of a change in % B on a reversed-phase separation of uracil (1), 19-nortestosterone (2) and epitestosterone (3) for two injection volumes. Absolute mass of each solute is constant. Chromatographic conditions: stationary phase: 2.1 x 150 mm ZirChrom-PBD, 3 µm particles; mobile phase: A: water, B: methanol; isocratic mode at 0.5 mL min^{-1}; temperature: isothermal at 90 °C; sample solvent: water/methanol 20:80 (v/v); detection: UV at 254 nm. Black star: peak by sample solvent; asterisk: peak by sample solvent is hidden by the uracil signal.

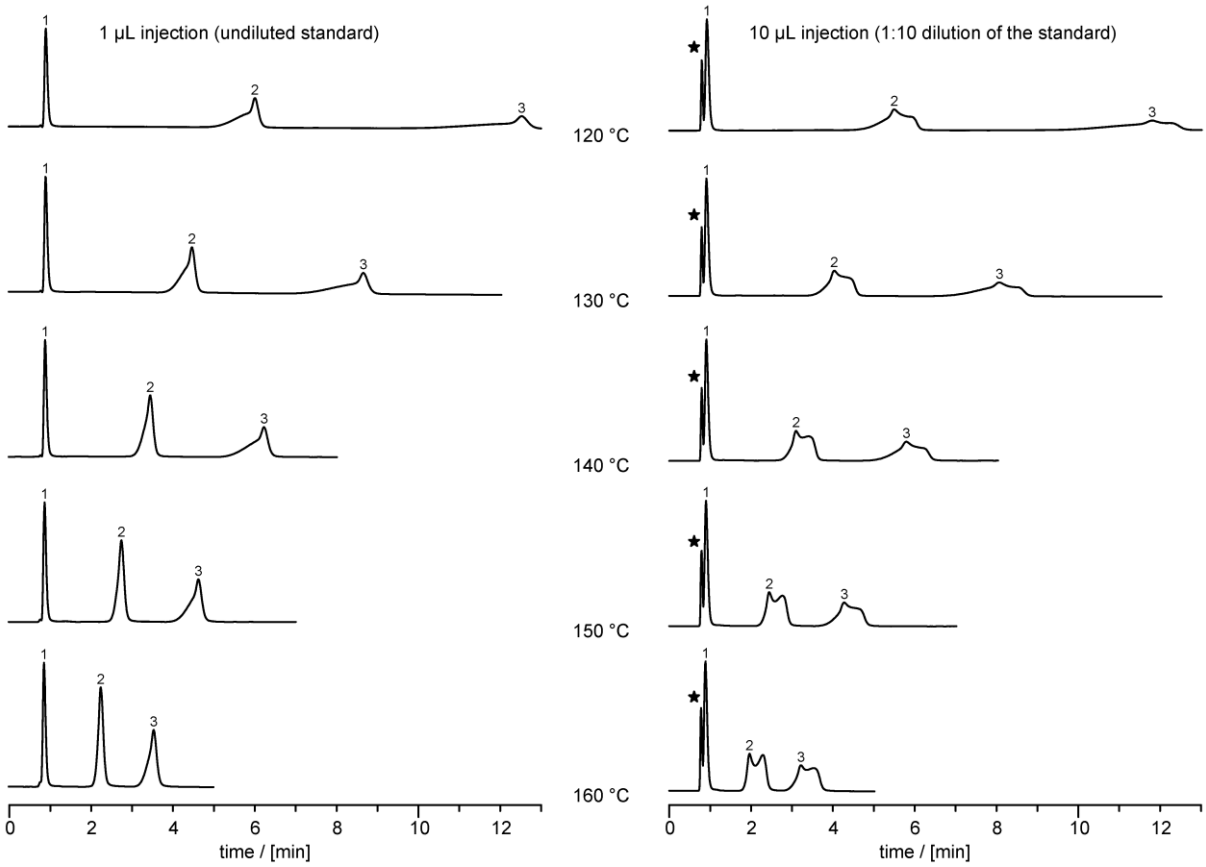

SI-Figure 2-6. Original chromatogram view of the peaks in Figure 2-2. Impact of a change in column temperature on a separation of uracil (1), 19-nortestosterone (2) and epitestosterone (3) for two injection volumes. Absolute mass of each analyte is constant. Chromatographic conditions: stationary phase: 2.1 x 150 mm ZirChrom-PBD, 3 µm particles; mobile phase: water; isocratic mode at 0.5 mL min^{-1}; temperature mode: isothermal; sample solvent: water/methanol 20:80 (v/v); detection: UV at 254 nm. Black star: peak by sample solvent.

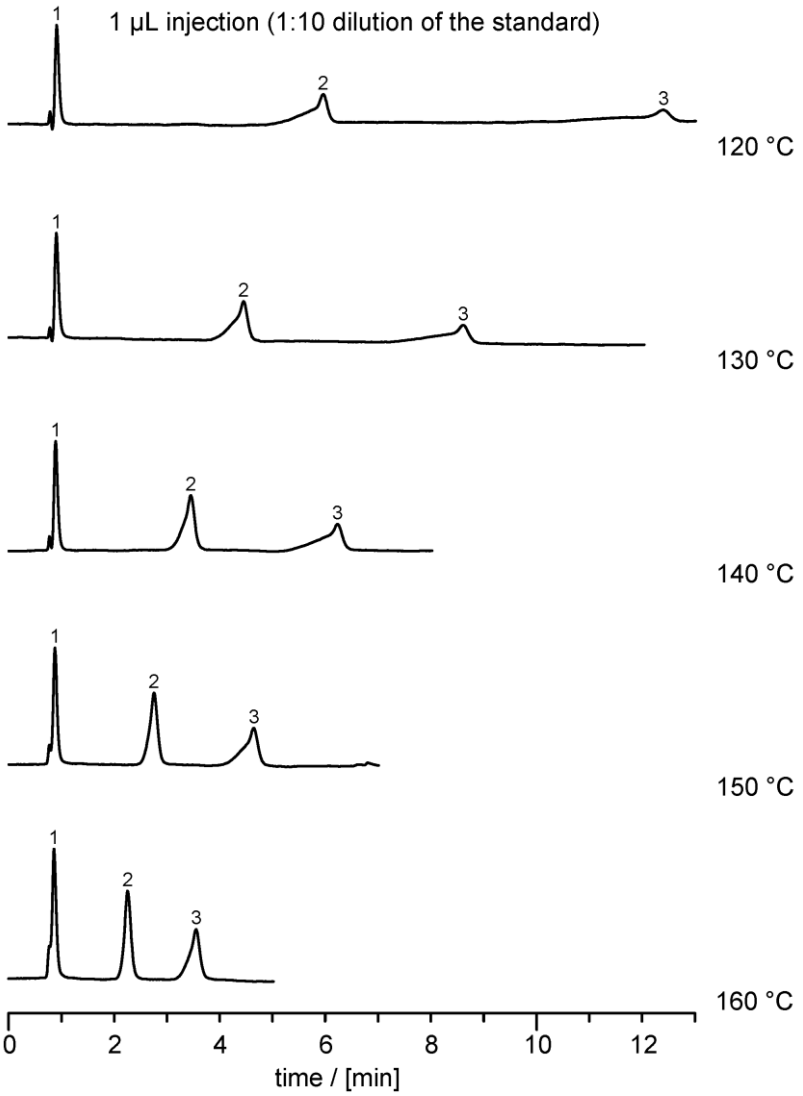

SI-Figure 2-7. Impact of a change in column temperature on a separation of uracil (1), 19-nortestosterone (2) and epitestosterone (3) (injection volume: 1 µL, 1:10 dilution). Absolute mass of each solute is one tenth compared to Figure 2-2. Chromatographic conditions: stationary phase: 2.1 x 150 mm ZirChrom-PBD, 3 µm particles; mobile phase: water; isocratic mode at 0.5 mL min^{-1}; temperature: isothermal; sample solvent: water/methanol 20:80 (v/v); detection: UV at 254 nm.

2.6.2 Tables

SI-Table 2-1. Tailing factors at five percent height for the peaks presented in the left column of SI-Figure 2-4 (1 µL injections).

Mobile phase H_2O/MeOH (v/v)	Tailing factor (uracil)	Tailing factor (19-nortestosterone)	Tailing factor (epitestosterone)
100:0	1.71	8.14	6.38
95:5	1.22	5.91	5.36
90:10	1.27	4.29	4.66
85:15	1.34	3.15	3.59
80:20	1.39	2.29	2.67
75:25	1.43	1.80	1.95

Chapter 3 Temperature stability of stationary phases

Redrafted from "J. Haun, T. Teutenberg, T. C. Schmidt, Long-term high-temperature and pH stability assessment of modern commercially available stationary phases by using retention factor analysis, Journal of Chromatography A, 2012, 1263, 99-107, DOI: 10.1016/j.chroma.2012.09.031"

High-temperature liquid chromatography provides several advantages concerning HPLC method development and is needed to realize special hyphenation techniques. However, hardware limitations and stationary phase degradation can prevent the successful application of this technique. Therefore, column stability is of major importance. The presented study contains results of long-term high-temperature stability tests for eight modern commercially available HPLC stationary phases. Six of them were silica-based reversed-phase C18 columns tested according to an earlier reported procedure (Teutenberg et al., 2009 [1]). On the basis of the extended data set that covers a wide range of column technologies, a comparative approach using retention factor analysis was evaluated in order to categorize the columns according to their long-term high-temperature stability at 150 °C and changing pH value. This approach offers a more objective alternative to conventional listings in which temperature maxima are compared for columns tested under different conditions. Additionally, customized tests are presented for one promising polymer-based C18 stationary phase and an amide column for hydrophilic interaction liquid chromatography.

3.1 Introduction

Numerous advantages of high-temperature HPLC and its potential regarding new applications, green(er) chemistry and the enabling of special hyphenation techniques have been described in several recent literature reviews [2-7]. However, column stability has been revealed to be the Achilles' heel of this technique. As column temperatures of more than 60 °C are often needed if organic modifiers in the mobile phase shall be replaced by water, the number of columns that do not deteriorate too fast is limited [5]. In general, column performance at high temperatures can be affected by hardware failures and by the deterioration of the stationary phase itself [2-7]. As a consequence of heating and cooling, high mechanical stress is applied to the column hardware increasing the risk of leakages. Mechanical stress is intensified by temperature gradients compared to isothermal operation [8]. Moreover, elevated temperatures can lead to deformation of different synthetic hardware materials (e.g. PEEK) resulting in flow path blockage or leakages [3]. The use of such materials is often not obvious to the practitioner if the corresponding parts (e.g. ferrules or frits) are hidden by the steel casing [3]. Furthermore, corrosion of steel parts, in particular of the inlet frit, can entail the release of metal ions that catalyze degradation processes of the stationary phase [9].

High-temperature stability of the stationary phase itself clearly depends on its chemistry, but also strongly on the composition, pH and purity of the mobile phase, as well as on choice of buffers and further additives. In general, a high water content of the mobile phase enforces degradation [10].

As a result of stationary phase degradation, a wash-out of stationary phase – often referred to as column bleed – can severely disturb several detection methods such as mass spectrometry, flame ionization or evaporative light scattering detection. A preselection of suitable columns can be done by using results of long-term high-temperature stability tests on which the presented study is focused and which describes changes in general column performance over the time of elution at high temperatures. However, the absolute interference caused by bleeding of the preselected column depends on conditions, time and detector, and therefore needs further application-specific evaluation as recently done by Zhang et al. [11] for $^{13}C/^{12}C$ isotope-ratio mass spectrometry.

In ambient temperature HPLC, the use of bonded silica phases is widespread because of several advantages like fast mass transfer, mechanical stability and batch-to-batch reproducibility. Unfortunately, silica gels are water-soluble and solubility increases with

temperature and pH, especially if pH exceeds a value of 8 [12]. At low pH values (<3), dissolution of the silica base is low, but bonded phase is lost due to hydrolysis [12]. Most silica-based stationary phases should not be used at temperatures above 60 °C [2] unless special technologies are used to increase stability.

On the other hand, alternative stationary phases on the basis of organic polymers, porous graphitic carbon and coated metal oxides (zirconia or titania) provide a much better stability concerning temperature (150–200 °C and above) and aggressive pH values [1, 13]. However, their use in non-academic environment is still limited because of their different retention mechanisms compared to silica phases and some material-dependent drawbacks. Polymer phases, for example, tend to shrink and swell at changing composition of the mobile phase [5, 14]. Furthermore, in case of porous graphitic carbon, strong secondary interactions, e.g. the polar retention effect on graphite, are observed and some analytes cannot be eluted within a reasonable time window because retention is too strong [15]. Coated metal oxide stationary phases can exhibit strong ion exchange interactions and other secondary interactions, e.g. ligand exchange with Lewis bases [16]. Some modified metal oxide phases are commercially available, where metal chelating compounds are used to suppress these secondary interactions, but this works at the expense of a pH range restriction.

In the following, several particle technologies are listed that have proven to increase high-temperature stability of silica-based stationary phases markedly and that resulted in commercially available columns for high-temperature HPLC. Initially, most of them were developed to increase the pH stability and to enlarge the pH range. Steric protection of the silica surface by using functional silanes with bulky isoalkyl side chains as bonded phase allowed extending the pH range down to 1 [17]. The development of bidentate phases with short alkyl bridges between the silicon atoms of two functional silanes improved chemical stability even toward higher pH values (about 11 for propyl-bridge, organic buffer, ambient temperature) [18]. Taking up this idea, polydentate phases as tested by Marin et al. in 2004 [19] were developed in which all functional silanes of the bonded phase were crosslinked to each other by ethyl bridges. This type of stationary phase was later enhanced by bonding a protective layer between the silica backbone and the functional groups [20]. This layer consists of silicon atoms that are dendrimerically crosslinked by ethyl bridges. In other approaches, graftings of organosilanes (with and without ethyl bridges) to the surface of the silica surface were used to increase temperature and pH stability. It was found that graftings containing ethyl bridges show higher temperature stability than those without [1]. Following a different concept, the use of polymer-encapsulated silica particles was evaluated in order to

merge the advantages of silica and polymer phases. Last but not least, pH and temperature stable columns were the result of the development of hybrid stationary phases [21]. These particles are stabilized by the introduction of terminal or bridging short alkyl groups to the silica structure of the particle providing hydrophobic shielding and C–Si bonds that are not susceptible to hydrolysis [21]. In contrast to other technologies which add a protective shield function to the silica surface, chemical stability of the whole particle is enhanced.

Many publications on evaluations of different stationary phases for the use in high-temperature HPLC exist (e.g. [1, 8, 13, 19-20, 22-27]) and several reviewers presented data with rankings and/or temperature limits for temperature stable phases [2-7, 10]. However, comparability of the results of different publications is not given in most cases due to the different methods and measurement conditions that were used during the evaluation of the column materials. A further problem is that often only one or two test substances are used for the stability evaluation resulting in an incomplete image of the performance changes caused by high temperatures. Therefore, one goal of this publication is the extension of the data basis for silica-based C18 stationary phases evaluated by using the high-temperature stability testing procedure recently reported by Teutenberg et al. [1]. The presented extension covers results for six new stationary phases. In contrast to [1], column stability will be discussed by using a comparative approach based on the extended data set. Additionally, high-temperature test results of one silica-hybrid column for hydrophilic interaction chromatography (HILIC) and one promising polymer-based reversed-phase column are presented in this paper for which measurement conditions had to be slightly changed.

3.2 Materials and methods

3.2.1 Tested columns

The tested columns and their dimensions are listed in Table 3-1. All of these columns were brand-new and unused prior to this study. Where possible, column dimensions and particle diameter were chosen to be 4.6 mm × 150 mm and 5 µm, respectively, as used by Teutenberg et al. [1].

Table 3-1. Tested HPLC columns.

No.	Manufacturer	Column description	Length (mm)	Inner diameter (mm)	Particle diameter (µm)	Pore size (Å)
1	AkzoNobel	Kromasil Eternity-2.5-C18	100	4.6	2.5	100
2	Interchim	Uptisphere Strategy C18-2	150	4.6	5	100
3	Interchim	Uptisphere Strategy C18-3	150	4.6	5	100
4	Supelco	Ascentis Express C18 (fused-core)	150	4.6	2.7	90
5	Waters	XSelect CSH C18	150	4.6	5	144
6	YMC	Triart C18	150	4.6	5	120
7	Showa Denko	Shodex ET-RP1 4D (polymer)	150	4.6	4	
8	Waters	XBridge Amide (HILIC)	150	4.6	3.5	130

3.2.1.1 Silica-based reversed-phase columns

According to the manufacturer, Kromasil Eternity columns contain a packing of silica particles that are modified by an organosilane grafting prior to functionalization and endcapping. This modification is claimed to substantially increase column life-time under extreme conditions (primarily pH, but also high temperatures). During the manufacturing process, parts of the organosilane penetrate the fully porous particle, thus giving rise to a merged organic/inorganic interfacial gradient in radial direction. This gradient represents the main difference to other grafting modified stationary phases, where the organosilane is mainly bonded to the surface of the particle to act as a protective shell. The pH range of the tested Kromasil Eternity column is stated to be 1–12. Unfortunately, no temperature maximum or temperature dependent pH range is given by the manufacturer.

The Interchim Uptisphere Strategy phases are claimed to be stable up to 100 °C and even higher temperatures. Stability of both phases was explained by a high bonding density and a multistage endcapping process. pH ranges are 1–10 and 1–12 for the C18-2 and C18-3 version, respectively. The main difference between both phases is the even higher bonding density of the C18-3 phase. The carbon load is 23% C compared to 19.7% C for C18-2. These phases are delivered as cartridge columns of the Modulo-cart Quick seal type. According to the manufacturer, this HPLC-column hardware is remarkably pressure-stable (up to 800 bars) and compatible to supercritical fluid chromatography.

The tested Ascentis Express C18 phase of Supelco is based on the fused-core technology by Advanced Material Technology (Wilmington, DE, USA) and is therefore an example of the modern third generation of shell particles according to the recent review of Guiochon and

Gritti [28]. As known from literature [29], pellicular particles, the predecessors of modern shell particles, could be used at considerably higher temperature (up to 120 °C) compared to fully porous silica at that time. This increase in temperature stability was attributed to the non-porous core of these particles. In contrast to pellicular particles, the non-porous core of the modern shell particles is surrounded by a thick layer of porous silica which potentially decreases temperature stability. For the tested Ascentis Express, a pH range of 2–9 and a temperature maximum of 60 °C are claimed by the manufacturer. We could not find publications where this maximum was exceeded for the Ascentis Express C18 but a study by Cunliffe et al. [30] indicates that another core–shell stationary phase can be operated successfully at elevated temperatures up to 100 °C.

The XSelect CSH stationary phase represents the third generation of hybrid phases by Waters. For its production, ethylene bridged hybrid (BEH) particles are modified prior to functionalization and endcapping by a controlled application of surface charges [31]. According to the manufacturer, this is done to provide a different selectivity, especially for basic compounds. The claimed temperature range (80 °C at low pH, 60 °C at high pH) is the same as for the Waters XBridge columns, a second generation hybrid based on BEH particles without surface charge modification. Regarding the XBridge columns, several authors [1, 11, 26, 32] reported about an excellent high-temperature performance that is superior to other silica-based stationary phases. Therefore, our goal was to investigate whether the additional modification of the XSelect CSH affects its high-temperature stability.

YMC pursues a different hybrid particle strategy for the Triart columns. According to the manufacturer, micro-reactor production technique allows producing particles which are built up of radially alternating inorganic and organic siloxane layers. Silanol activity should be suppressed by the application of a proprietary multistage endcapping process after the polymeric bonding of the C18 ligands. The claimed temperature stability is 70 °C at pH 1–7 and 40 °C at pH 7–12. Although these specifications are chosen conservatively, the manufacturer stresses the stability to be superior to other hybrid stationary phases.

3.2.1.2 Other stationary phase materials

In 2010, Vanhoenacker et al. reported about an excellent high-temperature performance and stability of a polymer-based C18 phase that could be operated in gradient elution without problems and exhibited an efficiency close to silica-based C18 phases [27]. This phase which is commercially available as Shodex ET-RP1 was tested.

The use of elevated temperatures in hydrophilic interaction liquid chromatography has recently proven to reduce analysis time without a significant decrease in separation efficiency [33]. According to [33], a laboratory study comparing different bare-silica columns revealed that the highest temperature maximum was observed for the XBridge HILIC hybrid particles (100 °C). While no changes in retention mechanisms are expected during degradation of bare-silica columns, it appears more interesting to monitor the high-temperature stability of bonded-phase HILIC columns such as the tested Waters XBridge Amide. Corresponding to the manufacturer's specifications, the Amide column can be used with mobile phase pH values between 2 and 11, and at temperatures up to 90 °C.

3.2.2 HPLC systems

Columns 1–7 were tested using a Beckman HPLC system (Beckman-Coulter, Krefeld, Germany) consisting of a System Gold Solvent Module 126, a System Gold DAD Module 168 and an LC 502 e autosampler. Data was processed using the Beckman 32 Karat software package (version 7.0 Build 1048). In case of column 8, the Beckman system was not available, so it was adequately replaced by a Shimadzu HPLC system (Duisburg, Germany) consisting of an SCL-10A_{SP} system controller, two LC-10AD_{VP} pumps, a DGU-14A degassing unit, an SIL-10AD_{VP} auto injector and an SPD-10A_{VP} diode array detector. Data processing was performed using the LCsolution software package (version 1.21 SP1, Shimadzu, Kyoto, Japan). For all experiments, a commercially available Metalox 200-C high-temperature column oven (Systec, New Grighton, USA) was used to control the temperature of the column and the mobile phase which is preheated to column temperature by means of an internal two-step system consisting of a heat-exchanger and a contact preheater.

3.2.3 Chemicals

Acetonitrile and methanol (LGC Promochem, Wesel, Germany) were both HPLC gradient grade. An Elix-10/MilliQ-Plus combination (Millipore, Schwalbach, Germany) was used to produce ultrapure water. All chemicals for buffer preparation were purchased from Sigma–Aldrich Corporation (Schnelldorf, Germany): crystalline phosphoric acid (≥ 99.999%, Aldrich), potassium phosphate monobasic anhydrous (≥ 99.5%, Fluka), potassium phosphate dibasic anhydrous (≥ 99.99%, Fluka), potassium phosphate tribasic (≥ 98%, Sigma), formic acid (~ 98%, Fluka) and ammonium formate (≥ 99%, Fluka). The pH value of the buffer solutions was fine-adjusted using potassium hydroxide solution (1 mol L^{-1}, Fluka) or a dilution of hydrochloric acid (≥ 32%, Fluka). All relevant information about the substances

used for the test mixtures is given in Table 3-2. Test mix solutions were always prepared freshly using the corresponding mobile phase as sample solvent.

Table 3-2. Relevant information about the test mix solutes.

Chemical	CAS No.	Manufacturer	Purity	Test mix	Conc. [mg L^{-1}]
Acenaphthene	83-32-9	Fluka	≥ 99.0%	Neue test	200
Amitriptyline hydrochloride	549-18-8	Sigma	≥ 98.0%	Neue test	100*
Dihydroxyacetone	96-26-4	Merck	≥ 98.0%	Neue test	3000
Dipropyl phthalate	131-16-8	Fluka	≥ 98.5%	Neue test	340
Naphthalene	91-20-3	Fluka	≥ 99.0%	Neue test	60
Propranolol hydrochloride	318-98-9	Sigma	≥ 99.0%	Neue test	400*
Propyl paraben	94-13-3	Fluka	≥ 99.0%	Neue test	20
n-Butyl benzoate	136-60-7	Supelco	≥ 99.9%	Column 7	270
n-Hexyl benzoate	6789-88-4	Aldrich	≥ 98.0%	Column 7	440
Methyl benzoate	93-58-3	Fluka	≥ 98.0%	Column 7	160
Uracil	66-22-8	Fluka	≥ 99.0%	Column 7	6
Acenaphthene	83-32-9	Fluka	≥ 99.0%	Column 8	100
Adenine	73-24-5	Fluka	≥ 99.0%	Column 8	100
Cytosine	71-30-7	Sigma	≥ 99.0%	Column 8	100
Thymine	65-71-4	Sigma	≥ 99.0%	Column 8	100

*concentration of pure analyte (without hydrochloride)

3.2.4 General high-temperature stability testing procedure

All silica-based C18 reversed-phase columns (i.e. 1–6) were tested using a procedure that was introduced by Teutenberg et al. [1]. Prior to the procedure, the columns' initial performance is characterized by a 20 µL injection of a Neue test mixture (compare Table 3-2, [34]). Other than in literature [1, 34], all Neue test mixtures were measured at 30 °C column temperature. The corresponding mobile phase consisting of a phosphate buffer (20 mM, pH 7.0)/methanol mixture (35:65, v/v) was isocratically pumped at a flow rate of 1 mL min^{-1} (unless otherwise noted).

The high-temperature stability test procedure itself is divided into three heating phases with different pH-conditions of the mobile phase. The first phase is at "neutral" pH (no buffer), the second at acidic conditions (buffered, pH 2.2) and the third at basic conditions (buffered, pH 12.0). Each phase is subdivided into five heating cycles. One heating cycle includes heating the column to 150 °C, holding the temperature for 5 h and cooling down to

30 °C. During all heating cycles, the mobile phase consists of a water (or 20 mM phosphate buffer, depending on the heating phase)/methanol mixture at a ratio of 90:10 (v/v) which is pumped isocratically at a flow rate of 1 mL min^{-1}. In-between the cycles, the column status is monitored by the application of the Neue test described above [1].

3.2.5 Polymer phase testing procedure

In case of the polymer phase (column 7), the procedure was modified by replacing the Neue test with a simpler column performance test. The Neue test [34] was designed to distinguish between hydrophobic interactions and other retention mechanisms closely related to the silica basis of many modern stationary phases (silanol activity). This silica basis is missing in case of the polymer phase. Therefore and for reasons of simplicity, the column performance test of the manufacturer was chosen to monitor the loss of column performance. This test mix contains three n-alkyl benzoates differing in their alkyl chain length, thus differing in hydrophobicity. Moreover, uracil is added to act as a dead time marker. Injection volume was 10 µL. As recommended, a mixture of water and acetonitrile (35:65, v/v) at a flow rate of 0.6 mL min^{-1} was used as the mobile phase for the isocratic separation of the solutes. However, all heating cycles were performed in the same way as described for the silica-based C18 columns (see Section 3.2.4).

3.2.6 HILIC phase testing procedure

Retention mechanisms and elution strength are different for hydrophilic interaction chromatography compared to reversed-phase liquid chromatography [35-36]. Consequently, several test conditions had to be adjusted for the amide column. Again, a column test mix of the manufacturer was chosen as a basis for the performance check between the heating cycles. This test mix contains the non-polar acenaphthene which acts as dead time marker as well as three polar and retained nucleobases. Isocratic conditions using a ratio of 20:80 (v/v) 100 mM ammonium formate buffer at pH 3/acetonitrile at 0.5 mL min^{-1} were chosen to elute 5 µL of the test mix in HILIC mode.

Although no analyte separation is measured during the heating cycles, high-temperature elution conditions had to be changed as well. A pronounced and direct increase in pressure drop over the column prohibited using the predominantly watery elution conditions of the original heating procedure. However, high water contents are generally avoided in hydrophilic interaction chromatography due to the high elution strength of water [35-36]. Therefore, an isocratic method using 20:80 (v/v) water (or buffer)/acetonitrile was applied during the

heating cycles. Again, 20 mM phosphate buffers at pH 2.2 and 12 were used for the acidic and basic heating phases.

3.3 Results and discussion

3.3.1 Silica-based reversed-phase columns

3.3.1.1 Hardware issues

In case of both Interchim cartridge columns, the results of the test procedure clearly indicate that the corresponding column hardware is not compatible to high-temperature liquid chromatography at 150 °C. As expected, mechanical stress due to heating and cooling of the column as well as thermal deformation of synthetic parts immediately produced leakages. The finger-tight fittings had to be re-fastened by using tools. In case of the C18-2 column, this action resulted in a fixation of the replaceable PEEK frit in the cartridge adapter. As a consequence, mechanical stress removed the frit from the column during operation and stationary phase was washed out. In case of the second column (C18-3), the frit was not removed, so there was no loss of stationary phase due to leakage. However, it was impossible to work without leakage after the fifth heating cycle of the neutral heating phase. Moreover, peak shape was severely distorted for each analyte at that point, allowing the assumption that the stationary phase itself was also severely degraded. The results for both Interchim phases are visualized in SI-Figure 3-1 and SI-Figure 3-2.

Column hardware also revealed to be the main weakness of the tested Kromasil Eternity column. Mechanical stress caused by heating to 150 °C and cooling led to leakages during every heating cycle. However, leakages could be suppressed by retightening the fittings. Although the Kromasil Eternity phase did not collapse completely after the neutral heating phase, a considerable loss of performance is visible. SI-Figure 3-3 clearly shows a retention time loss for all analytes accompanied by a significant fronting for all analytes except for propranolol which developed a tailing. These strong peak deformations point to a void volume at the column head that can be caused by a washout of stationary phase and/or particle dissolution. During the acidic heating phase, column backpressure increased by more than 100 bars which made it impossible to continue the column test procedure. Besides particle degradation, hardware failure in terms of thermal deformations could be a reason. In conclusion, the real potential of this phase is obscured by its poor hardware.

3.3.1.2 Stability comparison

High-temperature degradation can be visualized best for stationary phases that are most stable. Therefore, for the following comparisons only those stationary phases were selected for which at least the neutral elution heating phase was completed. Table 3-3 summarizes the compared stationary phases.

Table 3-3. Silica-based stationary phases to be compared.

Stationary phase	Protection	Diagram symbol	Origin
Agilent Zorbax SB C18	Sterical protection (bulky side chain)	○	[1]
AkzoNobel Kromasil Eternity C18	Grafting (org./inorg. gradient)	△	This study
Phenomenex Gemini NX C18	Grafting (with ethylene bridges)	■	[1]
Selerity Blaze 200	Polydentate	▲	[1]
Waters XBridge C18	Ethylene bridged hybrid (BEH)	◆	[1]
Waters XSelect CSH C18	Ethylene bridged hybrid (BEH)	□	This study
YMC Pack Pro C18	High-density bonded phase	◇	[1]
YMC Triart C18	Multilayer org./inorg. Hybrid	●	This study

The fundamental publications of Neue et al. [34, 37-38] in which the Neue test is described inspired us to a comparative data analysis approach for the assessment of high-temperature column stability. In their work, Neue et al. used retention factor analysis for the classification and characterization of silica-based reversed-phase packings. Here, retention factors are used to monitor column degradation. Exemplary results are shown in Figure 3-1. Four charts show changes in retention factors or retention factor ratios of selected marker substances as a result of the low-temperature performance tests before and in-between the heating cycles. On the x-axis the total duration of elution at 150 °C is plotted.

As can be seen from Figure 3-1, the basic heating phase is not included to the charts. This is because particle dissolution during the basic elution phase resulted in void volume formation causing a quick breakdown of column performance and peak quality for all silica-based stationary phases. Therefore, it can be concluded that the given conditions in combination with the column history (i.e. neutral and acidic phase) were too harsh to evaluate differences in stability among these stationary phases. However, it should be kept in mind that the procedure of Teutenberg et al. [1] was also used to differentiate between silica-based and alternative materials which provide a much higher stability toward high pH elution. Moreover, data analysis of the preceding two heating phases already offers much information on stationary phase degradation.

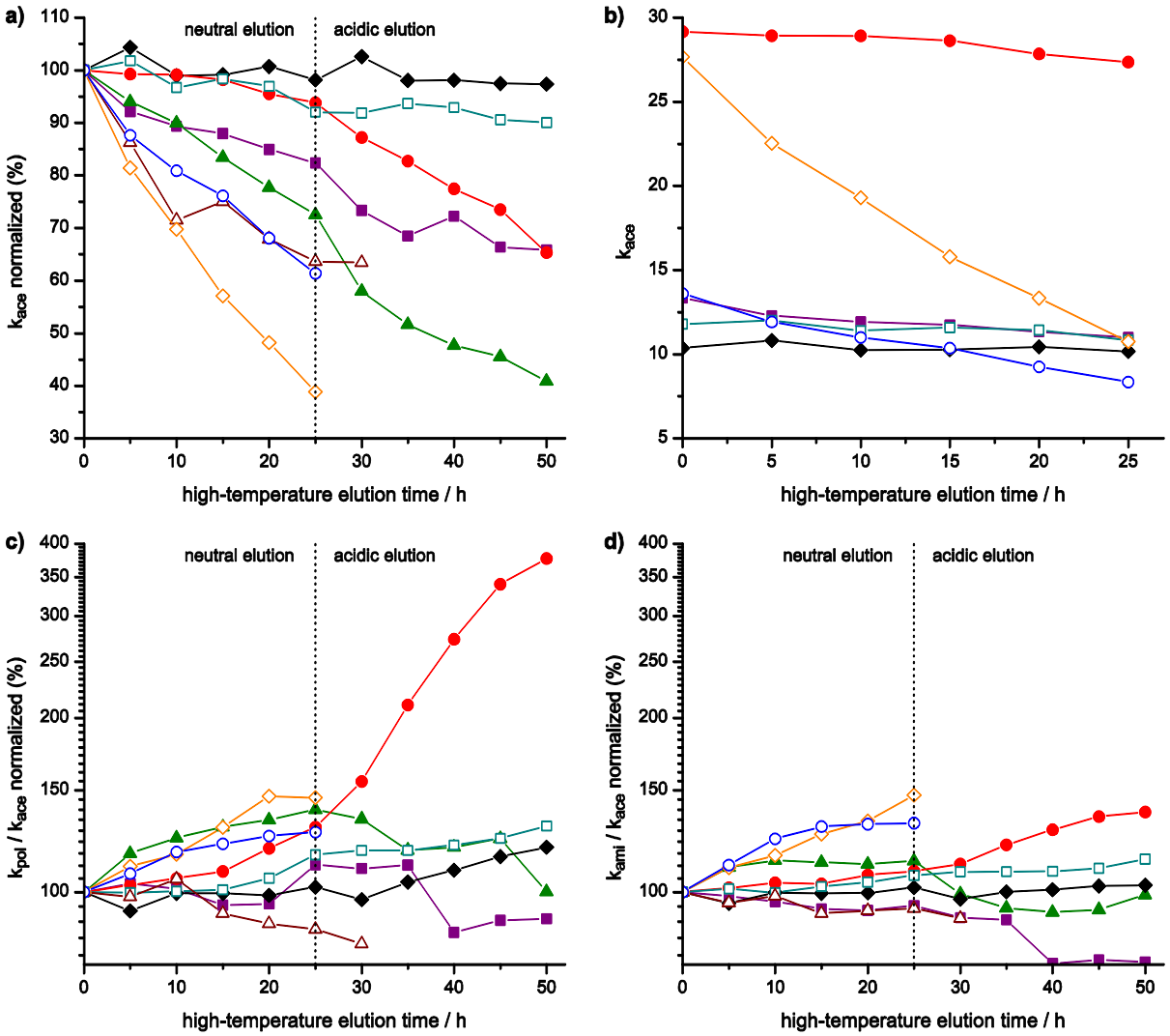

Figure 3-1. Retention factor analysis as a tool to visualize column degradation. Retention factor data originating from the low-temperature performance tests in-between the heating cycles are presented in dependence of the total high-temperature elution time. The lines are simple point-to-point-connections and not functional graphs. Normalized (a) and raw (b) data of the retention factor of acenaphthene (ace) for monitoring losses in hydrophobicity. (c) and (d) show normalized views of the retention factors of each basic marker, propranolol (pol) and amitriptyline (ami), corrected by the retention factor of acenaphthene for an approximation of the increase in silanophilic interactions. Symbol legend: see Table 3-3.

In Figure 3-1a the normalized retention factor of the hydrophobic marker acenaphthene is used to present approximately the losses in hydrophobicity. In this context, normalization is done by defining the mean retention factor resulting from the initial performance test as 100%. This way, general hydrophobicity differences between the columns in their brand-new status are compensated for. As hydrophobicity is the predominant retention mechanism in C18 reversed-phase chromatography, the illustration presented in Figure 3-1a allows for an approximation of the loss of general retentivity of the column. A very similar picture would

be obtained if the retention factor of the second hydrophobic marker naphthalene was chosen instead. The observed losses can be primarily explained by a hydrolytic loss of bonded phase, and beyond that by a loss of endcapping groups and temperature-induced dissolution of the whole particle. Over the time of neutral elution at 150 °C, all three hybrid phases show a remarkable stability. In contrast, quick degradation is observed for the YMC Pack Pro where protection of the particle against extreme conditions only happens via a high density of the bonded phase. Medium stability is observed for the stationary phases with surface protection technologies. By changing to acidic elution the difference between the two hybrid types becomes apparent (Figure 3-1a). Distinct losses of bonded phase are visible for the multilayer hybrid particles of YMC while the BEH-based stationary phases of Waters remain stable.

In order to account for the general hydrophobicity differences of the stationary phases, Figure 3-1b shows the uncorrected retention factor of acenaphthene for the columns in standard test format (150 mm × 4.6 mm, 5 µm particle diameter) over the time of the neutral heating phase. Although the disadvantageous scaling of the y-axis hides the previously shown column differences in degradation, Figure 3-1b presents the main advantage of the hybrid phase of YMC, its high initial hydrophobicity that remains constant during the neutral heating phase. This property can be beneficial for the analysis of moderately polar substances in superheated water chromatography and related hyphenation techniques because resolution of these compounds in purely or dominantly aqueous mobile phase conditions can be increased compared to reversed-phase C18 phases with low hydrophobicity.

As a result of bonded phase losses, increasing interactions with free surface silanols can entail elution order changes and deterioration of peaks of susceptible analytes. Especially bases tend to longer retention times accompanied by peak broadening in terms of a tailing. In this context, the Neue test includes two basic markers that can be used to monitor such a change in retention behavior, propranolol and amitriptyline. Retention of both markers is not independent from hydrophobic interactions and a possible loss of packing caused by particle dissolution must not be neglected. Therefore, retention factors of both basic markers have to be corrected when used to monitor silanophilic interactions. For Figure 3-1c and d, this was done by division by the retention factor of acenaphthene. Again, normalization was applied by setting the values of the measurements in columns' brand-new states to 100%. As can be seen from the results using propranolol (Figure 3-1c), at least three columns show a direct increase in silanophilic interactions during neutral heating phase. In contrast to that, the hybrid and grafting materials investigated in this study seem to be more stable. However, if pH is changed to 2.2, a severe increase in silanophilic activity can be observed for the Triart C18,

whereas for both Waters hybrid phases this change is quite low. In Figure 3-1d amitriptyline is used instead of propranolol. Regarding the Triart C18, the increase in retention of amitriptyline is by far not as pronounced as for propranolol (Figure 3-1c). An explanation could be that the retention of amitriptyline that can be described by "hydrophobically assisted ion exchange interactions" [39-40] is significantly influenced by hydrophobicity. The latter is strong for the Triart C18 column (Figure 3-1b) and is corrected via division by the retention factor of acenaphthene. The influence of hydrophobicity on the retention of propranolol is much lower whereas that of secondary interactions is comparably high. A similar observation was done by Neue et al. in their fundamental publication, however, in a different context [34]. Therefore, the retention factor ratio of propranolol and acenaphthene should be preferred to approximate the potential toward elution order changes caused by silanophilic interactions. Retention factor analysis of the polar markers of the Neue test, dipropyl phthalate and propylparaben, did not provide much additionally relevant information. This should be different if reversed-phase columns with a more polar bonded phase are compared to C18 phases. However, it should be noted that in general the retention factor ratio of the critical peak pair, dipropyl phthalate and naphthalene, decreases slowly with column degradation. This can also be seen from Figure 3-2 and Figure 3-3 which show the results of the XSelect CSH and the Triart C18 columns in the original style used by Teutenberg et al. [1].

In both cases (Figure 3-2 and Figure 3-3), column degradation leads to a better separation of the critical peak pair which co-eluted when the columns were new. Moreover, the change in elution order for the Triart column resulting from increasing silanophilic interactions during the acidic heating phase can be observed by comparing Figure 3-3b and c. In addition to retention factor analysis, these chromatogram illustrations present valuable information about peak shapes. For most of the silica-based C18 columns, except for the Blaze 200, a significant fronting of the hydrophobic and polar markers is observed as a result of the acidic phase pointing to void volume formation due to particle dissolution. At low temperatures, this phenomenon would be expected primarily for high pH elution [12]. The fronting effect is not observed for the Blaze 200 column [1]. We assume that the rigid dendrimer shells of the polydentate modification prohibit a complete particle collapse.

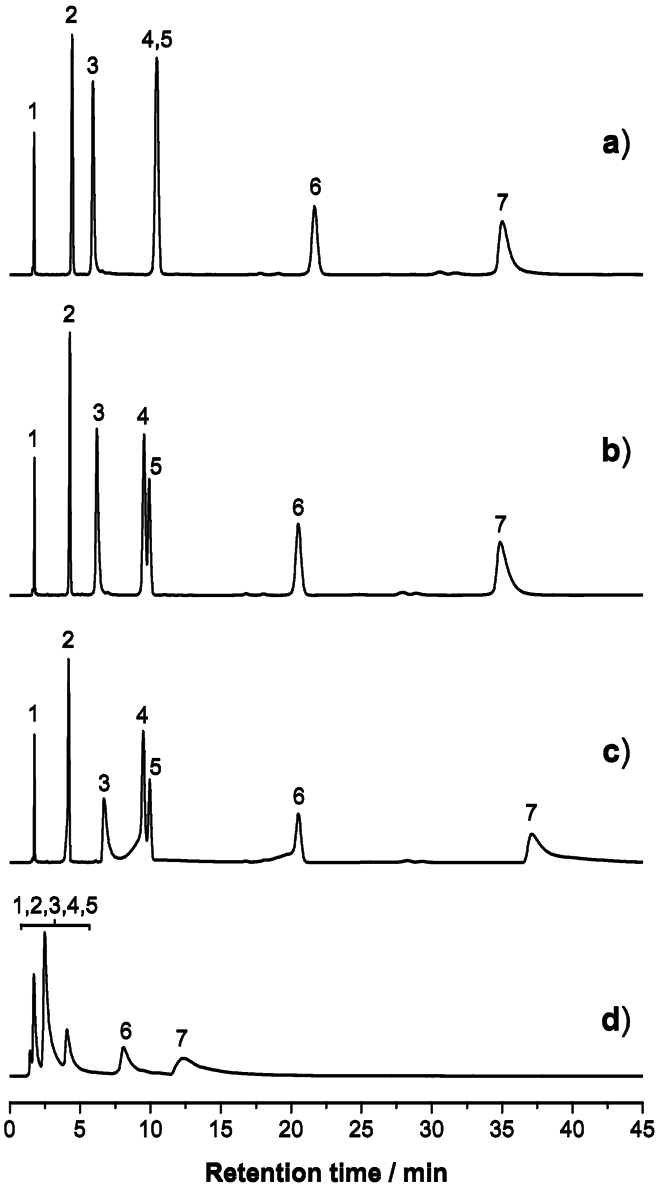

Figure 3-2. Column performance of the Waters XSelect CSH C18 column: (a) brand-new status, (b) after neutral heating phase, (c) after acidic heating phase and (d) after basic heating phase. Neue test analytes: dihydroxyacetone (1), propylparaben (2), propranolol (3), dipropyl phthalate (4), naphthalene (5), acenaphthene (6), and amitriptyline (7). Chromatographic conditions: isocratic, mobile phase: 35:65 (v/v) 20 mM phosphate buffer at pH 7/MeOH, flow rate: 1 mL min^{-1}; temperature: isothermal at 30 °C; UV-detection at 254 nm.

Regarding the XSelect CSH C18 (Figure 3-2), the results allow for an assessment of the influence of the surface charge modification on high-temperature stability in comparison to the unmodified XBridge phase. The performance of the XSelect CSH C18 at high temperatures is slightly weaker as can be seen from the losses in hydrophobicity (Figure 3-1a). The retention factor ratio of Figure 3-1c also shows a slightly worse behavior over time. Here, the surface charges of the modification seem to intensify the increase in surface

activity which is normally attributed to silanophilic interactions. The more bonded phase is lost, the higher the influence of the additional surface charges on retention of the analytes. However, high-temperature stability of the column (even at acidic conditions) is still superior to most silica-based columns due to the small loss of bonded phase. Furthermore, no change in the elution order is observed (Figure 3-2), although secondary interactions are increased.

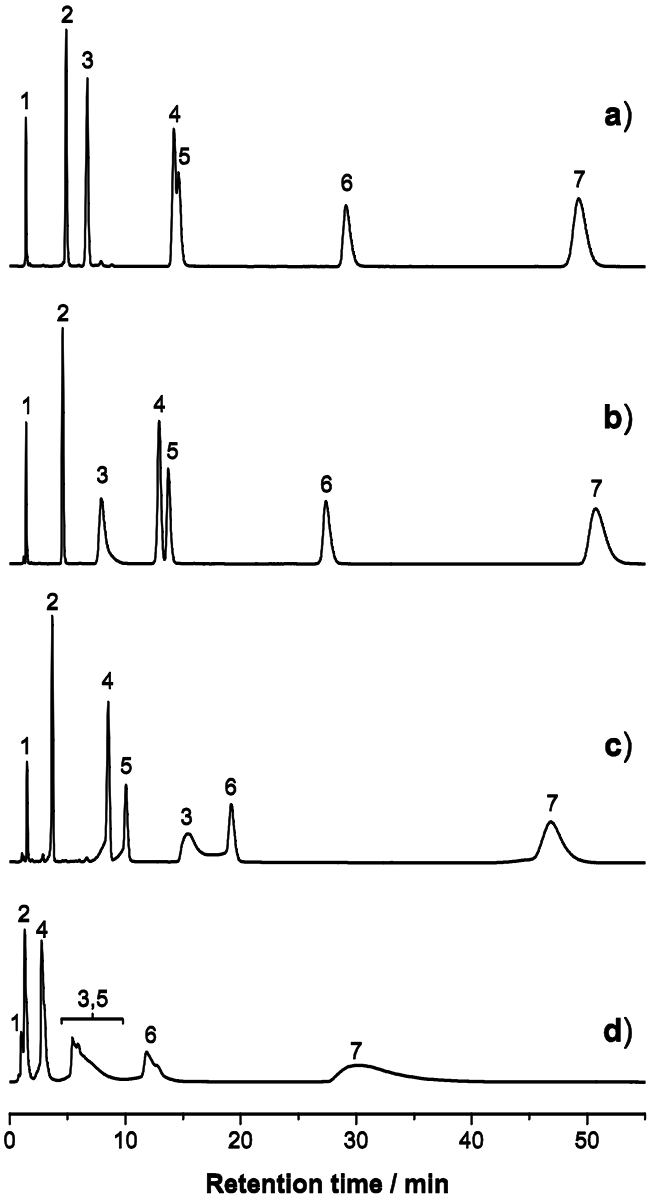

Figure 3-3. Column performance of the YMC Triart C18 column: (a) brand-new status, (b) after neutral heating phase, (c) after acidic heating phase and (d) after first cycle of the basic heating phase. Neue test analytes: dihydroxyacetone (1), propylparaben (2), propranolol (3), dipropyl phthalate (4), naphthalene (5), acenaphthene (6), and amitriptyline (7). Chromatographic conditions: isocratic, mobile phase: 35:65 (v/v) 20 mM phosphate buffer at pH 7/MeOH, flow rate: 1 mL min^{-1}; temperature: isothermal at 30 °C; UV-detection at 254 nm.

3.3.1.3 Shell particles

The Ascentis Express C18 was not part of the comparison because our results show that this particular phase rapidly degraded when operated at 150 °C (see SI-Figure 3-4). No hardware failure was obvious. Comparing the results to those of the fully porous Ascentis stationary phase tested in the earlier publication [1], the use of the core–shell stationary phase type does not enhance high-temperature stability. Therefore, the successful operation of other core–shell stationary phases at high temperatures may be caused rather by other modifications than by the core. In case of the Agilent Poroshell 120 SB-C18, the sterical protection of the silica surface by bulky alkyl side chains could be the reason for the reported temperature stability [30], because it provides a similar stability to the fully porous Zorbax SB C18 [1].

3.3.2 Other stationary phase materials

3.3.2.1 Showa Denko Shodex ET-RP1 4D (polymer phase)

The high-temperature test results for the Shodex column are shown in Figure 3-4.

As expected after the promising test results reported by Vanhoenacker et al. [27], the ET-RP1 material appeared to be comparably stable. Low hydrophobicity losses are visible over the time of neutral and acidic elution at 150 °C when looking at the retention of analytes 3 and 4. In contrast to many other polymer phases, retention is not solely obtained via the polymer. According to the manufacturer, the particle base material is a polyvinyl alcohol to which C18 functional groups are “anchored” as described by Vanhoenacker et al. [27]. Therefore, the losses in hydrophobicity could be explained by a loss of C18 groups. As a consequence of the basic heating phase, the bulk of the remaining C18 functionalization seems to be lost (Figure 3-4d) because retention of the retained solutes decreases markedly. However, it is very surprising to observe symmetrical peak shapes at that point of the procedure. This could not be observed for any of the previously tested columns. In conclusion, stationary phase degradation in case of the Shodex ET-RP1 includes losses of C18 phase, but void volume formation due to dissolution of the polymeric particle backbone can be considered to be very low, even at pH 12 and 150 °C. This offers new possibilities for a temperature-based optimization of separations which require basic mobile phase conditions.

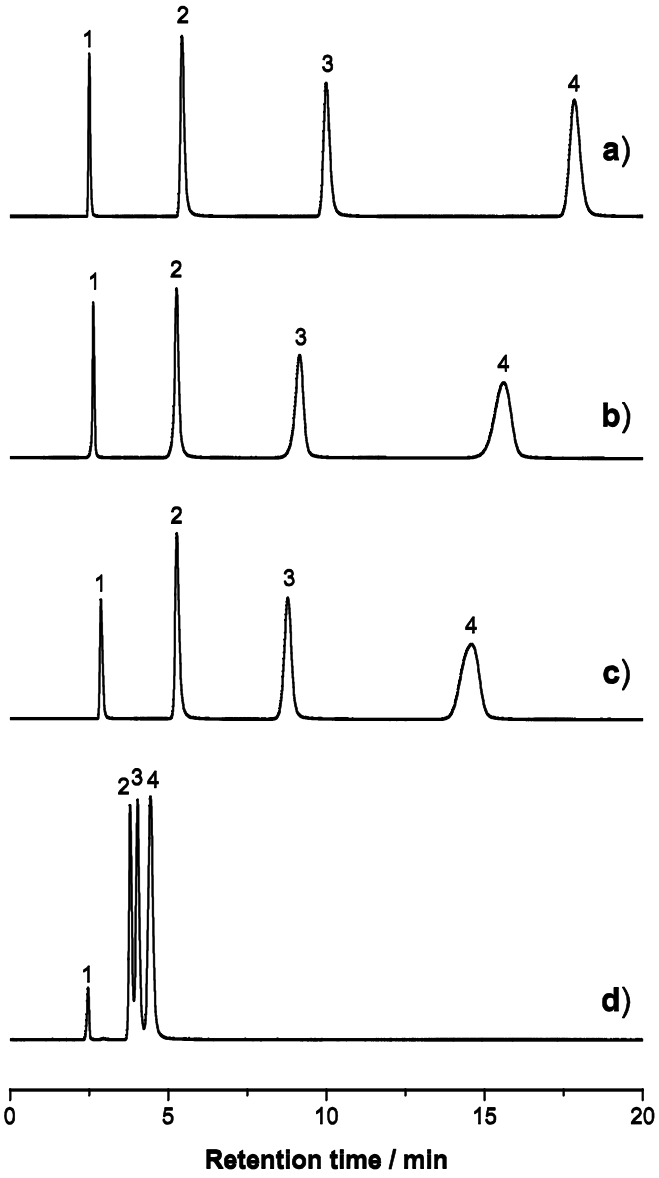

Figure 3-4. Column performance of the Showa Denko Shodex ET-RP1 4D polymer-based column: (a) brand-new status, (b) after neutral heating phase, (c) after acidic heating phase and (d) after basic heating phase. Analytes: uracil (1), methyl benzoate (2), n-butyl benzoate (3), and n-hexyl benzoate (4). Chromatographic conditions: isocratic, mobile phase: 35:65 (v/v) water/acetonitrile, flow rate: 0.6 mL min^{-1}; temperature: isothermal at 30 °C; UV-detection at 254 nm.

3.3.2.2 Waters XBridge Amide (HILIC phase)

As can be seen from Figure 3-5, column degradation of a bonded HILIC phase is not comparable to that of reversed-phase C18 columns. Bonded phase in this particular case consists of an amide group bonded to an organic linker silane. Over the time of the neutral and acidic heating phases, a probable loss of bonded phase results in increased retention times for adenine and cytosine. Surprisingly, column degradation during these heating phases does

not affect the retention of thymine leading us to the assumption that at least two completely independent retention mechanisms are the basis of the presented separation. The fact that adenine and cytosine each contain a primary amine that might be protonated at the given conditions points to an ionic interaction of these analytes with the stationary phase. The high buffer concentration of the test which, in theory, suppresses this kind of interaction even points to relatively strong ionic interaction that is enhanced by column degradation.

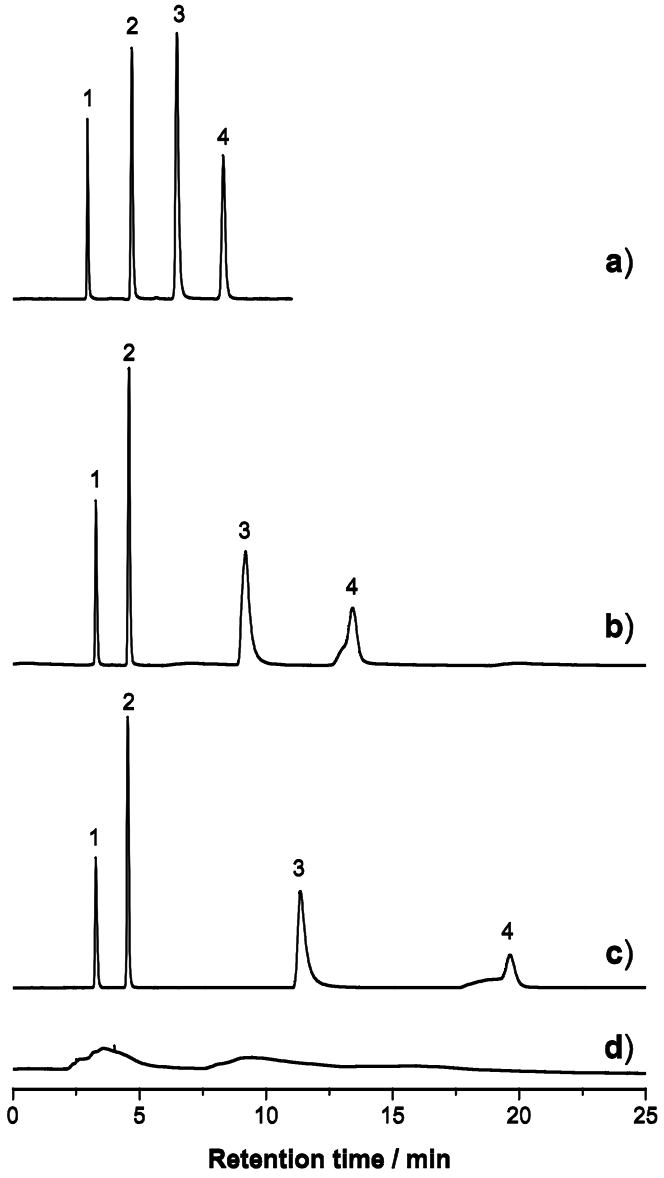

Figure 3-5. Column performance of the Waters XBridge Amide column (HILIC): (a) brand-new status, (b) after neutral heating phase, (c) after acidic heating phase and (d) after basic heating phase. Analytes: acenaphthene (1), thymine (2), adenine (3), and cytosine (4). Chromatographic conditions: isocratic, mobile phase: 20:80 (v/v) 100 mM ammonium formate buffer/acetonitrile at pH 3, flow rate: 0.5 mL min^{-1}; temperature: isothermal at 30 °C; UV-detection at 254 nm.

As known from the silica-based C18 phases, basic elution at pH 12 and 150 °C leads to a fast dissolution of the particles and an associated breakdown of performance. However, it can be concluded that Waters XBridge Amide phases can be used at high temperatures in HILIC mode, but are not as stable as the respective reversed-phase C18 equivalents.

3.4 Conclusions

A comparative approach based on retention factor analysis is now available to categorize silica-based reversed-phase columns according to their long-term high-temperature stability at 150 °C including a change in the mobile phase's pH. The method includes considerations on hydrophobicity losses as well as on silanophilic interactions which can cause elution order changes. The comparative analysis is based on column data that cover a wide range of technologies that are known to protect stationary phases from thermal and pH-driven degradation. The presented method allows for a more objective comparison of columns than conventionally reported listings according to temperature maxima where data is gathered by using several different experimental conditions. It was found that the core of core–shell particles has no significant influence on temperature stability of an HPLC column. According to our measurements, stationary phases based on ethylene bridged hybrid (BEH) technology still represent the most stable silica-based columns with regard to long-term thermal stability and changing pH, although the surface charge modification of the third generation decreases long-term stability to a small extent. In a fitted high-temperature test of an amide column, it turned out that BEH particles are as well a good basis for silica-based temperature-stable HILIC stationary phases, although long-term stability seems to be lower compared to the reversed-phase C18 versions.

The results of a further separate testing procedure for a polymer-based C18 phase are promising toward temperature optimization of basic separations and confirm the findings of Vanhoenacker et al. [27]. The peak shapes obtained were still symmetrical after breakdown of performance induced by elution at pH 12 and 150 °C.

In total, four of eight newly tested commercially available stationary phases expand the list of high-temperature compatible phases. In future studies, further in-depth characterization of the successfully stability-screened phases could reveal interesting information on chemical processes during column degradation.

Acknowledgements

The authors would like to thank for financial support from the German Federal Ministry of Economics and Technology within the agenda for the promotion of industrial cooperative research and development (IGF) based on a decision of the German Bundestag. The access was organized by the AiF, Arbeitsgemeinschaft industrieller Forschungsvereinigungen, Cologne, Germany (IGF-Project No. 16120N). Moreover, all column donations by the vendors are gratefully acknowledged.

3.5 References

[1] Teutenberg, T.; Hollebekkers, K.; Wiese, S.; Boergers, A. *Temperature and pH-stability of commercial stationary phases*. J. Sep. Sci. 2009, ***32***, 1262-1274.

[2] Heinisch, S.; Rocca, J. L. *Sense and nonsense of high-temperature liquid chromatography*. J. Chromatogr. A 2009, ***1216***, 642-658.

[3] Smith, R. M. *Superheated water chromatography - A green technology for the future*. J. Chromatogr. A 2008, ***1184***, 441-455.

[4] Teutenberg, T. *Potential of high temperature liquid chromatography for the improvement of separation efficiency—A review*. Anal. Chim. Acta 2009, ***643***, 1-12.

[5] Teutenberg, T. *High-Temperature Liquid Chromatography - A User's Guide for Method Development*. Royal Society of Chemistry: Cambridge, UK, 2010.

[6] Teutenberg, T. In *Extreme Chromatography: Faster, Hotter, Smaller*; Byrdwell, W. C.; Holcapek, M., Editors; AOCS Press: Urbana, IL, USA, 2011; pp. 129-174.

[7] Vanhoenacker, G.; Sandra, P. *High temperature and temperature programmed HPLC: possibilities and limitations*. Anal. Bioanal. Chem. 2008, ***390***, 245-248.

[8] Andersen, T.; Nguyen, Q. N.; Trones, R.; Greibrokk, T. *Mesoporous polybutadiene-modified zirconia for high-temperature packed capillary liquid chromatography: column preparation and temperature programming stability*. J. Chromatogr. A 2003, ***1018***, 7-18.

[9] Ma, L. J.; Carr, P. W. *Loss of Bonded Phase in Reversed-Phase Liquid Chromatography in Acidic Eluents and Practical Ways To Improve Column Stability*. Anal. Chem. 2007, ***79***, 4681-4686.

[10] Claessens, H. A.; van Straten, M. A. *Review on the chemical and thermal stability of stationary phases for reversed-phase liquid chromatography*. J. Chromatogr. A 2004, ***1060***, 23-41.

[11] Zhang, L. J.; Kujawinski, D. M.; Jochmann, M. A.; Schmidt, T. C. *High-temperature reversed-phase liquid chromatography coupled to isotope ratio mass spectrometry*. Rapid Commun. Mass Spectrom. 2011, ***25***, 2971-2980.

[12] Majors, R. E. *Stationary-Phase Technology in Separation Science*. LC GC N. Am. 2000, ***18*** *(Number 12, December)*, 1214-1227.

[13] Teutenberg, T.; Tuerk, J.; Holzhauser, M.; Giegold, S. *Temperature stability of reversed phase and normal phase stationary phases under aqueous conditions*. J. Sep. Sci. 2007, ***30***, 1101-1114.

[14] Snyder, L. R.; Kirkland, J. J.; Dolan, J. W. *Introduction to Modern Liquid Chromatography*. 3rd edition; John Wiley & Sons: Hoboken, NJ, USA, 2010.

[15] West, C.; Elfakir, C.; Lafosse, M. *Porous graphitic carbon: A versatile stationary phase for liquid chromatography*. J. Chromatogr. A 2010, ***1217***, 3201-3216.

[16] Nawrocki, J.; Dunlap, C.; McCormick, A.; Carr, P. W. *Part I. Chromatography using ultra-stable metal oxide-based stationary phases for HPLC*. J. Chromatogr. A 2004, ***1028***, 1-30.

[17] Kirkland, J. J.; Glajch, J. L.; Farlee, R. D. *Synthesis and Characterization of Highly Stable Bonded Phases for High-Performance Liquid Chromatography Column Packings*. Anal. Chem. 1989, ***61***, 2-11.

[18] Kirkland, J. J.; Adams, J. B.; van Straten, M. A.; Claessens, H. A. *Bidentate Silane Stationary Phases for Reversed-Phase High-Performance Liquid Chromatography*. Anal. Chem. 1998, ***70***, 4344-4352.

[19] Marin, S. J.; Jones, B. A.; Felix, W. D.; Clark, J. *Effect of high-temperature on high-performance liquid chromatography column stability and performance under temperature-programmed conditions*. J. Chromatogr. A 2004, ***1030***, 255-262.

[20] Lippert, J. A.; Johnson, T. M.; Lloyd, J. B.; Smith, J. P.; Johnson, B. T.; Furlow, J.; Proctor, A.; Marin, S. J. *Effects of elevated temperature and mobile phase composition on a novel C_{18} silica column*. J. Sep. Sci. 2007, ***30***, 1141-1149.

[21] Wyndham, K. D.; O'Gara, J. E.; Walter, T. H.; Glose, K. H.; Lawrence, N. L.; Alden, B. A.; Izzo, G. S.; Hudalla, C. J.; Iraneta, P. C. *Characterization and Evaluation of C_{18} HPLC Stationary Phases Based on Ethyl-bridged Hybrid Organic/Inorganic Particles*. Anal. Chem. 2003, ***75***, 6781-6788.

[22] Al-Khateeb, L.; Smith, R. M. *Superheated water chromatography on phenyl bonded hybrid stationary phases*. J. Chromatogr. A 2008, ***1201***, 61-64.

[23] Al-Khateeb, L. A.; Smith, R. M. *High-temperature liquid chromatography of steroids on a bonded hybrid column*. Anal. Bioanal. Chem. 2009, ***394***, 1255-1260.

[24] He, P.; Yang, Y. *Studies on the long-term thermal stability of stationary phases in subcritical water chromatography*. J. Chromatogr. A 2003, ***989***, 55-63.

[25] Li, J. W.; Carr, P. W. *Effect of Temperature on the Thermodynamic Properties, Kinetic Performance, and Stability of Polybutadiene-Coated Zirconia*. Anal. Chem. 1997, ***69***, 837-843.

[26] Liu, Y.; Grinberg, N.; Thompson, K. C.; Wenslow, R. M.; Neue, U. D.; Morrison, D.; Walter, T. H.; Gara, J. E. O.; Wyndham, K. D. *Evaluation of a C18 hybrid stationary phase using high-temperature chromatography*. Anal. Chim. Acta 2005, ***554***, 144-151.

[27] Vanhoenacker, G.; Pereira, A. D.; Kotsuka, T.; Cabooter, D.; Desmet, G.; Sandra, P. *Evaluation of a new polymeric stationary phase with reversed-phase properties for high temperature liquid chromatography*. J. Chromatogr. A 2010, ***1217***, 3217-3222.

[28] Guiochon, G.; Gritti, F. *Shell particles, trials, tribulations and triumphs*. J. Chromatogr. A 2011, ***1218***, 1915-1938.

[29] Chen, H.; Horvath, C. *Rapid Separation of Proteins by Reversed Phase HPLC at Elevated Temperatures.* Anal. Meth. Instr. 1993, ***1***, 213-222.

[30] Cunliffe, J. M.; Shen, J. X.; Wei, X. R.; Dreyer, D. P.; Hayes, R. N.; Clement, R. P. *Implementation of high-temperature superficially porous technologies for rapid LC-MS/MS diastereomer bioanalysis*. Bioanalysis 2011, ***3***, 735-743.

[31] Waters Corporation *Acquity UPLC CSH and XSelect HPLC columns (product brochure 720003928EN)*. Online resource: http://www.waters.com/webassets/cms/library/docs/720003928en.pdf (last accessed: March 3rd, 2014): Milford, MA, USA, 2011.

[32] Shen, S.; Lee, H.; McCaffrey, J.; Yee, N.; Senanayake, C.; Grinberg, N.; Clark, J. *High Temperature High Performance Liquid Chromatography of Substituted Anilines using a C_{18} Hybrid Stationary Phase*. J. Liq. Chromatogr. Relat. Technol. 2006, ***29***, 2823-2834.

[33] Louw, S.; Lynen, F.; Hanna-Brown, M.; Sandra, P. *High-efficiency hydrophilic interaction chromatography by coupling 25 cm x 4.6 mm ID x 5 µm silica columns and operation at 80 °C*. J. Chromatogr. A 2010, ***1217***, 514-521.

[34] Neue, U. D.; Serowik, E.; Iraneta, P.; Alden, B. A.; Walter, T. H. *Universal procedure for the assessment of the reproducibility and the classification of silica-based reversed-phase packings - I. Assessment of the reproducibility of reversed-phase packings*. J. Chromatogr. A 1999, ***849***, 87-100.

[35] Buszewski, B.; Noga, S. *Hydrophilic interaction liquid chromatography (HILIC)-a powerful separation technique*. Anal. Bioanal. Chem. 2012, ***402***, 231-247.

[36] Hemström, P.; Irgum, K. *Hydrophilic interaction chromatography*. J. Sep. Sci. 2006, ***29***, 1784-1821.

[37] Neue, U.; Van Tran, K.; Iraneta, P. C.; Alden, B. A. *Characterization of HPLC packings*. J. Sep. Sci. 2003, ***26***, 174-186.

[38] Neue, U. D.; Alden, B. A.; Walter, T. H. *Universal procedure for the assessment of the reproducibility and the classification of silica-based reversed-phase packings - II. Classification of reversed-phase packings*. J. Chromatogr. A 1999, ***849***, 101-116.

[39] Luo, H.; Ma, L. J.; Zhang, Y.; Carr, P. W. *Synthesis and characterization of silica-based hyper-crosslinked sulfonate-modified reversed stationary phases*. J. Chromatogr. A 2008, ***1182***, 41-55.

[40] Yang, X. Q.; Dai, J.; Carr, P. W. *Analysis and critical comparison of the reversed-phase and ion-exchange contributions to retention on polybutadiene coated zirconia and octadecyl silane bonded silica phases*. J. Chromatogr. A 2003, ***996***, 13-31.

3.6 Chapter appendix – additional figures

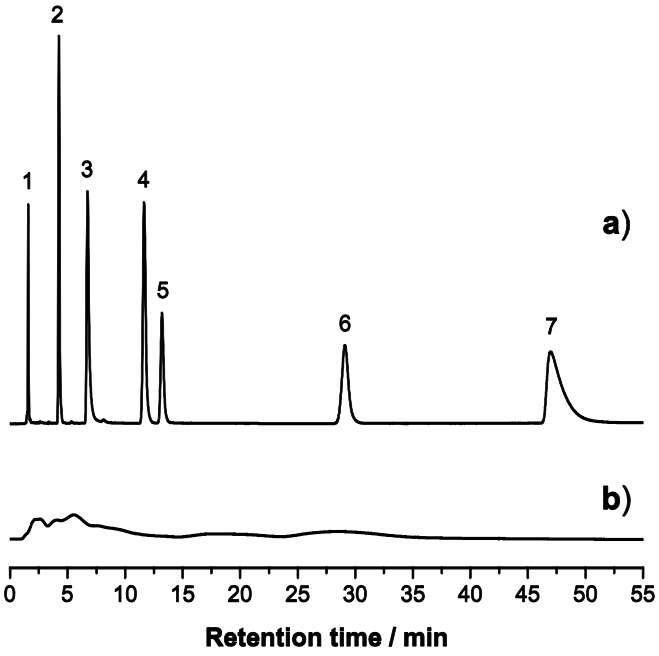

SI-Figure 3-1. Column performance of the Interchim Uptisphere Strategy C18-2 column: a) brand-new status and b) after fourth cycle of the neutral heating phase. Neue test analytes: dihydroxyacetone (1), propylparaben (2), propranolol (3), dipropyl phthalate (4), naphthalene (5), acenaphthene (6), amitriptyline (7). Chromatographic conditions: Isocratic, mobile phase: 35:65 (v/v) 20 mM phosphate buffer at pH 7/MeOH, flow rate: 1 mL min^{-1}; temperature: isothermal at 30 °C; UV-detection at 254 nm.

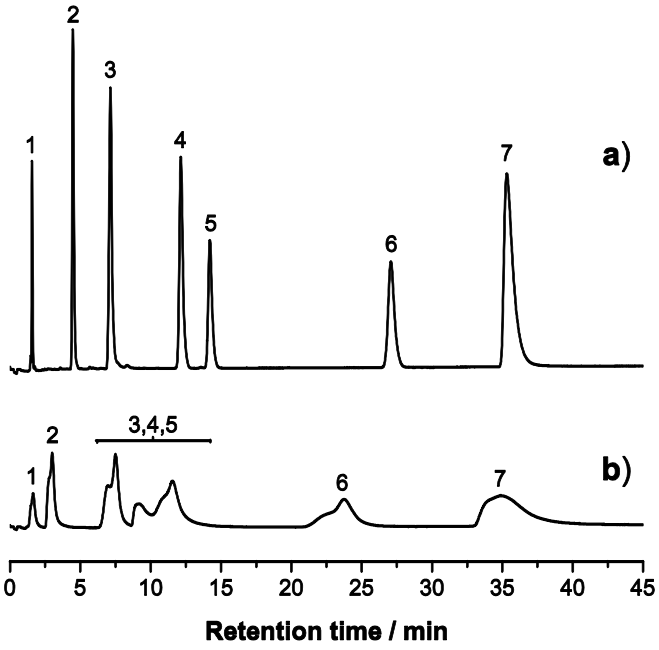

SI-Figure 3-2. Column performance of the Interchim Uptisphere Strategy C18-3 column: a) brand-new status and b) after neutral heating phase. For analytes and conditions see SI-Figure 3-1.

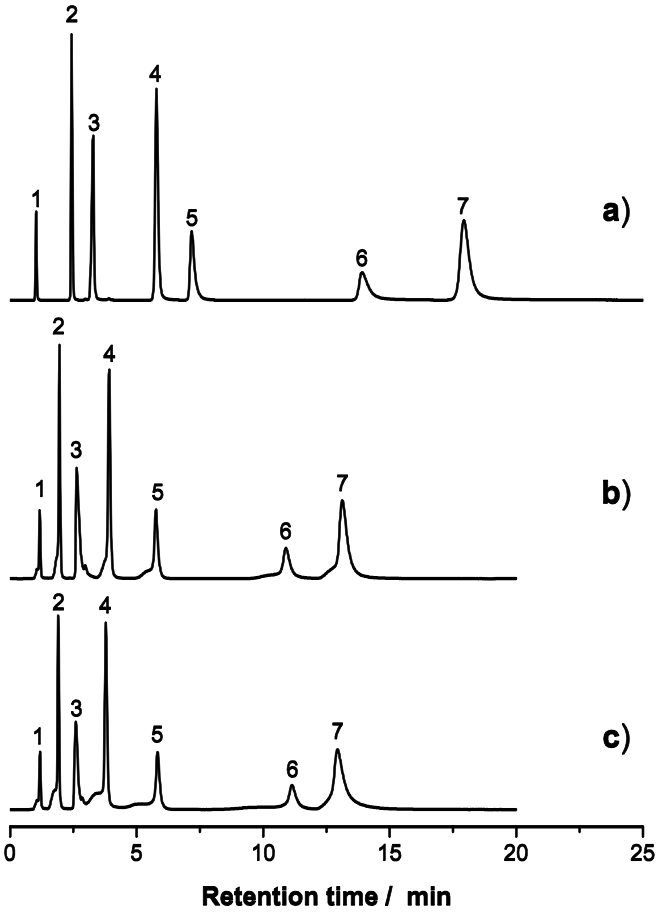

SI-Figure 3-3. Column performance of the AkzoNobel Kromasil Eternity-2.5-C18 column: a) brand-new status, b) after neutral heating phase and c) after first cycle of the acidic heating phase. Neue test analytes: dihydroxyacetone (1), propylparaben (2), propranolol (3), dipropyl phthalate (4), naphthalene (5), acenaphthene (6), amitriptyline (7). Chromatographic conditions: Isocratic, mobile phase: 35:65 (v/v) 20 mM phosphate buffer at pH 7/MeOH, flow rate: 1 mL min^{-1}; temperature: isothermal at 30 °C; UV-detection at 254 nm.

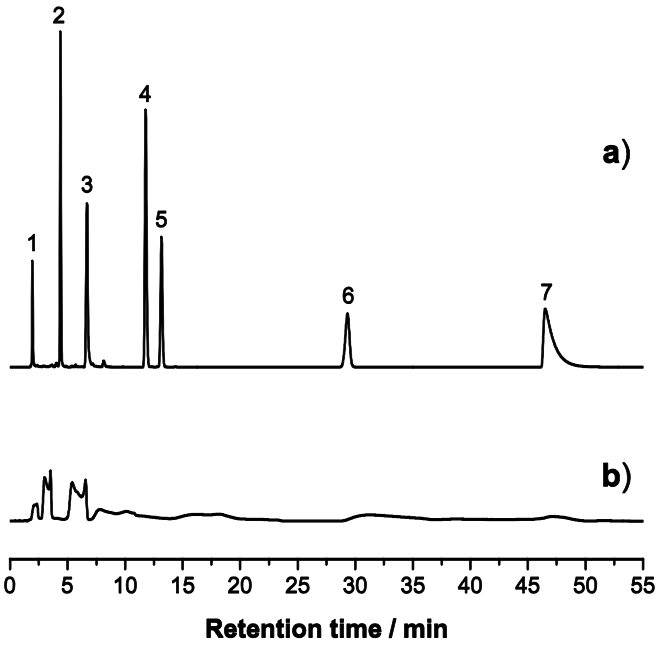

SI-Figure 3-4. Column performance of the Supelco Ascentis Express C18 column (fused-core): a) brand-new status and b) after neutral heating phase. Neue test analytes: dihydroxyacetone (1), propylparaben (2), propranolol (3), dipropyl phthalate (4), naphthalene (5), acenaphthene (6), amitriptyline (7). Chromatographic conditions: Isocratic, mobile phase: 35:65 (v/v) 20 mM phosphate buffer at pH 7/MeOH, flow rate: 0.7 mL min^{-1}; temperature: isothermal at 30 °C; UV-detection at 254 nm.

Chapter 4 Instrumentation and concept revision

The development of separation systems on the basis of online, comprehensive two-dimensional liquid chromatography (LC×LC) is a highly complex task, not just because of the high amount of variable operation parameters, but also due to the high demands on the instrumentation. Therefore, the practitioner should make as many decisions as possible prior to the implementation. Of course, an important source for decision-making support is the available literature on this subject. However, in consequence of the high instrumentation demands, reported methods are very often strongly connected to the respective hard- and software. The use of new or unconventional hardware potentially leads to problems and should therefore be carefully evaluated in advance. As a miniaturization of both liquid chromatographic dimensions is a central element of the concept, it is of major importance to become acquainted to the hard- and software that will be used as a development platform. Consequently, the development platform for the multidimensional system will be introduced in this chapter to give an overview on possibilities and practical limitations. On the basis of a critical reflection on the properties of the development platform, the two preliminary studies (Chapter 2 and Chapter 3) and recent literature, the decisions concerning the implementation of the multidimensional system are explained. This includes the choice of the stationary phases, column hardware dimensions, solvent systems, and the heating concept for both dimensions. At the end of this chapter, an overview scheme of the chosen concept for the final implementation of the multidimensional system is presented.

4.1 The development platform

4.1.1 The LC pump systems

Figure 4-1 shows a photograph of the NanoLC-Ultra 2D system that was used as the development platform for the miniaturized online LC×LC part of the multidimensional system. It was originally developed by Eksigent (now: part of AB Sciex, Dublin, CA, USA) for diverse LC applications in the field of biochemical analysis, most importantly for proteomics [1]. This requires multicolumn arrangements, for example trapping/desalination configurations, but as well stop-flow comprehensive two-dimensional approaches that combine strong cation exchange chromatography with C18 reversed phase chromatography as known from the MudPIT techniques [2-5]) [1].

Figure 4-1. The Eksigent NanoLC-Ultra 2D system – the development platform for the miniaturized online LC×LC part of the multidimensional system. 1: cover of the air-bath column oven compartment, 2: pump outlets of the two binary gradient pumps, 3: the two integrated 10-port 2-position valves, 4: capillary outlet gap.

The components of the NanoLC-Ultra 2D are not divided into modules as it is the case for the majority of commercially available HPLC systems, but are integrated in a compact system to allow short connection paths. Moreover, all connectors and unions are designed for 1/32” outer diameter (o.d.) capillaries instead of the 1/16” standard of conventional HPLC systems. Hence, extra-column volumes can be kept low as essentially needed for nano- and capillaryLC applications (compare Section 1.4.2). The compact system contains two self-priming/self-purging pneumatic binary gradient pumps which allow splitless delivery of nano- and capillaryLC flows at an extended pressure range up to 10,000 psi (~690 bars). Four

different flow rate ranges between 50 nL min^{-1} and 200 µL min^{-1} can be chosen by exchanging the internal flow modules. Moreover, high variability toward capillary system configurations and multicolumn applications is provided as two 10-port 2-position valves are integrated in the NanoLC-Ultra 2D. The work space is centralized to the column oven compartment (see Figure 4-1) that includes the two valves, the outlets of the two binary gradient pumps which are at the same time the gradient mixing tees, and an air-bath heater. The software allows for setting the temperature of this oven to values between room temperature (RT) +5 °C to at least 80 °C (accuracy: ±1 °C). However, it should be noted that the standard valves had a maximum temperature limit of 50 °C. Therefore, the manufacturer recommended not to exceed a temperature of 40 °C [1].

Although each of the valves could be programmed as an injection valve for full loop or time-based injection via the system's software, a satisfying solution for an automatic filling of the respective sample loop was missing. That was because Eksigent offered an optional separate injection module which was not available for the experiments. Instead, an available CTC HTS PAL autosampler was initially integrated and used in case of the solvent effect capillaryLC experiments in Chapter 2. The use of the separate injection module turned out to be disadvantageous with regard to the spatial arrangement of the modules that resulted in unacceptably long capillary ways in and out of the column oven compartment. Consequently, for the final implementation of the multidimensional system, one of the two integrated valves was used as an injector and the other as the modulator. The sample loop of the injector valve was filled manually (compare Section 5.2.3). For further one-dimensional evaluation experiments, the Eksigent ExpressLC-Ultra system (AB Sciex, Dublin, CA, USA) shown in Figure 4-2 was used.

The ExpressLC-Ultra [6] contains a pneumatic binary gradient pump that is identical in construction to those in the NanoLC-Ultra 2D system. In contrast to the latter system, the ExpressLC-Ultra provides a CCD-based multiwavelength detector that allows the acquisition of full spectra in a range of 200-375 nm (max. data acquisition rate: 100 Hz). The flow cell had a volume of 100 nL and a path-length of 5 mm. A further advantage of the ExpressLC-Ultra was its injection port. The sample loop that was mounted on an integrated 6-port 2-position valve was filled by the syringe of an HTC PAL autosampler (CTC Analytics, Zwingen, Switzerland). For this purpose, a needle port (see Figure 4-2) on top of the ExpressLC-Ultra with a bridging capillary to the injection valve was used.

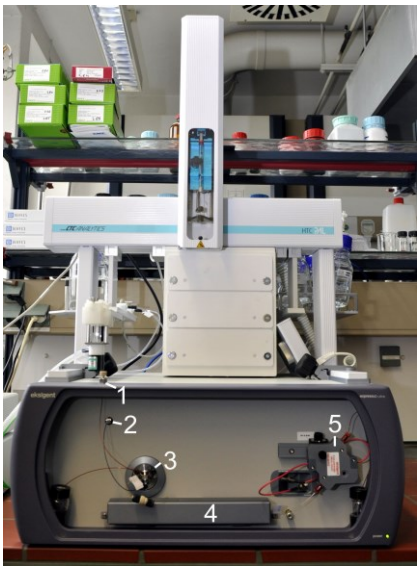

Figure 4-2. Eksigent ExpressLC-Ultra system with CTC HTC PAL autosampler on top. 1: needle port for injection. 2: binary gradient pump outlet. 3: injection valve. 4: contact heater for columns up to a length of 15 cm. 5: CCD-based multiwavelength UV-detector.

4.1.2 2-D capillary system setup

As already described in Section 1.2.3, the use of two synchronously switched 4-port 2-position valves allows for a simple 2-D capillary system setup (see Figure 1-2 on page 8). One advantage of that setup is that, in case of two equal modulation loops, capillary paths and tubing dimensions do not vary in each dimension if the valves are switched. The second advantage is that filling and flushing directions are consistent for both modulation loops. This is especially true when the D2 LC system is miniaturized as small differences in volume or sample path-length potentially result in significant retention time deviations for the same compound in consecutive D2 runs.

Although 4-port valves were not available and one of the two integrated valves of the NanoLC-Ultra 2D system needed to be used as an injector (see previous section), it was checked whether the development platform is capable of synchronized valve switching setups in general. Therefore, the scheme of Figure 1-2 was transferred to the two ten-port valves as presented in Figure 4-3.

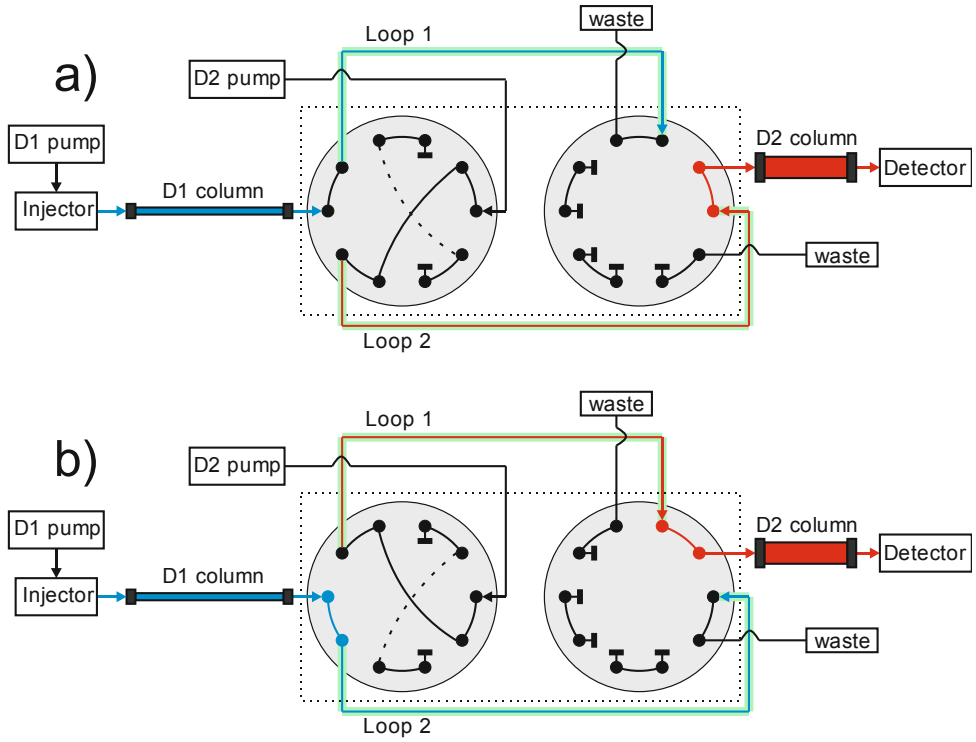

Figure 4-3. Two-loop modulation scheme using two synchronously switched 10-port 2-position valves for both valve positions, (a) and (b). Blue: sample path in first dimension. Red: sample path in second dimension. Green: modulation loops.

In order to keep the D2 capillary paths at constant length and tubing at constant volume, two equal capillaries have to be installed as port bridging capillaries on the left valve. Although this adds a further critical step in setting up the capillary system, the advantages of the synchronized 4-port valve concept persist. Therefore, the subsequent task was to program the NanoLC-Ultra 2D system for synchronized valve switching. Valve switching events can be set by entries in the gradient tables of the method files of the Eksigent software and the precise position of the valve has to be defined as “valve load” or “valve inject”. As each of the two valves is assigned to one of the binary pumps, events for both valves cannot be defined in a single gradient table. A straightforward solution to this would be the programming of the events at equal time values in two gradient tables, one for each pump and assigned valve. However, this did not result in a synchronized valve switching because small time deviations occurred during the processing of the two gradient method files. These were caused by variable flow stabilization times between method start signal and start of the gradient table processing for each pump. The only workaround for this problem was to change the connections of the system’s internal signal cables, so that both valves received the same signal, but were assigned to only one of the pumps. Finally, it can be concluded that

synchronized valve switching can generally be performed by the NanoLC-Ultra 2D system; however, a sufficient external injection solution would be required.

Instead, a single 10-port valve modulation was considered for the implementation of the multidimensional system, allowing the remaining valve to act as the injector to D1 (compare Section 4.1.1). An obvious advantage of a single-valve modulation is the fact that the abrasion by the large number of switching events affects the parts of only one valve. On the other hand, this comes at the price of the loss of an equal path length in D2 or the loss of consistent filling and flushing directions of the loops. A single-valve setup that is often used in nonminiaturized online LC×LC is based on a 10-port 2-position valve and is presented in Figure 4-4 (e.g. [7-10]).

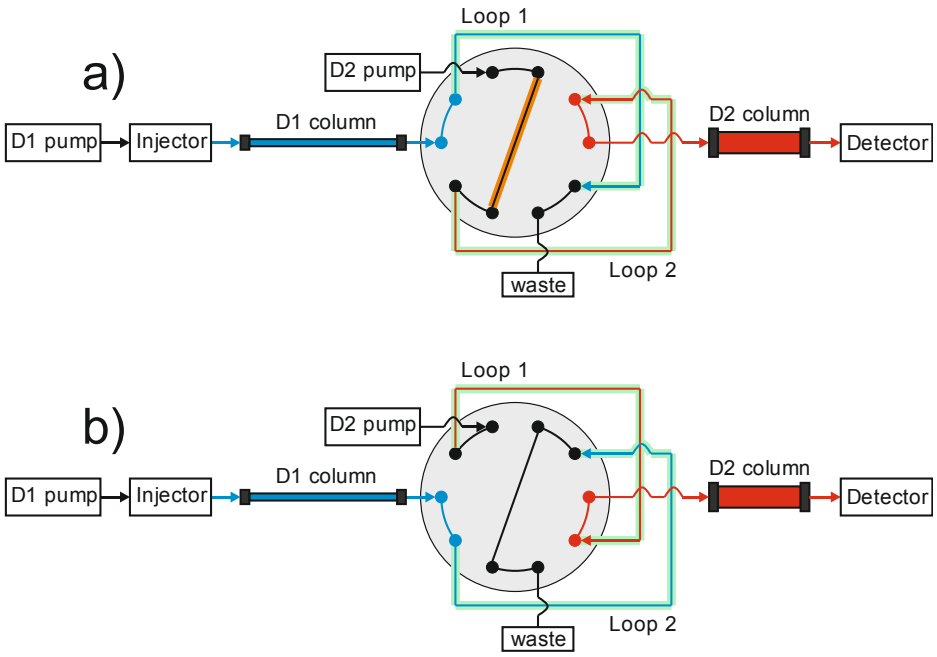

Figure 4-4. Conventionally used two-loop modulation setup using a single 10-port 2-position valve for both valve positions, (a) and (b). Blue: sample path in the first dimension. Red: sample path in the second dimension. Green: modulation loops. Orange: port bridging capillary in flow of second dimension.

As can be seen from comparing the D2 flow paths of both valve positions in Figure 4-4, a port bridging capillary that enables equal direction filling and flushing of the modulation loops lengthens the D2 flow path in position (a). The volume that is added by this capillary results in an additional delay before the D2 gradient can reach Loop 2. This means that slightly longer retention times are expected for the D2 runs flushing Loop 2 compared to those flushing Loop 1. Although this retention time deviation can usually be neglected at the high flow rates of nonminiaturized D2 systems, it potentially affects the results for

miniaturized D2 separations. The severity of this effect strongly depends on the D2 flow rate and the volume of the bridging capillary. Therefore, a setup was used for the multidimensional system that applied counter-flow flushing for one of the modulation loops as an alternative to the bridging capillary. The corresponding capillary system setup will be described in detail in Section 5.2.3.

4.1.3 Notes on the handling of miniaturized LC

The handling of miniaturized LC differs a bit from that of conventional LC and, therefore, discussion on difficulties is often charged with prejudices. In the following list, hints are provided that help avoiding problems.

- The manufacturers of miniaturized LC systems deliver tools that simplify the assembling of capillary systems and the general handling of small parts.
- As fused-silica is often used instead of PEEK or steel as the tubing material, the fittings have to be assembled more carefully to prevent the tubing from breakage. Modern fitting assemblies such as the EXP Ti-Lok fittings by Optimize Technologies (Oregon City, OR, USA), however, work with a second grip point to balance the pressure that is applied to the silica tubing.
- If no machine cut capillaries are available, rotary cutters should be used to obtain clean cuts of the tubing [11]. Otherwise, unwanted void volumes will be caused at the connection sites. A simple USB-microscope can be used to control the cut surface.
- Sample filtration and the use of high purity solvents are mandatory to avoid a plugging of parts of the capillary system. It was found during the experiments that the risk of capillary plugging is significantly decreased if the inner diameter of the tubing is ≥ 25 µm. Moreover, an acidification of watery mobile phases is a useful measure to inhibit microbial growth.

4.2 Mobile phases and elution modes

4.2.1 Mobile phase composition

As indicated in the introduction, retention and selectivity in liquid chromatography is significantly influenced by the choice of the mobile phase. In reversed-phase chromatography, the two most popular binary solvent systems are water/methanol and water/acetonitrile mainly due to their low viscosity maxima during gradient mixing [12] and their low UV-cutoff [13]. Methanol and acetonitrile differ in their chromatographic selectivity due to their different

chemical properties [14]. For example, the protic methanol can undergo polar-polar and ionic interactions. The aprotic acetonitrile, the stronger eluent of both, is more hydrophobic and undergoes stronger dipole-dipole interactions due to its -CN functional group [15]. Although the low flow rates and the absence of a detector generally allow the use of uncommon solvent systems in the first dimension of online LC×LC [13], it was decided to stick to these solvent systems because, first, miscibility is given at any ratio and, second, they were used in the solvent effect study described in Chapter 2. In accordance to this study, the water/methanol system qualifies for the first dimension since the transferred eluent strength to the second dimension is lower compared to the use of water/acetonitrile. At the same time, the water/acetonitrile system suits very well for the fast second dimension because viscosity in any mixture is significantly lower compared to that of the respective ratio of water/methanol [12], so the separation can be sped up using a higher linear mobile phase velocity (compare Section 1.3 and Equation 1-3).

The pH value influences retention of ionizable compounds [15]. Therefore, a variation of the pH between the two reversed-phase dimensions has been used by different researchers [10, 16-19] to increase the overall orthogonality of 2-D LC systems that apply reversed-phase stationary phases in both dimensions. However, pH variation was not considered for the first implementation of the multidimensional system to avoid potential problems caused by the buffer systems.

4.2.2 Elution mode

Both the use of isocratic and gradient elution provide advantages and disadvantages. Supporters of isocratic elution for RP×RP combinations usually bring forward that, first, wrap-around effects have minor influence on data analysis in approaches using a single D2 column as long as the solvent composition is not changed between the D2 runs [20]. Second, solvent strength in first and second dimension can easier be matched to avoid solvent strength effects. Third, the stability of the ion source spray for MS detection is maximized. And fourth, there is no need to account for column re-equilibration and delay times other than the dead volume. Advantages of gradient elution are band compression within the gradient window, increased peak capacity, and the possibility to refocus most peaks at the column head. The latter point is especially important in the second dimension to counteract different types of peak broadening, and thus as well analyte dilution and less pronounced solvent (strength) effects (compare Section 2.3.1) [13]. Moreover, in isocratic mode, it becomes increasingly

difficult to find the optimum solvent compositions for samples with increasing number of solutes. Therefore, a higher load of unseparated compounds is transferred to the MS detector.

In this respect, the application of gradients in both dimensions (dual-gradient mode) provides the highest potential for the separation of complex samples and – at full gradient range in every second dimension run – puts the highest demands on the LC hardware. Therefore, full range linear dual-gradient elution was chosen to get an idea of the capabilities of the miniaturized online LC×LC part.

4.3 Stationary phases

4.3.1 General notes

In 2-D LC, the optimum choice of stationary phases strongly depends on the sample composition and usually needs its own evaluation including an orthogonality comparison of different stationary phase combinations. However, this was out of the scope of this thesis. Instead, an example combination of phases was used to prove instrumental feasibility of the miniaturized online LC×LC.

4.3.2 The first dimension

It has become common practice for the combination of two reversed-phase dimensions in online LC×LC to use a less retentive D1 column to avoid the necessity of a too strong eluent in D1 that would be as well a strong eluent in D2. However, this practice is inconsistent with the need for good sensitivities as on-column focusing decreases with the retentivity of the material. This is especially true for a nanoLC column where the sample volume has to be adapted in conjunction with the inner diameter.

Reeh [21] used a short 10 mm × 2.1 mm i.d. Hypercarb phase by Thermo Fisher Scientific (Dreieich, Germany) that was serially coupled to a 5 mm × 2.1 mm i.d. C18 phase to enrich and focus polar pharmaceuticals that otherwise would elute with the void time on a C18 column. That way, sample volumes of up to 1 mL instead of a few microliters could be injected to the 2.1 mm i.d. column without negative effects on peak shapes. Moreover, a review of West et al. [22] described essential differences in retention behavior of compounds separated on porous graphitic carbon (PGC) phases such as Hypercarb compared to common reversed-phase C18 materials. At that time, this contradicted the popular opinion that a Hypercarb phase is simply a hydrophobic phase comparable to C18 phases. From this point of view, it was decided to employ Hypercarb as the stationary phase for the first dimension that

would include a large volume injection to counteract analyte dilution that is a major problem in online LC×LC approaches.

Stoll et al. [23] had already used carbon-clad zirconia particles in a high-temperature second dimension of a fast, online LC×LC approach. The authors pronounced the high retentivity and peak focusing abilities of the carbon-clad phase that was operated at 110 °C. Moreover, it had been reported that Hypercarb is extraordinary stable at high temperatures [24]. Therefore, it was decided that the first dimension column should be moderately heated to avoid a too strong retention and perhaps irreversible adsorption of certain compounds on the PGC material.

4.3.3 The second dimension

With regard to the differences in retention behavior to PGC phases [22], a reversed-phase C18 material was chosen for the fast second dimension. The results of the column stability study in Chapter 3 suggest the use of C18 particles on the basis of the BEH particle technology by Waters to obtain the maximum possible high-temperature stability. The use of polymer phases is not recommended due to the fast changes in mobile phase composition. Although the Showa Denko Shodex ET-RP1 4D stationary phase that was tested in Chapter 3 can be operated in gradient mode, fast gradients are still problematic. Moreover, the Shodex column is limited in its pressure stability. However, as was outlined in Chapter 3, it is an essential requirement that the column hardware in which the stationary phase is packed is also stable at the applied temperatures. Unfortunately, this point turned out to be the Achilles heel for the application of high-temperature LC in D2. The main problem was that the available capillary column hardware was either based on packed fused-silica capillaries that needed plastic parts for the fittings or even based on packed PEEK capillaries. Often, steel sheathings covered the packed capillaries to mimic the outer appearance of a usual HPLC column. In both cases, high temperatures cause at least deformation and a high potential of hardware failure. Although this situation required an alternative fast LC approach, an advantage of the consequent decrease of the oven temperature was that a broader range of stationary phase materials could be considered for use.

For example, sub-3-µm superficially porous (core-shell) stationary phases such as the Supelco Ascentis Express C18 phase tested in Chapter 3 were within this range. Since their emergence in 2006 [25-28], these materials have received much attention as alternatives to sub-2-µm fully porous particles known from UHPLC. The main benefit of sub-3-µm core-shell particles is that comparable optimum plate heights can be obtained at 2- to 3-times

increased column permeability [26, 29-30]. The reduced pressure drop allows the application of sub-3-µm core-shell materials even in 400 bar-standard-HPLC systems as long as extra-column volumes are carefully reduced [25, 31] as usually done in case of UHPLC systems. As the Eksigent NanoLC-Ultra 2D system does not provide the full pressure range of a conventional UHPLC system that can handle backpressures of 1000 bar, the option to use C18 functionalized sub-3-µm core-shell particles as the D2 stationary phase at moderately elevated temperature seemed to be a promising alternative to a pure high-temperature or UHPLC approach.

Correspondingly, 2.6 µm Kinetex C18 particles by Phenomenex (Aschaffenburg, Germany) were used for preliminary experiments. Later, for the study in Chapter 5, 2.6 µm SunShell C18 particles (ChromaNik Technologies, Osaka, Japan) were employed because it was claimed by the manufacturer that this comparably new stationary phase provides an increased analyte loading capacity compared to other sub-3-µm core-shell materials, especially in case of basic analytes [32].

4.3.4 D1 column dimensioning

As shown in Table 1-1, the column inner diameters of nanoLC packed-bed columns range between 25-100 µm. The largest inner diameter (100 µm) was chosen to be able to maximize the injection volume for the large volume injection. With regard to the high retentivity of the Hypercarb material, a comparably short 5 cm column packed with 5 µm particles was chosen.

4.3.5 D2 column dimensioning

The D2 column has to fulfill significantly more requirements compared to the D1 column as fast LC has to be performed.

The main arguments for choosing either a small or a large D2 column i.d. are visualized in Figure 4-5.

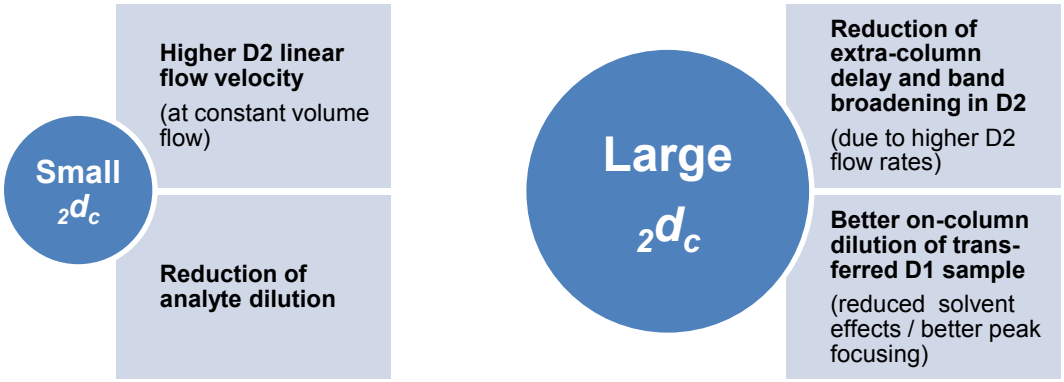

Figure 4-5. Main arguments for a smaller or larger inner diameter of the second dimension column ($_2d_c$) in online LC×LC techniques.

As can be seen from Figure 4-5, the preselection of the D2 column inner diameter is dominated by questions of speed and dilution effects. Both depicted variants provide pros and cons. A large diameter on the one hand increases analyte dilution simply by additional dispersion that occurs within the large column volume [33]. On the other hand, the transferred D1 solvent will be far better diluted, so the analyte bands potentially can be better refocused on the stationary phase. The latter process counteracts analyte dilution [13].

The question of speed, however, is of superior importance as fast LC is applied. As known from theory (see Section 1.3), chromatographic speed is proportional to the average linear mobile phase velocity (u). According to Equation 1-4, linear velocity can be increased by decreasing the column diameter at a constant flow rate. An increase of the column diameter implies that significantly higher flow rates are necessary to keep u constant, so solvent consumption increases as well. On the other hand, extra-column delay times as for example the gradient delay time are minimized for increased flow rates [34]. It can be concluded that a smaller column i.d. can enhance overall speed by increasing the speed of the separation itself, whereas the use of higher flow rates in combination with a larger column i.d. decreases the contribution of extra-column volumes to the analysis time.

This means that for an optimum of speed, the stationary phase in combination with the column i.d. should be chosen in a way that the optimum flow rate is high enough to keep the influence of the extra-column volumes low, but low enough to allow the use of a small i.d. column to optimize toward linear velocity. An essential requirement for a linear velocity optimization is that the latter does not result in significant efficiency losses which depend on

the stationary phase and the experimental conditions. However, in case of a sub-3-µm core-shell stationary phase at elevated temperature, this requirement is fulfilled [25, 35].

The influence of the extra-column volume on analysis time will be discussed by using the example of the gradient delay volume (V_{GD}). It is defined as the volume from the point of gradient mixing to the column head. The gradient delay time (t_{GD}) that is needed to flush this volume can be calculated by using the fundamental equation that defines the flow rate as volume per time [34], thus, it follows:

$$t_{GD} = \frac{V_{GD}}{F} \qquad \text{Equation 4-1}$$

where F is the volumetric flow rate.

If V_{GD} is held constant (as in Figure 4-6) Equation 4-1 results in functions of the type f(x) = b/x.

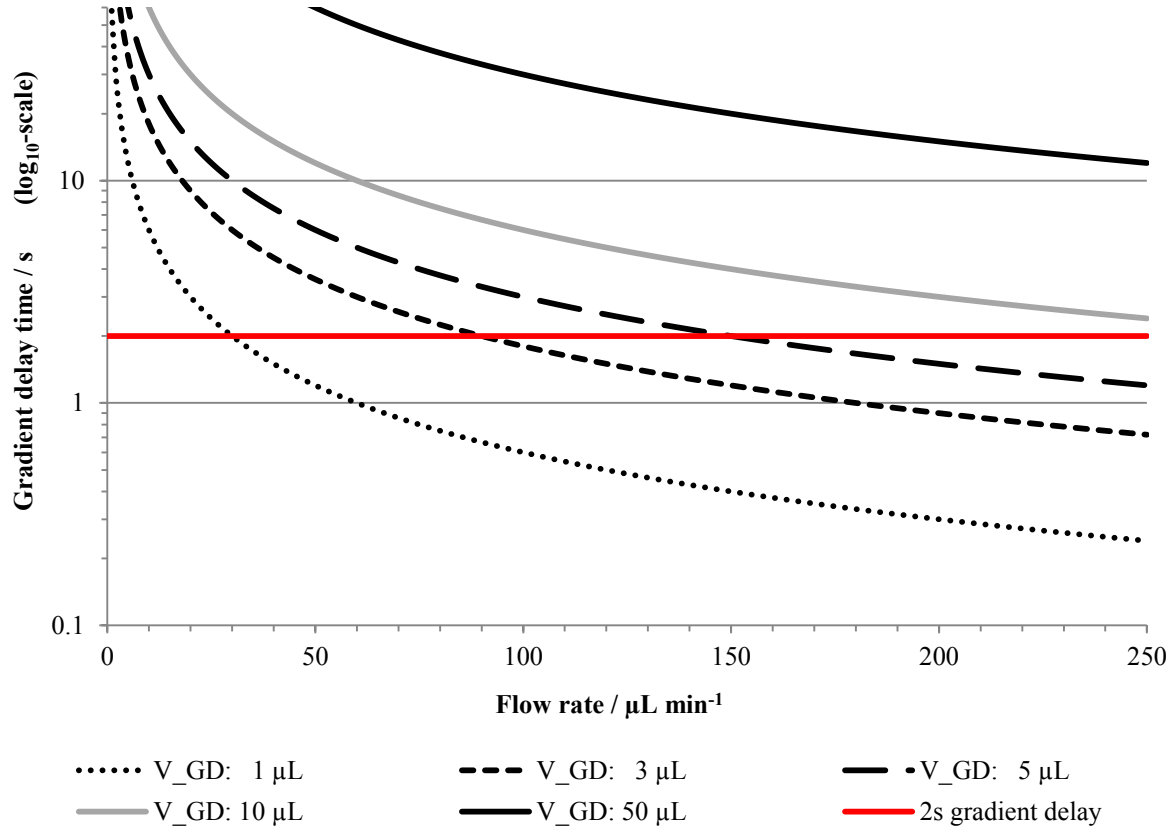

Figure 4-6. Dependence between flow rate and the resulting gradient delay time for different gradient delay volumes (V_GD).

The maximum value of the time scale in Figure 4-6 has been chosen intentionally as sixty seconds is the whole time that is available for one D2 cycle. As can be seen from Figure 4-6, the gradient delay time drastically increases at low flow rates. A 2 s gradient delay (3.3%) was set as a significance level. A delay below this tolerable value guarantees that the gradient delay time is not a significant part of the cycle time – keeping in mind that the extra-column volume from the column end to the detector will also be added to the analysis time. As shown in Figure 4-6, this significance level can only be reached by gradient delay volumes << 10 µL within the given flow rate range. Moreover, it can be seen from the equation and the figure that the gradient delay volumes have to be minimized together with the flow rate at an equal rate to keep the delay constant.

A gradient delay volume of 50 µL is a typical value for modern UHPLC instruments with small standard mixers (usually ~ 35 - 45 µL). Miniaturized mixers (1 – 25 µL) are available for capillary-UHPLC flow rates and columns. Accordingly, smaller gradient delay volumes below 10 µL can be obtained if the tubing dimensions are selected appropriately. The lowest delay volumes of around 1 µL can be obtained if no mixer is used. However, this potentially results in a baseline ripple for conventional piston-based pumps that affects the sensitivity of the detector. The Eksigent pump systems used for this study are pneumatic pumps that do not need a separate mixer post to the tee-connector that unifies and mixes the flows of both gradient channels. Thus, gradient delay volume is easily minimized to 1 µL for capillaryLC experiments including a 300 nL sample loop.

From Figure 4-6 it follows that D2 column inner diameter should allow a flow rate of at least 30, better 40 µL min^{-1} to avoid a too strong influence of the gradient delay in case of a 60 s cycle time.

The chromatogram in Figure 4-7, acquired on the ExpressLC-Ultra system by Leonhardt [36], implies that a flow rate of 40 µL min^{-1} can be easily performed on a 50 mm × 0.3 mm i.d. column packed with 2.6 µm Kinetex C18 particles.

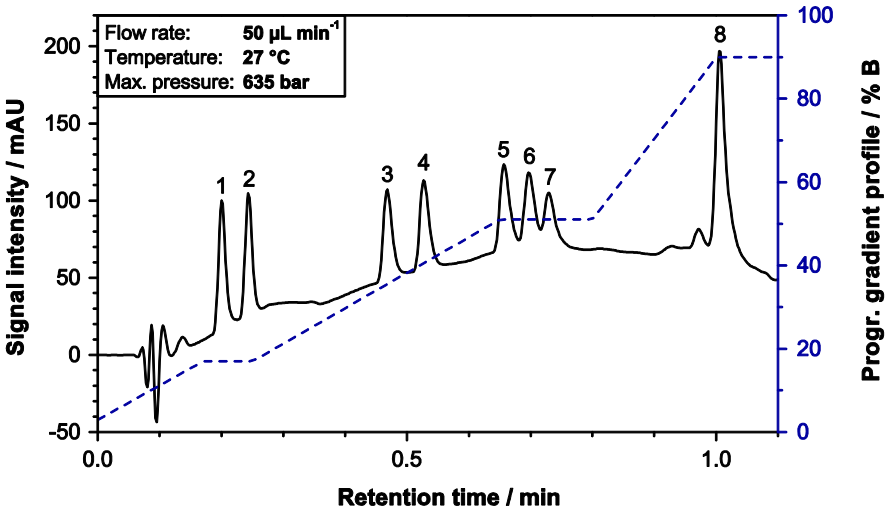

Figure 4-7. Separation of a mixture of eight pharmaceuticals on a 50 mm × 0.3 mm i.d. column packed with 2.6 µm core-shell Phenomenex Kinetex C18 particles. Mobile phase: (eluent A) 20 mM ammonium formate buffer at pH 3.3; (eluent B) acetonitrile. Temperature and gradient conditions calculated using DryLab Software. Injection volume: 0.1 µL. Analytes: (1) theophylline, (2) caffeine, (3) labetalol, (4) diphenhydramine, (5) bifonazol, (6) chrysin, (7) terfenadine, and (8) 1-ethyl-2-phenylindole. Detection wavelength: 205 nm. [36]

50 mm columns were the shortest available capillary-HPLC columns. The column inner diameter of 0.3 mm is already smaller than the 0.5 mm i.d. that is suggested by Eksigent for fast capillaryLC applications on both pump systems. The application of even smaller i.d.s was not considered with respect to the already high pressure drop and the need for high loading capabilities due to the transfer volume from D1.

It can be concluded that the final diameters were 0.1 and 0.3 mm for the first and second dimension, respectively. In order to compare these values to that of typical conventional online LC×LC setups which usually use 1 or 2.1 mm in D1 and 4.6 mm in D2, the relative difference of the column inner diameters of the two coupled LC dimensions (Δ i.d.) was calculated using Equation 4-2:

$$\Delta\, i.d. = \frac{{}_2d_c - {}_1d_c}{{}_2d_c} \qquad \text{Equation 4-2}$$

where ${}_2d_c$ is the i.d. of the second dimension, and ${}_1d_c$ is that of the first dimension.

The results are listed in Table 4-1.

Table 4-1. Comparison of the Δ i.d. between nonminiaturized online LC×LC and the miniaturized approach of this thesis. Conventional setups 1 and 2 show typical inner diameters of nonminiaturized online LC×LC systems that do not use a flow split between the dimensions.

	D1 column i.d.	D2 column i.d.	Δ i.d.
Conventional setup 1	1	4.6	0.78
Conventional setup 2	2.1	4.6	0.54
Multidimensional system	0.1	0.3	0.66

As can be seen from Table 4-1, the Δ i.d. used for the miniaturized online LC×LC system lies in between the Δ i.d.s of typical nonminiaturized online LC×LC systems. This indicates that the contribution to analyte dilution caused by the difference in inner diameter is not expected to be significantly higher or lower as in conventional LC×LC systems.

4.3.6 Note on column fittings

Usually, there is no discussion on column fittings as the capillary outer diameter (o.d.) is standardized to 1/16” in conventional HPLC. Several column manufacturers, however, still pack capillaryLC columns with the corresponding fittings for standard capillaries which are very large in comparison to the inner diameter of the column and the capillaries that are usually used in capillaryLC (o.d.: 1/32” or 360 µm). Consequently, PEEK sleeves – in case of 360 µm o.d. capillaries often two – are frequently used to bridge the gap between the outer diameter of the capillary and the connection bore size of the column end fitting (see Figure 4-8).

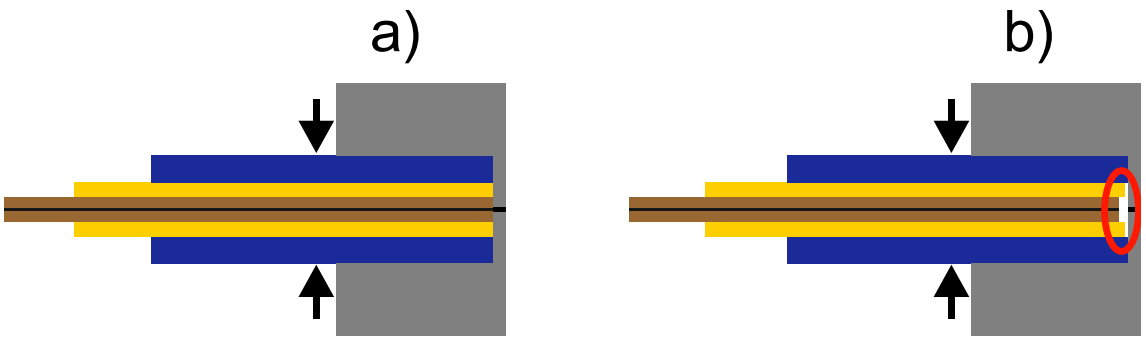

Figure 4-8. The use of PEEK tubing sleeves when mounting a 50 µm i.d. / 360 µm o.d. fused-silica capillary to a column end fitting for 1/16” capillaries. **(a)** Ideal arrangement before tightening the nut. **(b)** Void volume formation: dislocated inner sleeve and fused-silica capillary after tightening the nut. Grey: connection bore of the column end fitting. Brown: fused-silica capillary. Orange: PEEK sleeve 1/32” → 360 µm o.d. Blue: PEEK sleeve 1/16” → 1/32” o.d. Arrows: approximate grip of the ferrule.

In 2012, Gritti and Guiochon [37] who also worked with the Eksigent ExpressLC-Ultra system reported that significant extra-column band broadening can result from unwanted void volumes at the column end fittings. The same was observed in this thesis and by Leonhardt [36]. The void volumes can be formed as shown in Figure 4-8, or between the stacked sleeves or the sleeve and the capillary – up to the grip point. Accordingly, columns with end fittings for 1/32" o.d. capillaries should be used to avoid peak broadening, especially in case of the NanoLC-Ultra 2D and ExpressLC-Ultra pumps. Additionally, the use of zero-dead-volume fitting assemblies such as the EXP Ti-Lok fittings by Optimize Technologies is recommended where possible.

4.4 The simplified heating concept

As described in Sections 4.3.2 and 4.3.3, elevated temperature was intended for both columns. In order to keep the setup of the multidimensional system as simple as possible for the first experiments, it was decided to heat both LC dimensions equally by using the air-bath oven of the column compartment. This, however, required the replacement of the standard valves by models that are resistant at elevated temperatures. The new replacement valves (refer to 5.2.1 for details) were heat-proof up to 70 °C, so 60 °C was chosen as the oven temperature for isothermal heating of both LC dimensions.

4.5 Hyphenation of the MS instrument

Since the hybrid high-resolution mass spectrometer that should be hyphenated to the online LC×LC system was only available for short measurement campaigns at external locations, an older in-house hybrid tandem mass spectrometer, a 3200 QTRAP LC/MS/MS (AB Sciex, Darmstadt, Germany), was used for test installations (see Figure 4-9a).

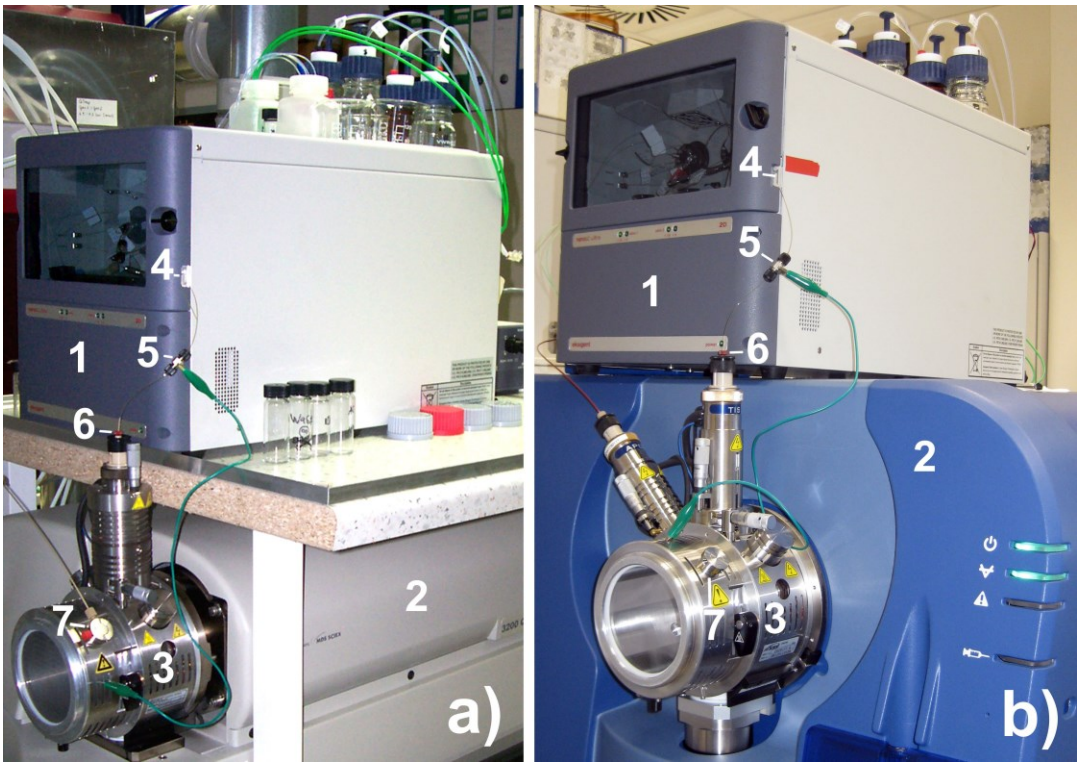

Figure 4-9. Test installations. Hyphenation of the Eksigent NanoLC-Ultra 2D to (a) a 3200 QTRAP LC/MS/MS and to (b) a TripleTOF 5600, all three instruments by AB Sciex. 1: Eksigent NanoLC-Ultra 2D, 2: respective MS-device, 3: ion source housing, 4: online LC×LC outlet, 5: stainless steel union for grounding, 6: inlet union to ion source / connection to TurboIonSpray emitter capillary for electrospray ionization, 7: grounding union for the hyphenation to nonminiaturized HPLC systems.

Despite its age, the QTRAP mass spectrometer was very well suited for this purpose as the ion source design was very similar to that of the TripleTOF 5600 instrument (AB Sciex, Darmstadt, Germany) which was later used for the implementation of the multidimensional system. The design similarity of the ion source is also visible from a comparison of photographs (a) and (b) in Figure 4-9. A freely suspended steel union (5) was used in both installations to shorten the post-D2-column flow path to the ion source inlet union (6) for a minimum post-D2-column dead volume. This way, the grounding union for use with conventional HPLC systems (7) could be skipped. The setup of Figure 4-9b deviates from the final setup described in Section 5.2 in only one point. The additional grounding steel union (5) was obsolete because the inlet union (6) of the ion source was replaced with a steel union in conjunction with a replacement of the emitter capillary. Thus, grounding could be achieved directly at the ion source inlet.

4.6 The concept

Figure 4-10 sums up the key features of the multidimensional system prior its final implementation.

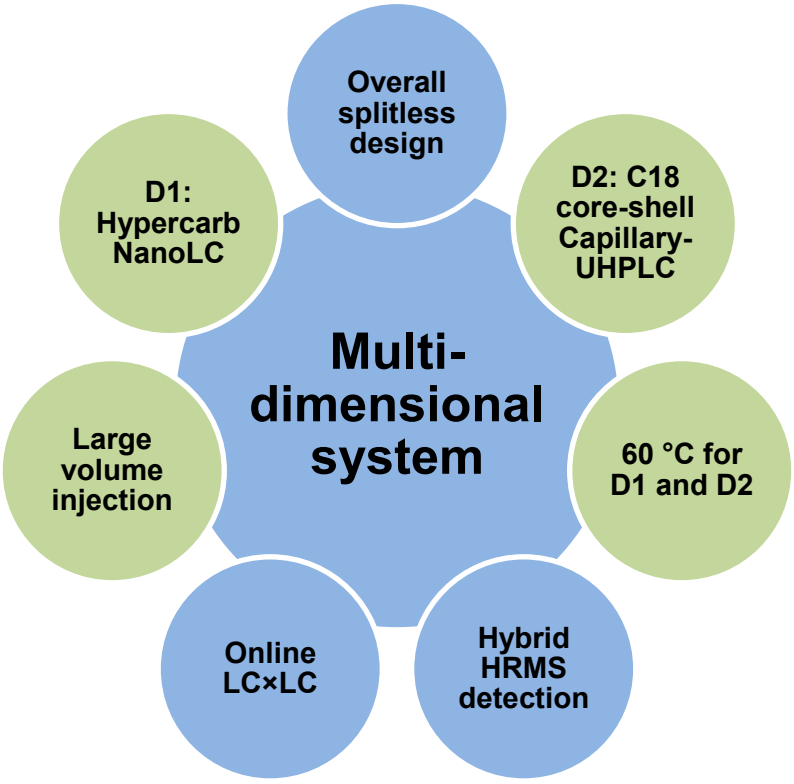

Figure 4-10. Overview of the concept for the implementation of the multidimensional system. Green: Variable features resulting from the considerations in this chapter. Blue: Basic features.

The online LC×LC and the hybrid high-resolution mass spectrometry (hybrid HRMS) constitute the fundaments of the concept. The splitless hyphenation of the two methods is facilitated by the consistent miniaturization of the LC dimensions. The application of a Hypercarb phase in D1 allows for a large volume injection. A sub-3-µm core-shell stationary phase with C18 functionalization is operated at extended pressure and elevated temperature to obtain the necessary D2 speed. A simplified heating of both columns is achieved by using a single compartment.

Acknowledgements

The author would like to thank for financial aid support the German Federal Ministry of Economics and Technology within the agenda for the promotion of industrial cooperative

research and development (IGF) on the basis of a decision by the German Bundestag. The access was opened by the member organization Environmental Technology and organized by the AiF, Arbeitsgemeinschaft industrieller Forschungsvereinigungen, Cologne, Germany (IGF Project No. 15928 N). AB Sciex and Julia Jasak, formerly Bayer CropScience, now AB Sciex, are acknowledged for providing a first opportunity to work with the TripleTOF 5600 system. Hagen Preik-Steinhoff (VICI International, Schenkon, Switzerland) is acknowledged for support on valve technology and Juergen Maier-Rosenkranz from Grace Discovery Sciences (Worms, Germany) for organizing the packing of micro-LC columns.

4.7 References

[1] Eksigent Technologies *data sheet: NanoLC-Ultra™ system*. Online resource: http://www.eksigent.com/Documents/Downloads/Literature/NanoLCUltra_DataSheet_0208_LR.pdf (last accessed: March 3rd, 2014), Dublin, CA, USA, 2008.

[2] Washburn, M. P.; Wolters, D.; Yates, J. R. *Large-scale analysis of the yeast proteome by multidimensional protein identification technology*. Nat. Biotechnol. 2001, ***19***, 242-247.

[3] Wolters, D. A.; Washburn, M. P.; Yates, J. R. *An Automated Multidimensional Protein Identification Technology for Shotgun Proteomics*. Anal. Chem. 2001, ***73***, 5683-5690.

[4] McDonald, W. H.; Ohi, R.; Miyamoto, D. T.; Mitchison, T. J.; Yates, J. R. *Comparison of three directly coupled HPLC MS/MS strategies for identification of proteins from complex mixtures: single-dimension LC-MS/MS, 2-phase MudPIT, and 3-phase MudPIT*. Int. J. Mass Spectrom. 2002, ***219***, 245-251.

[5] Motoyama, A.; Xu, T.; Ruse, C. I.; Wohlschlegel, J. A.; Yates, J. R. *Anion and Cation Mixed-Bed Ion Exchange for Enhanced Multidimensional Separations of Peptides and Phosphopeptides*. Anal. Chem. 2007, ***79***, 3623-3634.

[6] Eksigent Technologies *product note: Introducing the ExpressLC-Ultra® system: UHPLC with all the advantages of micro-LC*. Online resource: http://www.separations.nl/docs/system%20Eksigent%20ExpressLC%20ultra.pdf (last accessed: March 3rd, 2014), Dublin, CA, USA, 2010.

[7] van der Horst, A.; Schoenmakers, P. J. *Comprehensive two-dimensional liquid chromatography of polymers*. J. Chromatogr. A 2003, ***1000***, 693-709.

[8] Dugo, P.; Favoino, O.; Luppino, R.; Dugo, G.; Mondello, L. *Comprehensive Two-Dimensional Normal-Phase (Adsorption) - Reversed-Phase Liquid Chromatography*. Anal. Chem. 2004, ***76***, 2525-2530.

[9] Eggink, M.; Romero, W.; Vreuls, R. J.; Lingeman, H.; Niessen, W. M. A.; Irth, H. *Development and optimization of a system for comprehensive two-dimensional liquid chromatography with UV and mass spectrometric detection for the separation of complex samples by multi-step gradient elution*. J. Chromatogr. A 2008, ***1188***, 216-226.

[10] Donato, P.; Cacciola, F.; Sommella, E.; Fanali, C.; Dugo, L.; Dacha, M.; Campiglia, P.; Novellino, E.; Dugo, P.; Mondello, L. *Online Comprehensive RPLC x RPLC with Mass Spectrometry Detection for the Analysis of Proteome Samples*. Anal. Chem. 2011, ***83***, 2485-2491.

[11] New Objective Inc. *Cutting Fused Silica Tubing (product brochure)*. Online resource: http://www.presearch.co.uk/assets/aquilantscientific/products/brochures/1673/Cutting_fused_silica_tubing.pdf (last accessed: March 3rd, 2014).

[12] Teutenberg, T.; Wiese, S.; Wagner, P.; Gmehling, J. *High-temperature liquid chromatography. Part II: Determination of the viscosities of binary solvent mixtures—Implications for liquid chromatographic separations*. J. Chromatogr. A 2009, ***1216***, 8470-8479.

[13] Stoll, D. R.; Li, X. P.; Wang, X. O.; Carr, P. W.; Porter, S. E. G.; Rutan, S. C. *Fast, comprehensive two-dimensional liquid chromatography*. J. Chromatogr. A 2007, ***1168***, 3-43.

[14] Snyder, L. R.; Carr, P. W.; Rutan, S. C. *SOLVATOCHROMICALLY BASED SOLVENT-SELECTIVITY TRIANGLE*. J. Chromatogr. A 1993, ***656***, 537-547.

[15] Snyder, L. R.; Kirkland, J. J.; Dolan, J. W. *Introduction to Modern Liquid Chromatography*. 3rd edition; John Wiley & Sons: Hoboken, NJ, USA, 2010.

[16] Sommella, E.; Cacciola, F.; Donato, P.; Dugo, P.; Campiglia, P.; Mondello, L. *Development of an online capillary comprehensive 2D-LC system for the analysis of proteome samples*. J. Sep. Sci. 2012, ***35***, 530-533.

[17] Francois, I.; Cabooter, D.; Sandra, K.; Lynen, F.; Desmet, G.; Sandra, P. *Tryptic digest analysis by comprehensive reversed phase x two reversed phase liquid chromatography (RP-LC x 2RP-LC) at different pH's*. J. Sep. Sci. 2009, ***32***, 1137-1144.

[18] Gilar, M.; Olivova, P.; Daly, A. E.; Gebler, J. C. *Two-dimensional separation of peptides using RP-RP-HPLC system with different pH in first and second separation dimensions*. J. Sep. Sci. 2005, ***28***, 1694-1703.

[19] Mondello, L.; Donato, P.; Cacciola, F.; Fanali, C.; Dugo, P. *RP-LC x RP-LC analysis of a tryptic digest using a combination of totally porous and partially porous stationary phases*. J. Sep. Sci. 2010, ***33***, 1454-1461.

[20] Murphy, R. E.; Schure, M. R. In *MULTIDIMENSIONAL LIQUID CHROMATOGRAPHY - Theory and Applications in Industrial Chemistry and the Life Sciences*; Cohen, S. A.; Schure, M. R., Editors; Jon Wiley & Sons: Hoboken, NJ, USA, 2008; pp. 127-145.

[21] Reeh, A. *Entwicklung einer Onlineanreicherung für die Multikomponentenanalyse von Arzneimitteln mittels HPLC-MS unter Verwendung einer Chromatographiesimulationssoftware*. Master thesis, Fachbereich Chemie, Hochschule Niederrhein / University of Applied Sciences: Krefeld, Germany, 2011.

[22] West, C.; Elfakir, C.; Lafosse, M. *Porous graphitic carbon: A versatile stationary phase for liquid chromatography*. J. Chromatogr. A 2010, ***1217***, 3201-3216.

[23] Stoll, D. R.; Cohen, J. D.; Carr, P. W. *Fast, comprehensive online two-dimensional high performance liquid chromatography through the use of high temperature ultra-fast gradient elution reversed-phase liquid chromatography*. J. Chromatogr. A 2006, ***1122***, 123-137.

[24] Marin, S. J.; Jones, B. A.; Felix, W. D.; Clark, J. *Effect of high-temperature on high-performance liquid chromatography column stability and performance under temperature-programmed conditions*. J. Chromatogr. A 2004, ***1030***, 255-262.

[25] Kirkland, J. J.; Langlois, T. J.; DeStefano, J. J. *Fused Core Particles for HPLC Columns*. Am. Lab. 2007, ***39***, 18-21.

[26] Gritti, F.; Tanaka, N.; Guiochon, G. *Comparison of the fast gradient performance of new prototype silica monolithic columns and columns packed with fully porous and core-shell particles*. J. Chromatogr. A 2012, ***1236***, 28-41.

[27] Gritti, F.; Cavazzini, A.; Marchetti, N.; Guiochon, G. *Comparison between the efficiencies of columns packed with fully and partially porous C-18-bonded silica materials*. J. Chromatogr. A 2007, ***1157***, 289-303.

[28] DeStefano, J. J.; Langlois, T. J.; Kirkland, J. J. *Characteristics of Superficially-Porous Silica Particles for Fast HPLC: Some Performance Comparisons with Sub-2-µm Particles*. J. Chromatogr. Sci. 2008, ***46***, 254-260.

[29] Gritti, F.; Leonardis, I.; Shock, D.; Stevenson, P.; Shalliker, A.; Guiochon, G. *Performance of columns packed with the new shell particles, Kinetex-C-18*. J. Chromatogr. A 2010, ***1217***, 1589-1603.

[30] Gritti, F.; Leonardis, I.; Abia, J.; Guiochon, G. *Physical properties and structure of fine core-shell particles used as packing materials for chromatography Relationships between particle characteristics and column performance*. J. Chromatogr. A 2010, ***1217***, 3819-3843.

[31] Gritti, F.; Sanchez, C. A.; Farkas, T.; Guiochon, G. *Achieving the full performance of highly efficient columns by optimizing conventional benchmark high-performance liquid chromatography instruments*. J. Chromatogr. A 2010, ***1217***, 3000-3012.

[32] ChromaNik Technologies Inc. *SunShell HPLC column - Core Shell Particle (product description pdf-file)*. Online resource: http://www.dichrom.com/downloads/ChromaNik/SunShell_English_dichrom_072013_web.pdf (last accessed March 3rd, 2014).

[33] Schure, M. R. *Limit of Detection, Dilution Factors, and Technique Compatibility in Multidimensional Separations Utilizing Chromatography, Capillary Electrophoresis, and Field-Flow Fractionation*. Anal. Chem. 1999, ***71***, 1645-1657.

[34] Guillarme, D.; Nguyen, D. T. T.; Rudaz, S.; Veuthey, J. L. *Method transfer for fast liquid chromatography in pharmaceutical analysis: Application to short columns packed with small particle. Part II: Gradient experiments*. Eur. J. Pharm. Biopharm. 2008, ***68***, 430-440.

[35] Gritti, F.; Guiochon, G. *Facts and Legends About Columns Packed with Sub-3-µm Core-Shell Particles*. LC GC N. Am. 2012, ***30***, 586-595.

[36] Leonhardt, J. *Entwicklung einer umfassenden zweidimensionalen HPLC auf Basis von Nano- und Kapillarsäulen mit UV- und massenspektrometrischer Detektion*. Master thesis, Fachbereich Chemie, Hochschule Niederrhein / University of Applied Sciences: Krefeld, Germany, 2011.

[37] Gritti, F.; Guiochon, G. *Kinetic performance of narrow-bore columns on a micro-system for high performance liquid chromatography*. J. Chromatogr. A 2012, ***1236***, 105-114.

Chapter 5 The multidimensional system

Redrafted from "J. Haun, J. Leonhardt, C. Portner, T. Hetzel, J. Tuerk, T. Teutenberg, T. C. Schmidt, Online and Splitless NanoLC × CapillaryLC with Quadrupole/Time-of-Flight Mass Spectrometric Detection for Comprehensive Screening Analysis of Complex Samples, Analytical Chemistry, 2013, 85 (21), 10083-10090, DOI: 10.1021/ac402002m"

A novel multidimensional separation system based on on-line comprehensive two-dimensional liquid chromatography and hybrid high-resolution mass spectrometry has been developed for the qualitative screening analysis and characterization of complex samples. The core of the system is a consistently miniaturized two-dimensional liquid chromatography that makes the rapid second dimension compatible with mass spectrometry without the need for any flow split. Elevated temperature, ultrahigh pressure, and a superficially porous sub-3-µm stationary phase provide a fast second dimension separation and a sufficient sampling frequency without a first dimension flow stop. A highly loadable porous graphitic carbon stationary phase is employed in the first dimension to implement large volume injections that help countervailing dilution caused by the sampling process between the two dimensions. Exemplarily, separations of a 99-component standard mixture and a complex wastewater sample were used to demonstrate the performance of the dual-gradient system. In the second dimension, 30 s gradients at a cycle time of 1 min were employed. One multidimensional separation took 80-90 min (~120 min including extended hold and re-equilibration in the first dimension). This approach represents a cost-efficient alternative to on-line LC×LC strategies working with conventionally sized columns in the rapid second dimension, as solvent consumption is drastically decreased and analytes still are detectable at environmentally relevant concentrations.

5.1 Introduction

Hyphenation of liquid chromatography and mass spectrometry (LC-MS) is widely accepted and used for the analysis of complex environmental samples that can contain hundreds of semi- and nonvolatile substances [1]. For a target screening of a limited number of analytes with reference standards, a sufficient identification of the targets can often be achieved by fragmentation experiments carried out on conventional unit-resolution tandem mass spectrometers (MS/MS). In contrast, the application of hybrid full-scan high-resolution mass spectrometers (hybrid HRMS), such as quadrupole/time-of-flight (QqTOF) or linear ion trap/orbitrap, can help to avoid false positives resulting from the limitations of conventional MS/MS [2]. The additional high mass accuracy and mass resolving power enhance selectivity against the background signals of the matrix and allow the determination of the "exact mass" as well as retrospective data analysis [2]. These benefits of hybrid HRMS are pronounced in the case of screening for suspected or unknown compounds. However, co-eluting isobars can still lead to false positive results. Moreover, matrix effects resulting from coelution of a large amount of ionizable matrix compounds can suppress ionization of the analytes in the ion source [3-4]. One approach to minimize coelutions is to simply increase the peak capacity of the chromatographic system, for example, by using ultrahigh-performance liquid chromatography (UHPLC) [5]. However, the introduction of additional selectivity in terms of a second chromatographic dimension which helps to separate the analytes from interfering matrix is a more promising approach for avoiding matrix effects in particular.

In the past decade, comprehensive two-dimensional liquid chromatography (LC×LC) has gained much interest, as can be seen from several reviews [6-10]. This boost in publications on LC×LC surely coincides with the commercialization of promising hardware such as UHPLC systems or the sub-3-µm superficially porous particles [9]. Hyphenation of LC×LC to mass spectrometry (MS) was recently reviewed in a devoted book edited by Mondello [11-12]. In principle, all possible effects and problems known from the hyphenation of one-dimensional liquid chromatography (1-D LC) to mass spectrometry can as well arise for the LC×LC-MS combination, as the MS is still connected to only one liquid chromatographic dimension, which is the second dimension (D2). Depending on the LC×LC mode in use, however, the operating conditions of the D2 can be dictated by the Murphy-Schure-Foley (M-S-F) criterion that every peak of the first dimension (D1) has to be sampled about three to four times for a low-loss conservation of the D1 separation [10, 13]. This rule does not necessarily affect D2 conditions of off-line operated LC×LC systems, where there is no time

dependence between both LC dimensions [14-17]. Nevertheless, it means a major constraint to systems used in the on-line mode, especially in case of a fast single-column D2 system. Here, the maximum D2 run time is defined by the time in which one fraction of the D1 effluent is collected [10]. Thus, to fulfill the M-S-F criterion, D2 speed has to be very fast, otherwise resolution is decreased by undersampling [9]. Therefore, much attention is given to shorten D2 run times that are typically around 20 to 120 s. Speed is usually gained by the application of flow rates as high as 1 to 5 mL min^{-1} on short D2 columns with diameters of 1 mm and above [10-12]. Apart from the economically inefficient solvent consumption, a flow splitter is necessary to avoid overloading the ion source of the mass spectrometer. Upper tolerable flow rate limit of common electrospray ionization (ESI) sources is approximately 1 mL min^{-1}, and for atmospheric pressure chemical ionization (APCI), it is 2 mL min^{-1} [11], however, these values are already far above the optimum. The necessity for a flow split inevitably adds losses of sensitivity [18].

Besides the possible interface overload, the practitioner has to pay attention to the data acquisition rate of the respective mass spectrometer, especially if older quadrupole-based MS systems are used, as resulting peak widths for short D2 runs can be 1-2 s and below [19]. Although fast-scanning systems of the latest generation may be capable of measuring the minimum-needed 6 to 10 data points per peak under certain conditions (e.g., reduced mass-to-charge ratio (*m/z*) range), it is recommended in the literature to switch to time-of-flight (TOF) type MS as the high data acquisition rates are more than sufficient and independent of the selected *m/z* range [11, 18]. The application of multiple D2 systems operated in parallel allows decreasing the critical D2 speed [20-22]; however, besides increased complexity, additional hardware such as columns, valves and costly MS detectors would be necessary. The alternate use of stop-flow methods also allows for a sufficient number of D1 eluate samples, but overall analysis time is drastically increased, because the D1 has to be stopped after each eluate sample to allow the D2 separation to be performed [23-26].

A different way to decrease the solvent load to the mass spectrometer is the miniaturization of the D2 to capillaryLC. Miniaturized LC×LC systems with MS detection mainly originate from the field of proteomics [27-32]. In order to achieve high peak capacities, most of them are either operated in (automated) offline mode [30], in stop-flow mode [29] or use a step-gradient [27, 31-32] ion exchange chromatography (IEC) in D1 to allow independently long D2 run times. To the best of our knowledge, the only hitherto reported on-line LC×LC system with miniaturized D2 was developed by Opiteck et al. who applied IEC in D1 and reversed-

phase chromatography in D2 to separate protein mixtures within two hours (48 fractions, 150 s each) [28].

The goal of the present work was to develop a multidimensional system for the qualitative screening analysis of complex samples on the basis of a consistently miniaturized, on-line dual-gradient LC×LC system hyphenated to hybrid HRMS detection. The system should feature a large volume injection and a completely splitless design to increase sensitivity and prevent sample losses. Supporting technologies known from nonminiaturized on-line LC×LC were used to increase second dimension speed, among those elevated temperature [10, 33-34], ultrahigh pressures [35-36] and a superficially porous sub-3-µm stationary phase [36-37].

5.2 Materials and methods

5.2.1 HPLC instrumentation

As a development platform for the LC×LC part of the multidimensional system, an Eksigent NanoLC-Ultra 2D pump system (AB Sciex, Dublin, CA, USA) was used. Its operation was controlled by a PC and Eksigent software version 3.12.1. Apart from a column oven compartment with two integrated 10-port 2-position valves, the Eksigent system contains two binary-gradient pneumatic pumps which can be variably adjusted to different nano- and microflow ranges by exchanging the respective flow module. The standard nanoflow module (50-500 nL min^{-1}) was applied for the D1 gradient pump. In the case of the D2 pump, the standard flow module was replaced by a module with a flow range of 5-50 µL min^{-1}. As flow delivery is performed without splitting, gradients can reliably be mixed at back pressures of up to ~ 690 bar (10 kpsi).

A superficially porous sub-3-µm stationary phase was used for the packing of the D2 column. Therefore, 2.6 µm SunShell C18 particles (ChromaNik Technologies, Osaka, Japan) were packed into a custom 50 mm × 0.3 mm inner diameter (i.d.) column by Grace Davison (Worms, Germany). A Hypercarb column (50 mm × 0.1 mm i.d., 5 µm particles, Thermo Fisher Scientific, Dreieich, Germany) was used in D1.

The air-bath oven was used to apply an isothermal temperature of 60 °C with an accuracy of ±1 °C on both columns and all other parts inside the compartment. The two integrated 10-port 2-position valves were not designed to be constantly operated at elevated temperature. In order to avoid severely increased rotor abrasion, two custom replacement valves (C72NX-4670DY-EKS, Cheminert Nanovolume, 100 µm port bore size, 1/32” fittings, VICI International, Schenkon, Switzerland) were mounted to the actuators.

5.2.2 MS instrumentation

The hybrid HRMS instrument used for the implementation of the multidimensional system was a TripleTOF 5600 by AB Sciex (Darmstadt, Germany) equipped with a DuoSpray ion source and a TurboIonSpray probe for ESI experiments. For the sake of low dead volumes between D2 column and detection, the mass spectrometer was modified. The standard emitter tip inside the TurboIonSpray probe was replaced by an emitter with an i.d. of 50 µm. As recommended by the manufacturer, grounding was achieved by clipping a grounding cable on one end to the slots of the source housing and on the other end directly to the inlet steel union of the ion source. MS data acquisition was controlled using a separate PC with AB Sciex Analyst TF 1.5.1. Acquired data including mass spectra were analyzed using the AB Sciex PeakView 1.2.0.1 software out of the D2 raw data.

5.2.3 Capillary system, modulation and injection

The design of the capillary system of the multidimensional system is schematically illustrated in Figure 5-1.

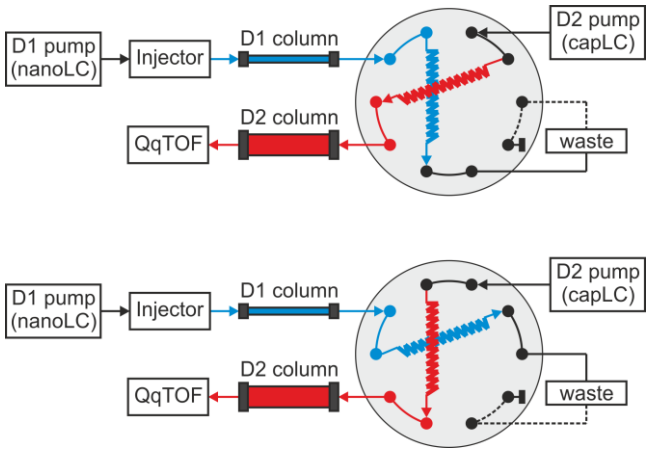

Figure 5-1. Scheme of the capillary system for both modulation valve positions. Blue: sample path in first dimension. Red: sample path in second dimension.

As is often found in the literature [18, 33, 38-42], the online LC×LC interface consists of a two-loop modulation composed of a single 10-port 2-position valve. In contrast to many interfaces of this type, counter-flow emptying of one of the two loops is used for the benefit of equal capillary volumes in D2 comparing both valve positions. Regarding the increased influence of extra-column volumes in miniaturized LC, this modification prevents retention time shifts between two consecutive D2 runs caused by an otherwise necessary port-to-port bridging capillary. In order to implement the modulation scheme of Figure 5-1, the left 10-

port valve of the Eksigent system was used as an injector to D1, and the right valve was used as the modulation valve. The injection loop to D1 was a 20 cm, 100 µm i.d. PEEKsil capillary (Upchurch Scientific, Oak Harbor, WA, USA) with a calculated volume of 1.57 µL. Prior to each 2-D analysis, this sample loop was manually filled by using a Hamilton syringe (Bonaduz, Switzerland) that was mounted to the injection valve via a capillary and a Luer lock adapter. All connection capillaries of the capillary system including both modulation loops were 360 µm outer diameter (o.d.) fused-silica purchased from Postnova Analytics (Landsberg, Germany), and they were cut to size by a Shortix GC (SGT, Middelburg, The Netherlands) rotating diamond cutter. Inner diameters of the connection capillaries were 25 and 50 µm for the first and second dimension, respectively. Both modulation loops had an equal length of 15.5 cm and an i.d. of 50 µm to avoid additional pressure drop due to restriction of the D2 pathway. The compact arrangement of pump outlets and switching valves inside the air-bath column oven compartment resulted in low extra-column dead volumes throughout the whole capillary system. Accordingly, low gradient delay volumes – calculated from the gradient mixing tee to the head of the column – were established, ~85 nL and ~1 µL for D1 and D2, respectively. In the case of D1, the injection loop does not contribute to gradient delay, as it is switched out of flow prior to gradient start.

5.2.4 Solvents

Ultrapure water (J.T. Baker, LC/MS reagent grade) was purchased from Mallinckrodt Baker (Griesheim, Germany). Acetonitrile and methanol were both LC-MS Optigrade from Promochem (LGC Standards, Wesel, Germany). All LC eluents were acidified by adding 0.1% formic acid (FA) by volume (puriss. p.a., ~ 98%, Sigma-Aldrich, Schnelldorf, Germany).

5.2.5 Standard mix and real sample

Ninety-nine substances were chosen as targets for a suspected screening of wastewater samples. These included 73 pharmaceutical drugs (among others: antibiotics, cytostatics, X-ray contrast media, steroids, beta blockers, and psychotropics), 4 metabolites of sulfonamide antibiotics, 13 pesticides, 6 mycotoxins, and 3 corrosion inhibitors. A detailed list of all substances is provided in SI-Table 5-1. Several of them are toxic, cytotoxic, carcinogenic, or possess other harmful properties. The safety data sheets provide details on handling and discharge. A multicomponent test mix containing each target in a mass concentration of 1 µg mL^{-1} was prepared in water/acetonitrile (95:5, v/v) acidified by 0.1% FA.

Groskreutz et al. recently confirmed the applicability of a new 2-D LC technique by using wastewater as a model matrix [43]. Analogously, the complex sample that was exemplarily analyzed to demonstrate the performance of our approach was a 200 mL wastewater sample taken at the inlet of the secondary (or biological) treatment step of a municipal sewage plant. Since this sample type contains very harmful substances as well as pathogenic bacteria and viruses, corresponding laboratory equipment and safety measures are needed. Sample pretreatment prior to the 2-D analysis included an adjustment of the pH to 3 using hydrochloric acid, the addition of deuterated internal standards, and solid-phase extraction (SPE) through a 200 mg Oasis HLB cartridge (Waters, Eschborn, Germany). The internal standards, 100 ng each, were bisoprolol-*d5* (LGC Standards), isoproturon-*d6* (Pestanal, Sigma-Aldrich) and racemic metoprolol-*d7* (Campro Scientific, Berlin, Germany). The SPE contained the following steps: conditioning, 5 mL methanol (5 min residence time); equilibration, 5 mL water at pH 3; sample application; washing, 5 mL of a water/methanol mixture (95:5, v/v); drying for 5 min; elution, 3 x 3 mL of methanol; the eluent was evaporated in a nitrogen stream at 40 °C, and the residue was redissolved in 2 mL of water/acetonitrile (95:5, v/v) acidified by 0.1% FA.

Both the test mix and the pretreated wastewater sample were filtered through a 0.2 µm CHROMAFIL RC 20/25 disposable syringe filter by Macherey-Nagel (Düren, Germany) prior to injection. Between the injections of wastewater samples, it is recommended to measure at least one blank as strongly retained substances may disturb the analysis of the next sample.

5.2.6 First dimension gradient programming and injection

In the first dimension, a water + 0.1% FA (eluent A) – methanol + 0.1% FA (eluent B) gradient at a flow rate of 200 nL min^{-1} was applied according to the following program: 8 min hold at 1% B, 1-99% B in 45 min, 35 min hold at 99% B, 99-1% B in 5 min, and 16 min re-equilibration (~11 column volumes). During the initial 8 min of isocratic elution, the sample loop was switched into flow and the full loop volume (1.57 µL) was injected to D1.

5.2.7 Second dimension gradient programming

In an earlier work on a unidimensional micro-LC system using an identically constructed binary gradient pump, we found that 30 s linear gradients can be performed with high accuracy and repeatability [44]. However, a pump-system dependent restriction is that fast gradients must not start or end at 0% of one of the eluent channels but at about 3-5% to ensure correct mixing and to prevent the eluent of one pump channel from entering the other.

Therefore, in the second dimension, a water + 0.1% FA (eluent A) – acetonitrile + 0.1% FA (eluent B) gradient at a flow rate of 40 µL min^{-1} was programmed as follows: 3-97% B in 0.5 min, 0.1 min hold at 97% B, 97-3% B in 0.1 min, and 0.3 min re-equilibration at 3% B (~6.8 column volumes). The gradient delay was 0.025 min. Overall, each gradient cycle took 1 min. As the D2 cycle time usually equals the time for D1 fraction collection, the resulting transfer volume to D2 was 200 nL. As a consequence of a necessary pump refill, however, the transfer volume could not be held constant over the whole analysis time.

5.2.8 Modulation at limited D2 pump volume

The used pneumatic pumps work like syringe pumps and, therefore, have a limited volume specified as 600 µL per gradient pump (300 µL per channel). We found that 13 consecutive D2 cycles could be run without interruption by an automatic pump restroke. The subsequent pump-stop, refill, and restart including flow and temperature stabilization at 3% B took 31 s on average (±1 s, standard deviation per 2-D analysis: 0.6 s). Then, the next 13 D2 cycles were run and so forth.

One option was to collect 303 nL in each 13th D1 fraction (1 min + 31 s of refill time). In order to avoid a solvent strength effect which might significantly affect the analyte's peak shape and retention time in D2 [45-46], it was instead decided to split the larger fraction in two parts. During flow stabilization at 3% B, the last fraction collected prior to each pump refill was flushed to the D2 column. Although most analytes are trapped, unretained analytes are potentially lost – if the overall signal intensity is so low that no data analysis is possible in adjacent fractions – as they are flushed to the detector that is not acquiring data during the pump refill procedure. Subsequent to the next modulation valve switching, the remaining 103 nL that is collected during the 31 s of the pump refill procedure was transferred to D2 by the first of the next 13 D2 gradient cycles. By using the split transfer, 303 nL – in the following counted as one D1 fraction – could be analyzed in one D2 gradient cycle. The according modulation valve actuation was achieved by setting switching events in the gradient table of the repeated D2 pump method every full minute from 0 to 13 min. The described D1 fractionation is visualized in SI-Figure 5-1. The dependence of D1 retention time to the D1 fraction numbers is given in Table 5-1.

Table 5-1. Relation between D1 fractions and D1 retention times.

D1 fraction	Collection time (min:s)	D2 gradient cycle	D1 retention time (min)
1 – 12	1:00	2 – 13	0 – 12
13	1:31	14	12 – 13.52
14 – 25	1:00	15 – 26	13.52 – 25.52
26	1:31	27	25.52 – 27.03
27 – 38	1:00	28 – 39	27.03 – 39.03
39	1:31	40	39.03 – 40.55
40 – 51	1:00	41 – 52	40.55 – 52.55
52	1:31	53	52.55 – 54.07
53 – 64	1:00	54 – 65	54.07 – 66.07
65	1:31	66	66.07 – 67.58
66 – 77	1:00	67 – 78	67.58 – 79.58
78	1:31	79	79.58 – 81.10
79 – 90	1:00	80 – 91	81.10 – 93.10
91	1:31	92	93.10 – 94.62
92 – 103	1:00	93 – 104	94.62 – 106.62

5.2.9 MS Parameters

Information-dependent acquisition (IDA) [47-48] was chosen as the MS strategy for a suspected screening, making use of both the single HRMS and the MS/MS functionalities of the QqTOF detector. In the primary experiments, "survey TOF scans" were carried out for an *m/z* range of 65-1000 in positive ESI ionization mode. Per IDA cycle (i.e., every 150 ms), the four most intensive precursor ions were chosen for sequential MS/MS scans with an *m/z* range of 50-1000 in order to obtain structural information from the respective product ion spectra. Based on the IDA cycle length, the programmed data acquisition rate was ~6.7 Hz. The following ion source parameters were held constant during detection: the curtain gas was set to 10 psi, ion source gas 1 and 2 to 25 psi, IonSpray voltage floating to 5500 V, declustering potential to 80 V, and temperature to 500 °C. The collision energy was 10 and 40 eV for the survey TOF scan and the product ion scans, respectively.

5.2.10 Preparation of contour plots

Contour plots were generated in the following way: The corresponding MS chromatograms were exported to ASCII files, each containing ~5200-5800 data points for 13 consecutive D2 gradient runs. Consequently, the real data acquisition rate was not constant and ranged from ~6.7 to 7.4 Hz. To achieve a constant data point number, linear interpolation was performed

in Excel 2010 (Microsoft, Redmont, WA) to 49998 data points per file. Each file was then cut to achieve one chromatogram per D2 gradient run (i.e., 3846 points per chromatogram). Visualizations were prepared using OriginPro 9 by OriginLab (Northampton, MA).

5.3 Results and discussion

5.3.1 Evaluation of system performance

At first, the 99-component mix was measured using the development system to gather LC×LC retention information on all of the 99 targets. Figure 5-2a shows a colored contour plot of the corresponding total ion current (TIC)-chromatogram.

As expected from a TIC, this perspective offers only limited information on the exact location of the analytes. Nonetheless, the high accuracy of the D2 gradient pump at the short cycle of 1 min can be seen from the noise lines at about 0.55, 0.59 and 0.78 min D2 retention time. The first two are observed at the end of the gradient, and the third occurs at the start of re-equilibration phase. Only for the signals of one series of 13 gradient cycles (compare the Section 5.2.8), a constant shift of about 0.01 min (0.6 s) to higher D2 retention is visible in Figure 5-2a. This is not an inaccuracy of the pump but a timer asynchronism caused by the use of two different computers and softwares for controlling the LC and the MS device. Thus, MS acquisition starts a bit too early for the shifted data.

The precise location of the analyte peaks in the 2-D chromatogram was determined from extracted ion chromatograms (XIC). The monoisotopic mass of a target's protonated molecular ion $[M+H]^+$ ±0.005 Da was chosen as the extraction window. In most cases, accurate mass verification allowed unambiguous identification of the target ions. Where necessary, the IDA MS/MS fragmentation pattern was additionally used. A detailed list containing the retention data of all targets is presented in SI-Table 5-2. Figure 5-2c contains an analyte map providing the locations of the peak maxima for every target after LC×LC separation of the 99-component standard mix. Peak width is not accounted for in this view and, therefore, separate spots do not necessarily mean baseline-separated compounds. Nonetheless, more than 90% of the targets resulted in countable spots that are spread over the chromatographic area. The results clearly underline that there is a significant difference in the selectivities of porous graphitic carbon (PGC) and C18 reversed-phase stationary phases, as is well-known from literature [49]. The additional selectivity helps to avoid coelution of isobars, as illustrated by the example of ifosfamide and cyclophosphamide in SI-Figure 5-2.

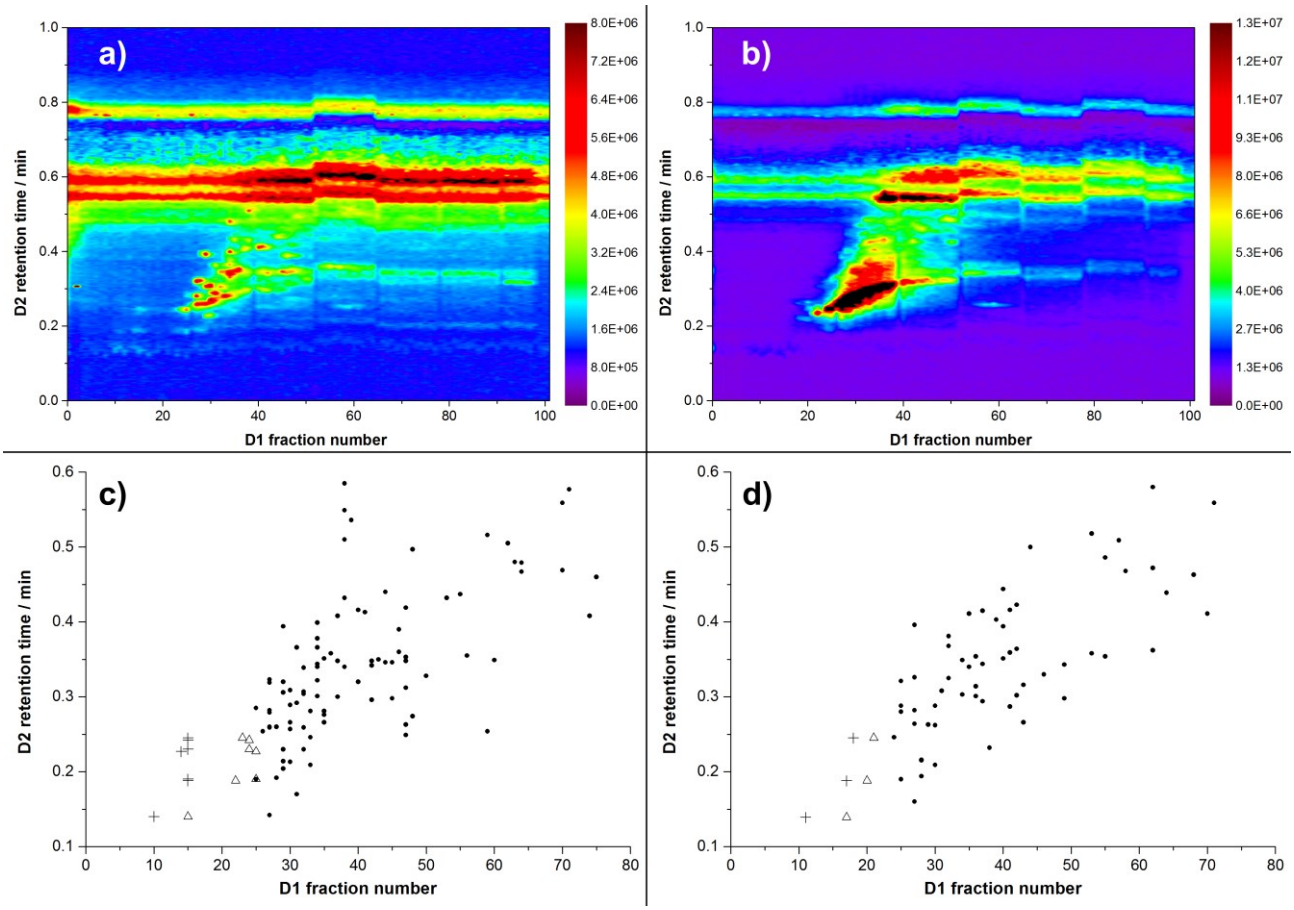

Figure 5-2. **(a)** and **(b)** Contour plots of the TIC chromatograms showing the LC×LC separations of a 99-component standard mix and a wastewater sample, respectively. Color code: signal intensity in counts s^{-1}. Black: intensities above maximum of color code. D1: Hypercarb 50 mm × 0.1 mm i.d., 5 µm. Mobile phase: water + 0.1% FA (A) – methanol + 0.1% FA (B) at 200 nL min^{-1}. D2: SunShell C18 50 mm × 0.3 mm i.d., 2.6 µm. Mobile phase: water + 0.1% FA (A) – acetonitrile + 0.1% FA (B) at 40 µL min^{-1}. Both dimensions operated in solvent gradient mode at 60 °C. D2 gradient cycle length: 1 min. Detection: TripleTOF 5600, TOF survey scan in positive ESI mode. Injection volume: 1.57 µL. For further details, refer to Section 5.2. **(c)** and **(d)** Analyte maps for the standard mix and the targets in the wastewater sample, respectively, based on the analytes' peak maxima presented as ●. D1 double peaks are highlighted by + and Δ for first and second maximum, respectively (see Section 5.3.3 for peak shape discussion).

Surface coverage is often used as a measure of orthogonality in LC×LC [50]. Therefore, the ratio between the convex hull [51-52] that includes all analytes and the rectangle given by the minimum and maximum retention values in both dimensions was calculated as an approximation and comparative value. The area of the convex hull, an eight-sided irregular polygon, was determined using a vector-based method described by Dück et al. [53]. This resulted in a surface coverage of 0.61 (or 61%). For more details, see chapter appendix Section 5.6.3.

5.3.2 Measurement of the wastewater sample

The TIC-chromatogram of the on-line LC×LC separation of the wastewater sample is presented in Figure 5-2b. As overall signal intensities drastically increased compared to the standard, the influence of noise signals decreased. The highly populated area described by D1 fraction numbers 20-40 and D2 retention times 0.2-0.4 highlights the importance of using a second dimension to separate the solutes in this type of water sample. Looking at the high signal intensities in this area, the application of only one of the dimensions would result in significantly increased coelutions and stronger suppression of analyte ionization by ionizable matrix.

Using the results of the 99-component standard mix, a suspected screening was performed for the wastewater sample. Sixty-five of the 99 suspected targets and, additionally, all three deuterated internal standards were found in the sample (see SI-Table 5-3 for details).

5.3.3 Two-dimensional peak shapes

In Figure 5-3, the XIC-chromatograms of 10 analytes in the standard mix were summed. These analytes represent different (border) regions of the analyte map (Figure 5-2c). This way, Figure 5-3 can be used to give an overview on the different types and extremes of peak shapes that were observed using the presented method.

An extremely distorted peak shape is observed for metformin (1). It was the only analyte of the mixture for which peak focusing could not be established on any of the columns. The very low retention of metformin was severely disturbed by the injected solvent and the temperature conditions that were applied. Missing first dimension focusing (~fractions 10 to 25) is marked in the analyte maps by spots for both D1 peak maxima (Figure 5-2, c and d). Although first dimension focusing was established for gemcitabine (2), second dimension focusing was still missing. All peaks apart from that of metformin and gemcitabine were focused in D2. Thus, the border for D2 focusing was at about 10 s (or 0.17 min) D2 retention time, which is still very close to D2 dead time (~0.09 min). The symmetrical peak shape of sulfapyridine (4) is an example for those of many peaks that eluted in the impact range of both gradients. The mass concentration of the targets in the standard mix had been chosen very high (1 $\mu g\ mL^{-1}$) to ensure detection of all analytes. This, however, leads in several cases to a peak broadening and, depending on the retention behavior of the analytes, results in a more or less pronounced tailing as in case of tramadol (3), venlafaxine (6), and clarithromycin (7). For those analytes eluting in D1 hold time at a maximum % B, as in case of pipamperone (5), diuron (8), and fenofibrate (10), strong tailing was observed.

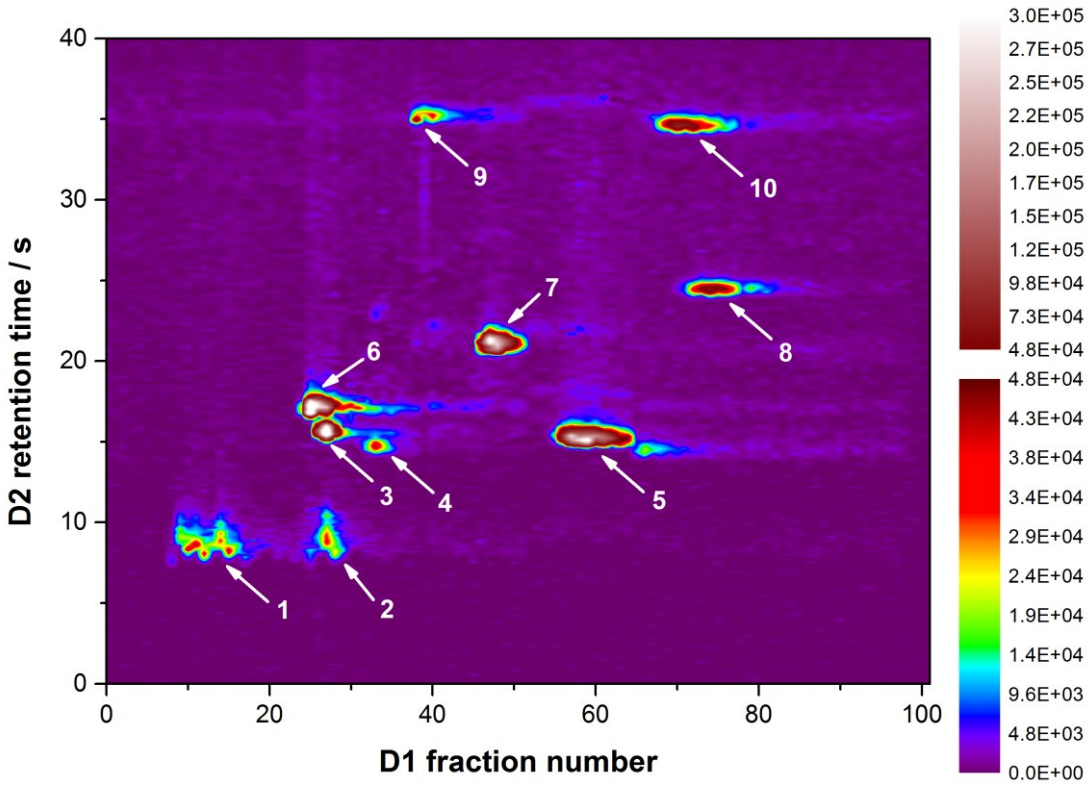

Figure 5-3. Chromatogram of summed XICs for 10 substances. Sample: 99-component standard mix. Color codes: signal intensity in counts s^{-1}. White: intensities from 3.0×10^5 to 4.7×10^5 counts s^{-1}. Analytes: metformin (1), gemcitabine (2), tramadol (3), sulfapyridine (4), pipamperone (5), venlafaxine (6), clarithromycin (7), diuron (8), HT-2 toxin (9), fenofibrate (10). Extracted *m/z*: protonated molecular ion $[M+H]^+ \pm 0.005$.

Looking closely to the peaks in Figure 5-3, especially those with tailing, a slightly serpentine form of the peaks in the direction of D1 is visible instead of a straight orientation. This effect (~0.002 min D2 retention deviation) is caused by the fact that one of the two modulation loops is emptied in the opposite flow direction. The effect of the enlarged fractions can be seen best for analytes 5, 8, and 9. The stepwise injection of the enlarged fraction leads to peak broadening and therefore to an intensity collapse for this fraction. Thus, peaks seem to be cut in two parts. For pipamperone, this effect is mixed with the retention shift due to the timer asynchronism (see the Section 5.3.1, compare Figure 5-2a).

Overall, the lowest observable D1 width for identifiable peaks was three to four fractions. This was also true for the analytes in the wastewater sample, so the M-S-F criterion was fulfilled for all identified compounds. Identification of analytes eluting in the region of the enlarged fractions was not hampered as these analytes were found in adjacent fractions as well.

5.3.4 Performance of the LC dimensions

5.3.4.1 The first dimension

The decision to select Hypercarb in D1 was not solely based on orthogonality criteria. As demonstrated by Stoll et al., who used a carbon-clad zirconia phase in a high-temperature second dimension [34], carbon stationary phases provide extraordinary retentivity and peak focusing abilities, even at high temperatures and disadvantageous sample solvent conditions. These properties of the Hypercarb phase were needed to implement the large volume injection at elevated temperatures, especially as samples containing a stronger solvent (5% acetonitrile) than the initial mobile phase (3% methanol) were injected. As can be seen from Figure 5-2 (c,d) and Figure 5-3, peak splitting could be successfully avoided for the majority of targets. Although the high retentivity is beneficial for the large volume injection, it extends retention time of late eluting compounds (Figure 5-3).

Stability of the D1 retention times between wastewater and standard mix (mean of absolute fraction deviations, 3.4; standard deviation, 2.6) makes it clear that for future quantification methods and a proper identification via D1 retention time, standard addition approaches will be essential. The high load of sample matrix due to the large volume injection as well as the high analyte concentrations in the standard mix surely contributed to the observed deviations. However, retention data of the internal standards and, where available, the IDA-MS/MS experiments could be used to unambiguously identify the targeted wastewater contaminants.

5.3.4.2 The second dimension

As can be seen from Figure 5-4, the SunShell C18 column in D2 provided sharp, symmetrical peak shapes for almost all analytes at high transfer volume conditions and comparably high solute concentration. The high performance of D2 was underlined by very stable retention times. The mean of the absolute D2 retention time deviations between the targets in the water sample and standard (compare SI-Table 5-2) was 0.003 min (standard deviation: 0.003 min). This makes it clear that matrix effects that affect first dimension retention are absent in the second dimension. A similar retention time stability of D2 was observed within one sample (i.e., regarding the differences between D1 fractions). The average peak width was 2 s. Although faster gradients may be performed, the QqTOF-MS acquisition rate dominated by the already optimized IDA cycles would not allow a sufficient number of data points for significantly narrower peaks.

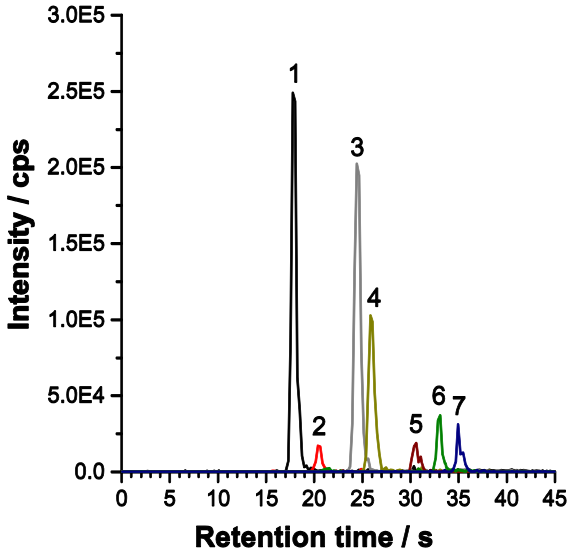

Figure 5-4. Second dimension XIC-chromatogram overlay for seven analytes in first dimension fraction 38 of the standard mixture. Analytes: (1) 5-methyl-1*H*-benzotriazole, (2) prednisolone, (3) isoproturon, (4) stachybotrylactam, (5) picoxystrobin, (6) simvastatin and (7) HT-2 toxin. Extracted *m/z*: protonated molecular ion $[M+H]^+ \pm 0.0005$.

5.3.5 Sensitivity of the system

The same wastewater sample had been analyzed on conventional 1-D LC-MS/MS systems with triple quadrupole detection using validated methods. The analyte list of these measurements contained 56 of the 99 targets. These were quantified using multiple reaction monitoring methods. The results listed in SI-Table 5-3 allow a rough estimation of the detection performance of the multidimensional system. Environmentally relevant analyte concentrations in the lower ng mL^{-1} range or even below – depending on the analyte – were detected. This is a good starting point for further optimizations toward the ng L^{-1} range. However, these supplemental values cannot replace future in-depth sensitivity validations of methods developed on the basis of the multidimensional system.

5.3.6 Solvent consumption

The overall D2 solvent consumption of the presented miniaturized on-line LC×LC was compared to that of conventional fast D2 approaches that use flow rates between 1 and 5 mL min^{-1}. While conventional fast D2 systems consume 0.6 to 3 L of solvent over 10 h, only 0.024 L are needed by a miniaturized D2 system operated at 40 µL min^{-1}. Keeping the rising solvent costs in mind, this trivial comparison underlines the economic advantage of miniaturized, on-line LC×LC systems over the nonminiaturized versions.

5.4 Conclusions and outlook

The presented multidimensional system provides the opportunity to use the advantages of on-line LC×LC and hybrid detection for the screening analysis of complex samples. As the LC×LC is consistently miniaturized, a fast operation of the second LC dimension is possible at low flow rates. Consequently, the hyphenated systems work in full compatibility without the need for a flow split. The capabilities of the highly customizable system were demonstrated by a suspected screening of 99 targets in a wastewater sample. PGC employed in the first and core-shell C18 in the second dimension provided a good LC×LC performance for the separation of the wastewater contaminants (convex hull surface coverage: ~0.6). D2 retention time turned out to be a reliable additional criterion for the identification of suspected compounds, as its stability was very high. The overall splitless design of the capillary system in combination with the large volume injection in the first LC dimension allowed countervailing the sensitivity losses due to modulation and resulted in sufficiently high sensitivity to detect the contaminants at environmentally relevant concentrations. The overall low solvent consumption of the system makes the multidimensional system an economically attractive and environmentally friendly alternative to existing systems based on on-line LC×LC approaches that use conventionally sized D2 columns. For future use, separate heating of both columns could be beneficial for an additional optimization of the first dimension toward analyte focusing at very low and very high retention times. A continuous-flow pump in the second dimension should be considered to simplify system programming and data analysis by making the refill procedure obsolete. For future quantification experiments, a continuous flow delivery is a must as only constant D1 eluate sampling and constant transfer to D2 ensure true (quantitative) comprehensiveness of the multidimensional system [54]. The existing screening approach should already allow an extension of the data analysis to suspected and unknown analytes without reference material.

Acknowledgements

The authors would like to thank for financial aid support the German Federal Ministry of Economics and Technology within the agenda for the promotion of industrial cooperative research and development (IGF) on the basis of a decision by the German Bundestag. The access was opened by the member organization Environmental Technology and organized by the AiF, Arbeitsgemeinschaft industrieller Forschungsvereinigungen, Cologne, Germany (IGF Project No. 15928 N). Hagen Preik-Steinhoff (VICI International, Schenkon, Switzerland) is acknowledged for support on valve technology and Juergen Maier-

Rosenkranz from Grace Discovery Sciences (Worms, Germany) for organizing the packing of micro-LC columns. The Ruhrverband (Essen, Germany) is acknowledged for providing the wastewater sample and Helmut Gräwe (IUTA, Duisburg, Germany) for sample pretreatment. Last but not least, we would like to thank Thomas Ternes and Michael Schlüsener (German Federal Institute of Hydrology (BfG), Koblenz, Germany) for giving us the opportunity to work with the TripleTOF 5600 system.

5.5 References

[1] Richardson, S. D. *Environmental Mass Spectrometry: Emerging Contaminants and Current Issues*. Anal. Chem. 2012, ***84***, 747-778.

[2] Krauss, M.; Singer, H.; Hollender, J. *LC-high resolution MS in environmental analysis: from target screening to the identification of unknowns*. Anal. Bioanal. Chem. 2010, ***397***, 943-951.

[3] Van Eeckhaut, A.; Lanckmans, K.; Sarre, S.; Smolders, I.; Michotte, Y. *Validation of bioanalytical LC-MS/MS assays: Evaluation of matrix effects*. J. Chromatogr. B 2009, ***877***, 2198-2207.

[4] Gosetti, F.; Mazzucco, E.; Zampieri, D.; Gennaro, M. C. *Signal suppression/enhancement in high-performance liquid chromatography tandem mass spectrometry*. J. Chromatogr. A 2010, ***1217***, 3929-3937.

[5] Neue, U. D. *Peak capacity in unidimensional chromatography*. J. Chromatogr. A 2008, ***1184***, 107-130.

[6] Dugo, P.; Cacciola, F.; Kumm, T.; Dugo, G.; Mondello, L. *Comprehensive multidimensional liquid chromatography: Theory and applications*. J. Chromatogr. A 2008, ***1184***, 353-368.

[7] Francois, I.; Sandra, K.; Sandra, P. *Comprehensive liquid chromatography: Fundamental aspects and practical considerations-A review*. Anal. Chim. Acta 2009, ***641***, 14-31.

[8] Guiochon, G.; Marchetti, N.; Mriziq, K.; Shalliker, R. A. *Implementations of two-dimensional liquid chromatography*. J. Chromatogr. A 2008, ***1189***, 109-168.

[9] Stoll, D. R. *Recent progress in online, comprehensive two-dimensional high-performance liquid chromatography for non-proteomic applications*. Anal. Bioanal. Chem. 2010, ***397***, 979-986.

[10] Stoll, D. R.; Li, X. P.; Wang, X. O.; Carr, P. W.; Porter, S. E. G.; Rutan, S. C. *Fast, comprehensive two-dimensional liquid chromatography*. J. Chromatogr. A 2007, ***1168***, 3-43.

[11] Dugo, P.; Mondello, L.; Cacciola, F.; Donato, P. In *Comprehensive Chromatography in Combination with Mass Spectrometry*; Mondello, L., Editor; Wiley Series on Mass Spectrometry; Wiley: Hoboken, NJ, USA, 2011; pp. 331-390.

[12] Dugo, P.; Mondello, L.; Cacciola, F.; Donato, P. In *Comprehensive Chromatography in Combination with Mass Spectrometry*; Mondello, L., Editor; Wiley Series on Mass Spectrometry; Wiley: Hoboken, NJ, USA, 2011; pp. 391-427.

[13] Murphy, R. E.; Schure, M. R.; Foley, J. P. *Effect of Sampling Rate on Resolution in Comprehensive Two-Dimensional Liquid Chromatography*. Anal. Chem. 1998, ***70***, 1585-1594.

[14] Eeltink, S.; Dolman, S.; Vivo-Truyols, G.; Schoenmakers, P.; Swart, R.; Ursem, M.; Desmet, G. *Selection of Column Dimensions and Gradient Conditions to Maximize the Peak-Production Rate in Comprehensive Off-Line Two-Dimensional Liquid Chromatography Using Monolithic Columns*. Anal. Chem. 2010, ***82***, 7015-7020.

[15] Horvath, K.; Fairchild, J.; Guiochon, G. *Optimization strategies for off-line two-dimensional liquid chromatography*. J. Chromatogr. A 2009, ***1216***, 2511-2518.

[16] Liang, Z.; Li, K. Y.; Wang, X. L.; Ke, Y. X.; Jin, Y.; Liang, X. M. *Combination of off-line two-dimensional hydrophilic interaction liquid chromatography for polar fraction and two-dimensional hydrophilic interaction liquid chromatography x reversed-phase liquid chromatography for medium-polar fraction in a traditional Chinese medicine*. J. Chromatogr. A 2012, ***1224***, 61-69.

[17] Kalili, K. M.; de Villiers, A. *Off-line comprehensive 2-dimensional hydrophilic interaction x reversed phase liquid chromatography analysis of procyanidins*. J. Chromatogr. A 2009, ***1216***, 6274-6284.

[18] Francois, I.; Sandra, K.; Sandra, P. In *Comprehensive Chromatography in Combination with Mass Spectrometry*; Mondello, L., Editor; Wiley Series on Mass Spectrometry; Wiley: Hoboken, NJ, USA, 2011; pp. 281-330.

[19] Opiteck, G. J.; Jorgenson, J. W.; Anderegg, R. J. *Two-Dimensional SEC/RPLC Coupled to Mass Spectrometry for the Analysis of Peptides*. Anal. Chem. 1997, ***69***, 2283-2291.

[20] Tanaka, N.; Kimura, H.; Tokuda, D.; Hosoya, K.; Ikegami, T.; Ishizuka, N.; Minakuchi, H.; Nakanishi, K.; Shintani, Y.; Furuno, M.; Cabrera, K. *Simple and Comprehensive Two-Dimensional Reversed-Phase HPLC Using Monolithic Silica Columns*. Anal. Chem. 2004, ***76***, 1273-1281.

[21] Alexander, A. J.; Ma, L. J. *Comprehensive two-dimensional liquid chromatography separations of pharmaceutical samples using dual Fused-Core columns in the 2nd dimension*. J. Chromatogr. A 2009, ***1216***, 1338-1345.

[22] Fairchild, J. N.; Horvath, K.; Guiochon, G. *Theoretical advantages and drawbacks of on-line, multidimensional liquid chromatography using multiple columns operated in parallel*. J. Chromatogr. A 2009, ***1216***, 6210-6217.

[23] Dugo, P.; Fawzy, N.; Cichello, F.; Cacciola, F.; Donato, P.; Mondello, L. *Stop-flow comprehensive two-dimensional liquid chromatography combined with mass spectrometric detection for phospholipid analysis*. J. Chromatogr. A 2013, ***1278***, 46-53.

[24] Kalili, K. M.; de Villiers, A. *Systematic optimisation and evaluation of on-line, off-line and stop-flow comprehensive hydrophilic interaction chromatography x reversed phase liquid chromatographic analysis of procyanidins, Part I: Theoretical considerations*. J. Chromatogr. A 2013, ***1289***, 58-68.

[25] Blahova, E.; Jandera, P.; Cacciola, F.; Mondello, L. *Two-dimensional and serial column reversed-phase separation of phenolic antioxidants on octadecyl-, polyethyleneglycol-, and pentafluorophenylpropyl-silica columns*. J. Sep. Sci. 2006, ***29***, 555-566.

[26] Bedani, F.; Kok, W. T.; Janssen, H. G. *A theoretical basis for parameter selection and instrument design in comprehensive size-exclusion chromatography x liquid chromatography*. J. Chromatogr. A 2006, ***1133***, 126-134.

[27] Kajdan, T.; Cortes, H.; Kuppannan, K.; Young, S. A. *Development of a comprehensive multidimensional liquid chromatography system with tandem mass spectrometry detection for detailed characterization of recombinant proteins*. J. Chromatogr. A 2008, ***1189***, 183-195.

[28] Opiteck, G. J.; Lewis, K. C.; Jorgenson, J. W.; Anderegg, R. J. *Comprehensive On-Line LC/LC/MS of Proteins*. Anal. Chem. 1997, ***69***, 1518-1524.

[29] Sommella, E.; Cacciola, F.; Donato, P.; Dugo, P.; Campiglia, P.; Mondello, L. *Development of an online capillary comprehensive 2D-LC system for the analysis of proteome samples*. J. Sep. Sci. 2012, ***35***, 530-533.

[30] Wilson, S. R.; Jankowski, M.; Pepaj, M.; Mihailova, A.; Boix, F.; Truyols, G. V.; Lundanes, E.; Greibrokk, T. *2D LC Separation and Determination of Bradykinin in Rat Muscle Tissue Dialysate with On-Line SPE-HILIC-SPE-RP-MS*. Chromatographia 2007, ***66***, 469-474.

[31] Zhang, J. A.; Lanham, K. A.; Peterson, R. E.; Heideman, W.; Li, L. J. *Characterization of the adult zebrafish cardiac proteome using online pH gradient strong cation exchange-RP 2D LC coupled with ESI MS/MS*. J. Sep. Sci. 2010, ***33***, 1462-1471.

[32] Wang, Y.; Zhang, J.; Liu, C. L.; Gu, X.; Zhang, X. M. *Nano-flow multidimensional liquid chromatography with electrospray ionization time-of-flight mass spectrometry for proteome analysis of hepatocellular carcinoma*. Anal. Chim. Acta 2005, ***530***, 227-235.

[33] Stoll, D. R.; Carr, P. W. *Fast, Comprehensive Two-Dimensional HPLC Separation of Tryptic Peptides Based on High-Temperature HPLC*. J. Am. Chem. Soc. 2005, ***127***, 5034-5035.

[34] Stoll, D. R.; Cohen, J. D.; Carr, P. W. *Fast, comprehensive online two-dimensional high performance liquid chromatography through the use of high temperature ultra-*

fast gradient elution reversed-phase liquid chromatography. J. Chromatogr. A 2006, ***1122***, 123-137.

[35] Huidobro, A. L.; Pruim, P.; Schoenmakers, P.; Barbas, C. *Ultra rapid liquid chromatography as second dimension in a comprehensive two-dimensional method for the screening of pharmaceutical samples in stability and stress studies*. J. Chromatogr. A 2008, ***1190***, 182-190.

[36] Cacciola, F.; Donato, P.; Giuffrida, D.; Torre, G.; Dugo, P.; Mondello, L. *Ultra high pressure in the second dimension of a comprehensive two-dimensional liquid chromatographic system for carotenoid separation in red chili peppers*. J. Chromatogr. A 2012, ***1255***, 244-251.

[37] Li, X. P.; Stoll, D. R.; Carr, P. W. *Equation for Peak Capacity Estimation in Two-Dimensional Liquid Chromatography*. Anal. Chem. 2009, ***81***, 845-850.

[38] Eggink, M.; Romero, W.; Vreuls, R. J.; Lingeman, H.; Niessen, W. M. A.; Irth, H. *Development and optimization of a system for comprehensive two-dimensional liquid chromatography with UV and mass spectrometric detection for the separation of complex samples by multi-step gradient elution*. J. Chromatogr. A 2008, ***1188***, 216-226.

[39] Jandera, P.; Fischer, J.; Lahovska, H.; Novotna, K.; Cesla, P.; Kolarova, L. *Two-dimensional liquid chromatography normal-phase and reversed-phase separation of (co)oligomers*. J. Chromatogr. A 2006, ***1119***, 3-10.

[40] Dugo, P.; Favoino, O.; Luppino, R.; Dugo, G.; Mondello, L. *Comprehensive Two-Dimensional Normal-Phase (Adsorption) - Reversed-Phase Liquid Chromatography*. Anal. Chem. 2004, ***76***, 2525-2530.

[41] van der Horst, A.; Schoenmakers, P. J. *Comprehensive two-dimensional liquid chromatography of polymers*. J. Chromatogr. A 2003, ***1000***, 693-709.

[42] van der Klift, E. J. C.; Vivo-Truyols, G.; Claassen, F. W.; van Holthoon, F. L.; van Beek, T. A. *Comprehensive two-dimensional liquid chromatography with ultraviolet, evaporative light scattering and mass spectrometric detection of triacylglycerols in corn oil*. J. Chromatogr. A 2008, ***1178***, 43-55.

[43] Groskreutz, S. R.; Swenson, M. M.; Secor, L. B.; Stoll, D. R. *Selective comprehensive multidimensional separation for resolution enhancement in high performance liquid chromatography. Part II: Applications*. J. Chromatogr. A 2012, ***1228***, 41-50.

[44] Teutenberg, T.; Leonhardt, J.; Wiese, S. *Method Development for Fast Separation of Polycyclic Aromatic Hydrocarbons Using Micro-LC - The Importance of the Dwell Volume*. The Column 2012, ***8***, 9-12.

[45] Haun, J.; Teutenberg, T.; Schmidt, T. C. *Influence of temperature on peak shape and solvent compatibility: Implications for two-dimensional liquid chromatography*. J. Sep. Sci. 2012, ***35***, 1723-1730.

[46] Jandera, P. *Programmed elution in comprehensive two-dimensional liquid chromatography*. J. Chromatogr. A 2012, ***1255***, 112-129.

[47] Decaestecker, T. N.; Casteele, S. R. V.; Wallemacq, P. E.; Van Peteghem, C. H.; Defore, D. L.; Van Bocxlaer, J. F. *Information-Dependent Acquisition-Mediated LC-MS/MS Screening Procedure with Semiquantitative Potential*. Anal. Chem. 2004, ***76***, 6365-6373.

[48] Decaestecker, T. N.; Clauwaert, K. M.; Van Bocxlaer, J. F.; Lambert, W. E.; Van den Eeckhout, E. G.; Van Peteghem, C. H.; De Leenheer, A. P. *Evaluation of automated single mass spectrometry to tandem mass spectrometry function switching for comprehensive drug profiling analysis using a quadrupole time-of-flight mass spectrometer*. Rapid Commun. Mass Spectrom. 2000, ***14***, 1787-1792.

[49] West, C.; Elfakir, C.; Lafosse, M. *Porous graphitic carbon: A versatile stationary phase for liquid chromatography*. J. Chromatogr. A 2010, ***1217***, 3201-3216.

[50] Gilar, M.; Fridrich, J.; Schure, M. R.; Jaworski, A. *Comparison of Orthogonality Estimation Methods for the Two-Dimensional Separations of Peptides*. Anal. Chem. 2012, ***84***, 8722-8732.

[51] Rutan, S. C.; Davis, J. M.; Carr, P. W. *Fractional coverage metrics based on ecological home range for calculation of the effective peak capacity in comprehensive two-dimensional separations*. J. Chromatogr. A 2012, ***1255***, 267-276.

[52] Semard, G.; Peulon-Agasse, V.; Bruchet, A.; Bouillon, J. P.; Cardinael, P. *Convex hull: A new method to determine the separation space used and to optimize operating conditions for comprehensive two-dimensional gas chromatography*. J. Chromatogr. A 2010, ***1217***, 5449-5454.

[53] Dück, R.; Sonderfeld, H.; Schmitz, O. J. *A simple method for the determination of peak distribution in comprehensive two-dimensional liquid chromatography*. J. Chromatogr. A 2012, ***1246***, 69-75.

[54] Schoenmakers, P.; Marriott, P.; Beens, J. *Nomenclature and Conventions in Comprehensive Multidimensional Chromatography*. LC GC Eur. 2003, ***16***, 335-339.

5.6 Chapter appendix

5.6.1 First dimension fractionation

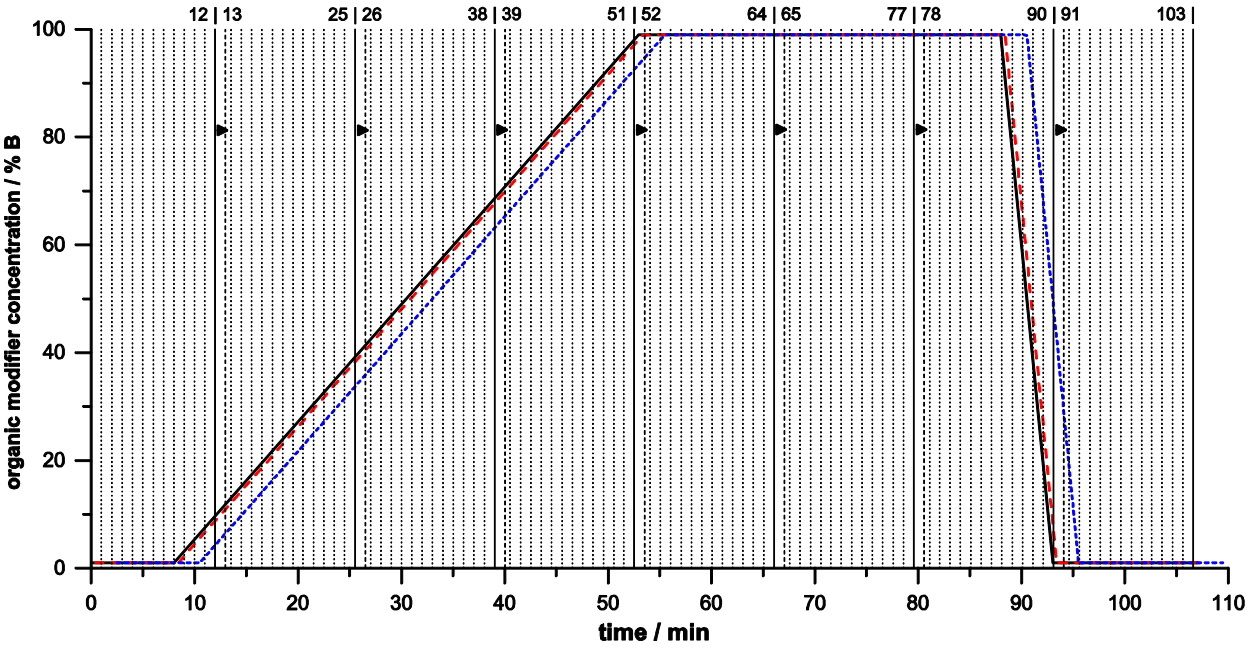

SI-Figure 5-1. Gradient profile and fractionation of the first dimension.

SI-Figure 5-1 visualizes the applied programming of gradient and fractionation in the first liquid chromatographic dimension. The black line describes the programmed gradient. The dashed red and blue lines show the gradient delay at the column head and at the head of the modulation loop, respectively. The modulation valve switching events are given by the vertical lines. Thus, the duration for collection of each fraction is given by the space between two consecutive vertical lines. Those modulation valve events that at the same time represent the time stamps of the end of a second dimension chromatogram are marked by the continuous vertical lines. Those sets of two fractions that are measured and counted as one fraction are highlighted by the black arrow heads. The valve events that cut these large fractions for the stepwise injection to the second dimension are shown as dashed lines. As described in the manuscript, this cut is necessary to avoid a solvent strength effect by an otherwise too large transfer volume to the second dimension. The numbers on top of the continuous vertical lines may help counting the first dimension fractions.

The dashed blue line can be used to approximate the concentration of the organic modifier content of the first dimension fractions that are transferred to the second dimension.

5.6.2 IDA-mode: Distinguishing between isobaric substances at the example of ifosfamide and cyclophosphamide

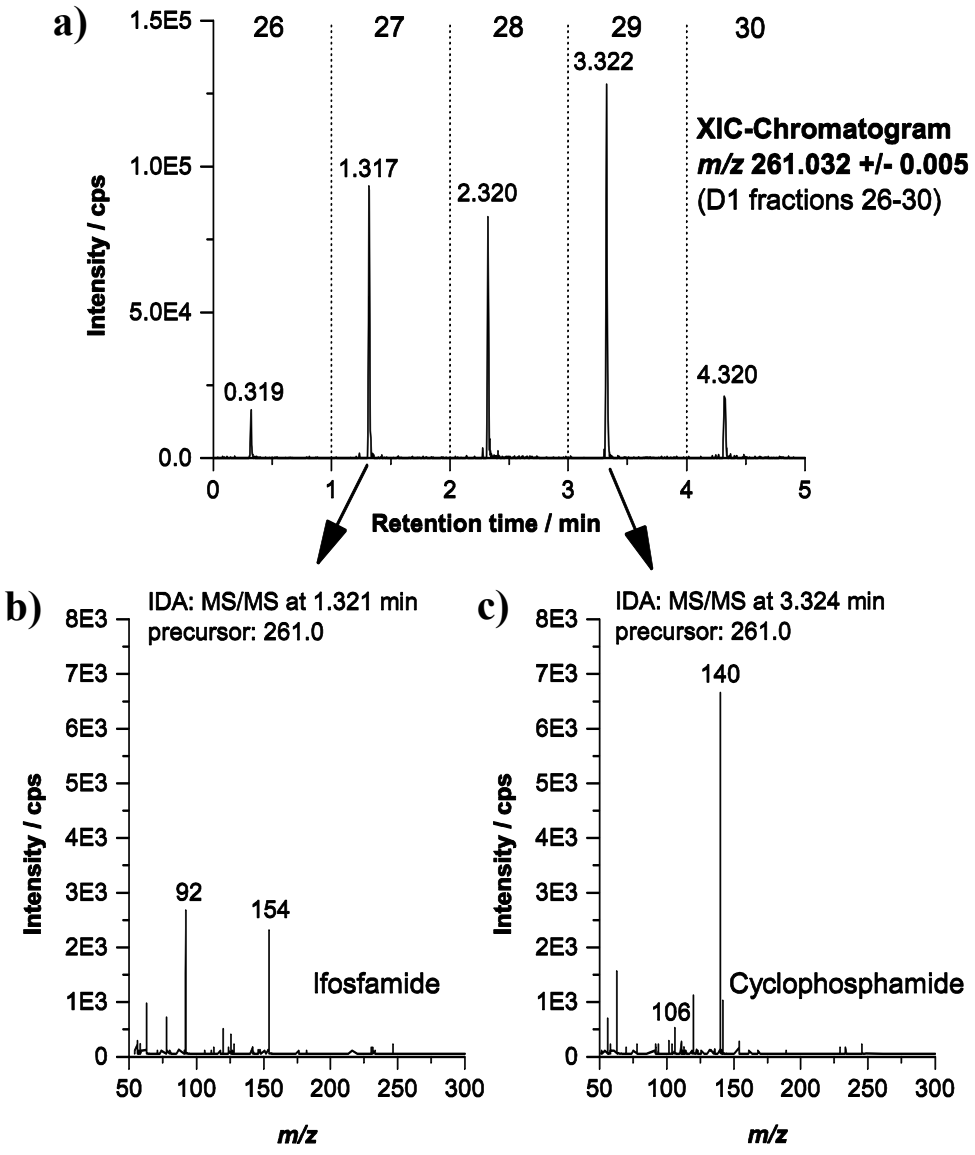

SI-Figure 5-2. **(a)** Uncut second dimension XIC-chromatogram (*m/z* 261.032 ± 0.005) showing the partial separation of the two isobaric compounds ifosfamide and cyclophosphamide over five D1 fractions. Sample: 99-component standard mixture. Corresponding D1 fraction numbers are given on top. Measurement conditions as in Figure 5-2a. (**b)** and **(c)** Mass spectra obtained from MS/MS-product ion scans for the same precursor ion 261.0 at 1.321 and 3.324 min retention time, respectively, of the XIC-chromatogram presented in a).

As can be seen from SI-Figure 5-2a, the two isobaric compounds ifosfamide and cyclophosphamide (molecular formula for both: $C_7H_{15}N_2O_2Cl_2P$) would coelute in the second dimension without the preseparation on the Hypercarb column in the first dimension. An

MS/MS-product ion scan would result in a mixed spectrum containing fragments of both substances. As no multiple reaction monitoring (MRM) experiments are programmed in a suspected screening, it would not be possible to differentiate between the two compounds. The application of the Hypercarb first dimension resulted at least in a double-peak with maxima in the D1 fractions 27 and 29. If now MS/MS product ion scans are applied at the two maxima (SI-Figure 5-2, b and c) clean product ion spectra can be obtained that contain only fragments of one of both substances.

In summary, the IDA-mode which is a prerequisite for a suspected screening in 1-D or 2-D LC-MS requires at least a partial separation of isobaric compounds. Otherwise, it is not possible to distinguish between the isobars. The additional selectivity of a 2-D LC approach can help to separate isobars which as co-eluting compounds could not be identified in a suspected screening. The example given in SI-Figure 5-2 underlines that it is not necessary to baseline-separate the peaks in the LC-dimensions as long as IDA experiments can be performed on the peak maxima.

5.6.3 Calculation of the surface coverage as a measure of orthogonality

As described in the manuscript, the surface coverage for the LC×LC separation of the 99-component standard mixture was calculated using the convex hull that includes all analyte spots (SI-Figure 5-3).

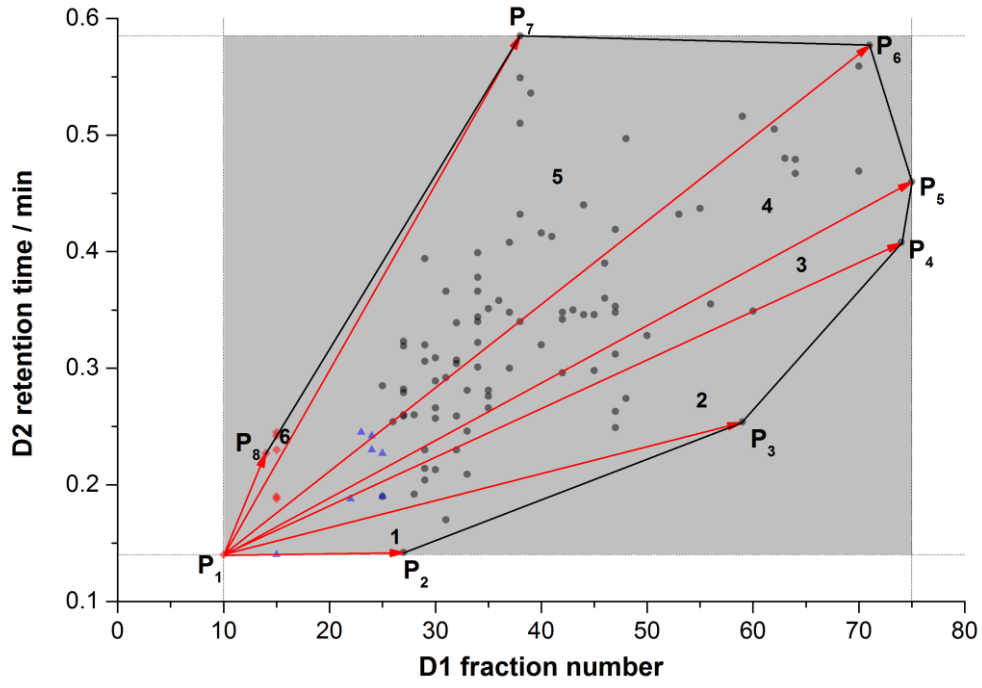

SI-Figure 5-3. The areas used for the calculation of the surface coverage.

In this case, the convex hull is an eight-sided irregular polygon which is described by the points P_1 to P_8. The area of this convex hull was calculated by a vector method that Dück et al. used in their work [53]. Accordingly, the area of the convex hull can be divided in six scalene triangles that are numbered in SI-Figure 5-3. Each of these triangles can be described by two vectors that have the same corner point as origin and the other corner points as heads. The vectors that were used to determine the six areas are marked red in SI-Figure 5-3. P_1 was chosen as the origin of all vectors.

The coordinates for the eight corner points of the convex hull were: P_1 (10 | 0.140), P_2 (27 | 0.142), P_3 (59 | 0.254), P_4 (74 | 0.408), P_5 (75 | 0.460), P_6 (71 | 0.577), P_7 (38 | 0.585) and P_8 (14 | 0.227).

Using these points, seven vectors with the origin in point P_1 can be calculated using Equation 5-1:

$$\overrightarrow{P_1P_k} = \begin{pmatrix} x_k - 10 \\ y_k - 0.140 \end{pmatrix} \qquad \text{Equation 5-1}$$

Thus, the seven vectors are:

$$\overrightarrow{P_1P_2} = \begin{pmatrix} 27 - 10 \\ 0.142 - 0.140 \end{pmatrix} = \begin{pmatrix} 17 \\ 0.002 \end{pmatrix},\ \overrightarrow{P_1P_3} = \begin{pmatrix} 49 \\ 0.114 \end{pmatrix},\ \overrightarrow{P_1P_4} = \begin{pmatrix} 64 \\ 0.268 \end{pmatrix},$$

$$\overrightarrow{P_1P_5} = \begin{pmatrix} 65 \\ 0.320 \end{pmatrix},\ \overrightarrow{P_1P_6} = \begin{pmatrix} 61 \\ 0.437 \end{pmatrix},\ \overrightarrow{P_1P_7} = \begin{pmatrix} 28 \\ 0.445 \end{pmatrix},\ \text{and } \overrightarrow{P_1P_8} = \begin{pmatrix} 4 \\ 0.087 \end{pmatrix}$$

The triangular area (A_Δ) described by two vectors $\vec{a}$ and $\vec{b}$ can be obtained by using the half of the absolute value of the cross product of the vectors:

$$A_\Delta(\vec{a}, \vec{b}) = 0.5\ \left|\vec{a} \times \vec{b}\right| = 0.5\ |x_a y_b - x_b y_a| \qquad \text{Equation 5-2}$$

Now, the triangular areas 1 to 6 of SI-Figure 5-3 can be calculated using Equation 5-2:

$$A_{\Delta 1}\left(\overrightarrow{P_1P_2}, \overrightarrow{P_1P_3}\right) = 0.5\ \left|\overrightarrow{P_1P_2} \times \overrightarrow{P_1P_3}\right| = 0.5\ |17 \cdot 0.114 - 49 \cdot 0.002| = 0.92,$$

$$A_{\Delta 2}\left(\overrightarrow{P_1P_3}, \overrightarrow{P_1P_4}\right) = 2.918,\ A_{\Delta 3}\left(\overrightarrow{P_1P_4}, \overrightarrow{P_1P_5}\right) = 1.53,\ A_{\Delta 4}\left(\overrightarrow{P_1P_5}, \overrightarrow{P_1P_6}\right) = 4.4425,$$

$$A_{\Delta 5}\left(\overrightarrow{P_1P_6}, \overrightarrow{P_1P_7}\right) = 7.4545,\ A_{\Delta 6}\left(\overrightarrow{P_1P_7}, \overrightarrow{P_1P_8}\right) = 0.328$$

The area of the convex hull is the sum of these six areas, i.e., 17.593.

The rectangular area $A_{\square}$ that would have to be populated if the two LC dimensions were fully orthogonal (grey rectangular area in SI-Figure 5-3) was calculated using the minimum and maximum values of the x- and y-coordinates of the analyte spots on the map according to the following equation.

$$A_{\square} = (x_{max} - x_{min}) \cdot (y_{max} - y_{min}) = (75 - 10) \cdot (0.585 - 0.140) = 28.925$$

The surface coverage can now be approximated by the area ratio of the convex hull and the quadratical area which is ~0.61 (or 61%).

5.6.4 Tables

SI-Table 5-1. Detailed list of compounds used for the 99-component standard mixture.

Analyte	purchased as	CAS No.	Purity*	Source
5,6-Dimethyl-1*H*-benzotriazole	5,6-Dimethyl-1*H*-benzotriazole monohydrate	4184-79-6	99%	Aldrich
5-Methyl-1*H*-benzotriazole	5-Methyl-1*H*-benzotriazole	136-85-6	≥ 98%	Fluka
Acetylsulfadiazine	N^4-Acetylsulfadiazine	127-74-2	99%	IUTA**
Acetylsulfadimidine	N^4-Acetylsulfamethazine	100-90-3	99%	IUTA**
Acetylsulfamerazine	N^4-Acetylsulfamerazine	127-73-1	99%	IUTA**
Acetylsulfamethoxazole	N^4-Acetylsulfamethoxazole	21312-10-7		LGC Standards
Allopurinol	Allopurinol	315-30-0		Sigma
Ampicillin	Ampicillin	69-53-4		Sigma
Atenolol	Atenolol	29122-68-7	≥ 98%	Sigma
Atorvastatin	Atorvastatin calcium salt	134523-03-8		Dr. Ehrenstorfer
Azithromycin	Azithromycin	83905-01-5	≥ 95%	Sigma
Benzotriazole	Benzotriazole	95-14-7	99%	Sigma-Aldrich
Bezafibrate	Bezafibrate	41859-67-0	≥ 98%	Sigma
Bisoprolol	Bisoprolol fumarate	104344-23-2		LGC Standards
Carbamazepine	Carbamazepine	298-46-4		Sigma
Carbetamide	Carbetamide	16118-49-3	Pestanal	Fluka
Cefalexin	Cephalexin hydrate	15686-71-2		Sigma
Chloramphenicol	Chloramphenicol	56-75-7	≥ 98%	Sigma
Chlorbromuron	Chlorobromouron	13360-45-7	Pestanal	Fluka
Chloridazon	Chloridazon	1698-60-8	Pestanal	Fluka
Chlorprothixene	Chlorprothixene hydrochloride	6469-93-8		Sigma
Cilastatin	Cilastatin sodium salt	81129-83-1	≥ 98%	Sigma
Citalopram	Citalopram hydrobromide	59729-32-7		Sigma
Clarithromycin	Clarithromycin	81103-11-9		LGC Standards
Clenbuterol	Clenbuterol hydrochloride	21898-19-1	≥ 95%	Sigma
Climbazole	Climbazole	38083-17-9	Pestanal	Fluka
Clindamycin	Clindamycin hydrochloride	21462-39-5		Sigma
Clozapine	Clozapine	5786-21-0		Sigma
Cyclophosphamide	Cyclophosphamide monohydrate	6055-19-2	≥ 97%	Sigma
Dapsone	Dapsone	80-08-0		Campro Scientific
Dehydrato-Erythromycin	Erythromycin	114-07-8		Sigma-Aldrich

Analyte	purchased as	CAS No.	Purity*	Source
Diacetoxyscirpenol	Diacetoxyscirpenol	2270-40-8		Sigma
Diatrizoic acid	Amidotrizoic acid dihydrate	50978-11-5		LGC Standards
Diclofenac	Diclofenac sodium salt	15307-79-6		Sigma
Dimpylate	Diazinon	333-41-5	Pestanal	Fluka
Diuron	Diuron	330-54-1	Pestanal	Fluka
Enalapril	Enalapril maleate	76095-16-4		Campro Scientific
Fenofibrate	Fenofibrate	49562-28-9	≥ 99%	Sigma
Fenofibric acid	Fenofibric acid	42017-89-0		Chemos
Fumonisin B1	Fuminosin B1	116355-83-0	95%	AppliChem
Fumonisin B2	Fuminosin B2	116355-84-1		Iris Biotech
Gemcitabine	Gemcitabine hydrochloride	122111-03-9		LGC Standards
Gliotoxin	Gliotoxin	67-99-2	≥ 98%	Fluka
HT-2 Toxin	HT2 Toxin	26934-87-2	98%	AppliChem
Hydrocortisone	Hydrocortisone	50-23-7		Dr. Ehrenstorfer
Ifosfamide	Ifosfamide	3778-73-2		Sigma
Iopromide	Iopromide	73334-07-3	≥ 99%	LGC Standards
Isoproturon	Isoproturon	34123-59-6	Pestanal	Fluka
Ketoprofen	Ketoprofen	22071-15-4	≥ 98%	Sigma
Lidocaine	Lidocaine	137-58-6		Sigma
Linuron	Linuron	330-55-2		Campro Scientific
Losartan	Losartan potassium salt	124750-99-8		Campro Scientific
Mefenamic acid	Mefenamic acid	61-68-7		Sigma
Megestrol	Megestrol acetate	595-33-5	Vetranal	Fluka
Melperone	Melperone hydrochloride	1622-79-3		Chemos
Metconazole	Metconazole	125116-23-6	Pestanal	Fluka
Metformin	1,1-Dimethylbiguanide hydrochloride	1115-70-4	97%	Aldrich
Metobromuron	Metobromuron	3060-89-7	Pestanal	Fluka
Metoprolol	(±)-Metoprolol (+)-tartrate	56392-17-7	≥ 98%	Sigma
Metronidazole	Metronidazole	443-48-1		Sigma
Mianserin	Mianserin hydrochloride	21535-47-7		Sigma
Mirtazapine	Mirtazapine	85650-52-8	≥ 98%	Sigma
Monuron	Monuron	150-68-5	Pestanal	Fluka
Nafcillin	Nafcillin sodium salt	985-16-0		Sigma
Naproxen	Naproxen	22204-53-1		Sigma-Aldrich
Oxazepam	Oxazepam	604-75-1		Sigma
Oxcarbazepine	Oxcarbazepine	28721-07-5	≥ 98%	Sigma
Paracetamol	Paracetamol	103-90-2		Fluka
Phenazone	Antipyrine	60-80-0		Fluka
Picoxystrobin	Picoxystrobin	117428-22-5		Campro Scientific
Pipamperone	Pipamperone dihydrochloride	2448-68-2	99%	Sigma
Piperacillin	Piperacillin sodium salt	59703-84-3		Sigma
Prednisolone	Prednisolone	50-24-8	≥ 99%	Sigma
Propranolol	(±)-Propranolol hydrochloride	318-98-9	≥ 98%	Sigma
Propyphenazone	Propyphenazone	479-92-5		LGC Standards
Quinoxyfen	Quinoxyfen	124495-18-7	Pestanal	Fluka

Analyte	purchased as	CAS No.	Purity*	Source
Ramipril	Ramipril	87333-19-5		Campro Scientific
Ranitidine	Ranitidine hydrochloride	66357-59-3		Campro Scientific
Ritalinic acid	Ritalinic acid	19395-41-6	99%	Aldrich
Roxithromycin	Roxithromycin	80214-83-1	≥ 90%	Sigma
Sertraline	Sertraline hydrochloride	79559-97-0		Campro Scientific
Simvastatin	Simvastatin	79902-63-9	≥ 97%	Sigma
Sotalol	Sotalol hydrochloride	959-24-0		Dr. Ehrenstorfer
Stachybotrylactam	Stachybotrylactam	163391-76-2	≥ 95%	Bioaustralis
Sulfadiazine	Sulfadiazine	68-35-9	≥ 99%	Sigma
Sulfadimethoxine	Sulfadimethoxine	122-11-2	≥ 98.5%	Fluka
Sulfadimidine	Sulfamethazine	57-68-1	≥ 99%	Sigma
Sulfamethizole	Sulfamethizole	144-82-1	≥ 99%	Fluka
Sulfamethoxazole	Sulfamethoxazole	723-46-6		Fluka
Sulfapyridine	Sulfapyridine	144-83-2	≥ 99%	Fluka
Tamoxifen	Tamoxifen citrate	54965-24-1		Fluka
Terbutaline	Terbutaline hemisulfate	23031-32-5		Sigma
Terbutryn	Terbutryn	886-50-0	Pestanal	Fluka
Tramadol	Tramadol hydrochloride	36282-47-0	≥ 99%	Sigma
Trimethoprim	Trimethoprim	738-70-5	≥ 98%	Sigma
Venlafaxine	Venlafaxine hydrochloride	99300-78-4	≥ 98%	Sigma
Warfarin	Warfarin	81-81-2		Campro Scientific
Xylometazoline	Xylometazoline hydrochloride	1218-35-5		Sigma
Zuclopenthixol	Zuclopenthixol	53772-83-1		Chemos

* Purity was at least pro analysi (p.a.) unless otherwise noted.

** These standards had been prepared in-house according to the procedure described in the following article: Pfeiffer, T.; Tuerk, J.; Fuchs, R. *Structural characterization of sulfadiazine metabolites using H/D exchange combined with various MS/MS experiments* J. Am. Soc. Mass Spectrom. 2005, ***16***, 1687–1694.

Manufacturer information in alphabetical order:

Products from Aldrich, Fluka and Sigma were purchased from Sigma-Aldrich, Schnelldorf, Germany; AppliChem, Darmstadt, Germany; Bioaustralis products via tebu-bio, Offenbach, Germany; Campro Scientific, Berlin, Germany; Chemos, Regenstauf, Germany; Dr. Ehrenstorfer, Augsburg, Germany; Iris Biotech, Marktredwitz, Germany; LGC Standards, Wesel, Germany.

SI-Table 5-2. Detailed result list of the LC×LC separation of the 99-component standard mixture (data basis of Figure 5-2c).

Analyte	Molecular formula of [M]	Monoisotopic mass* of $[M+H]^+$	---------- Standard mixture ----------			
			D1 max (fraction no.)	D2 retention time (min)	D2 retention time range (± x min)	Δ *m/z* (ppm)
5,6-Dimethyl-1*H*-benzotriazole	$C_8H_9N_3$	148.08692	50	0.328	0.002	-0.8
5-Methyl-1*H*-benzotriazole	$C_7H_7N_3$	134.07127	37	0.300	0.002	-3.8
Acetylsulfadiazine	$C_{12}H_{12}N_4O_3S$	293.07029	47	0.249	0.003	1.2
Acetylsulfadimidine	$C_{14}H_{16}N_4O_3S$	321.10159	48	0.274	0.002	-0.3
Acetylsulfamerazine	$C_{13}H_{14}N_4O_3S$	307.08594	47	0.263	0.002	0.5
Acetylsulfamethoxazole	$C_{12}H_{13}N_3O_4S$	296.06995	47	0.312	0.002	-1.0
Allopurinol	$C_5H_4N_4O$	137.04579	31	0.170	0.015	1.0
Ampicillin	$C_{16}H_{19}N_3O_4S$	350.11690	15 / 24	0.230	0.005	-0.6
Atenolol	$C_{14}H_{22}N_2O_3$	267.17032	25	0.190	0.005	2.5
Atorvastatin	$C_{33}H_{35}FN_2O_5$	559.26028	64	0.479	0.005	-1.4
Azithromycin	$C_{38}H_{72}N_2O_{12}$	749.51580	30	0.266	0.004	1.6
Benzotriazole	$C_6H_5N_3$	120.05562	32	0.259	0.003	2.3
Bezafibrate	$C_{19}H_{20}ClNO_4$	362.11536	55	0.437	0.003	0.1
Bisoprolol	$C_{18}H_{31}NO_4$	326.23259	31	0.292	0.003	3.4
Carbamazepine	$C_{15}H_{12}N_2O$	237.10224	34	0.366	0.005	-1.4
Carbetamide	$C_{12}H_{16}N_2O_3$	237.12337	37	0.348	0.005	-0.2
Cefalexin	$C_{16}H_{17}N_3O_4S$	348.10125	14 / 25	0.227	0.005	3.1
Chloramphenicol	$C_{11}H_{12}Cl_2N_2O_5$	323.01960	34	0.322	0.010	3.1
Chlorbromuron	$C_9H_{10}BrClN_2O_2$	292.96869	75	0.460	0.003	3.6
Chloridazon	$C_{10}H_8ClN_3O$	222.04287	45	0.298	0.003	0.7
Chlorprothixene	$C_{18}H_{18}ClNS$	316.09213	45	0.346	0.002	4.7
Cilastatin	$C_{16}H_{26}N_2O_5S$	359.16352	30	0.257	0.005	0.7
Citalopram	$C_{20}H_{21}FN_2O$	325.17107	30	0.309	0.002	2.0
Clarithromycin	$C_{38}H_{69}NO_{13}$	748.48417	47	0.353	0.002	3.3
Clenbuterol	$C_{12}H_{18}Cl_2N_2O$	277.08690	27	0.259	0.002	0.5
Climbazole	$C_{15}H_{17}ClN_2O_2$	293.10513	35	0.351	0.002	-0.4
Clindamycin	$C_{18}H_{33}ClN_2O_5S$	425.18715	27	0.282	0.002	2.2
Clozapine	$C_{18}H_{19}ClN_4$	327.13710	30	0.289	0.002	0.7
Cyclophosphamide	$C_7H_{15}Cl_2N_2O_2P$	261.03210	29	0.320	0.002	0.5
Dapsone	$C_{12}H_{12}N_2O_2S$	249.06923	35	0.281	0.003	-0.2
Dehydrato-Erythromycin	$C_{37}H_{65}NO_{12}$	716.45795	42	0.342	0.002	1.7
Diacetoxyscirpenol	$C_{19}H_{26}O_7$	367.17513	31	0.366	0.003	-0.4
Diatrizoic acid	$C_{11}H_9I_3N_2O_4$	614.77694	29	0.204	0.002	3.6
Diclofenac	$C_{14}H_{11}Cl_2NO_2$	296.02396	70	0.469	0.005	-4.3
Dimpylate	$C_{12}H_{21}N_2O_3PS$	305.10833	39	0.536	0.003	-1
Diuron	$C_9H_{10}Cl_2N_2O$	233.02429	74	0.408	0.002	2.8
Enalapril	$C_{20}H_{28}N_2O_5$	377.20710	32	0.307	0.002	3.8
Fenofibrate	$C_{20}H_{21}O_4Cl$	361.12020	71	0.577	0.002	0.2
Fenofibric acid	$C_{17}H_{15}ClO_4$	319.07316	63	0.480	0.015	3.2
Fumonisin B1	$C_{34}H_{59}NO_{15}$	722.39575	40	0.320	0.002	-0.3
Fumonisin B2	$C_{34}H_{59}NO_{14}$	706.40083	43	0.350	0.002	-0.8

Analyte	Molecular formula of [M]	Monoisotopic mass* of $[M+H]^+$	---------- Standard mixture ----------			
			D1 max (fraction no.)	D2 retention time (min)	D2 retention time range (± x min)	Δ *m/z* (ppm)
Gemcitabine	$C_9H_{11}F_2N_3O_4$	264.07904	27	0.142	0.007	2.1
Gliotoxin	$C_{13}H_{14}N_2O_4S_2$	327.04678	47	0.348	0.005	0.2
HT-2 Toxin	$C_{22}H_{32}O_8$	425.21699	38	0.585	0.005	-2.6
Hydrocortisone	$C_{21}H_{30}O_5$	363.21660	42	0.348	0.003	0.8
Ifosfamide	$C_7H_{15}Cl_2N_2O_2P$	261.03210	27	0.319	0.002	0.5
Iopromide	$C_{18}H_{24}I_3N_3O_8$	791.87705	30	0.213	0.002	1.1
Isoproturon	$C_{12}H_{18}N_2O$	207.14919	37	0.408	0.005	0.5
Ketoprofen	$C_{16}H_{14}O_3$	255.10157	40	0.416	0.002	0.7
Lidocaine	$C_{14}H_{22}N_2O$	235.18049	15 / 24	0.242	0.006	-0.7
Linuron	$C_9H_{10}Cl_2N_2O_2$	249.01921	64	0.467	0.003	-0.3
Losartan	$C_{22}H_{23}ClN_6O$	423.16946	46	0.390	0.003	1.7
Mefenamic acid	$C_{15}H_{15}NO_2$	242.11756	59	0.516	0.003	0.2
Megestrol	$C_{24}H_{32}O_4$	385.23734	48	0.497	0.002	2.1
Melperone	$C_{16}H_{22}FNO$	264.17582	33	0.281	0.002	-1.3
Metconazole	$C_{17}H_{22}ClN_3O$	320.15242	64	0.505	0.002	0.7
Metformin	$C_4H_{11}N_5$	130.10872	10 / 15	0.140	0.015	-0.3
Metobromuron	$C_9H_{11}BrN_2O_2$	259.00767	47	0.419	0.002	1.0
Metoprolol	$C_{15}H_{25}NO_3$	268.19072	28	0.260	0.005	-3.4
Metronidazole	$C_6H_9N_3O_3$	172.07167	29	0.214	0.003	0.8
Mianserin	$C_{18}H_{20}N_2$	265.16993	29	0.306	0.002	2.9
Mirtazapine	$C_{17}H_{19}N_3$	266.16517	26	0.254	0.003	2.2
Monuron	$C_9H_{11}ClN_2O$	199.06327	46	0.360	0.003	1.7
Nafcillin	$C_{21}H_{22}N_2O_5S$	415.13222	32	0.304	0.005	3.6
Naproxen	$C_{14}H_{14}O_3$	231.10157	53	0.432	0.002	2.4
Oxazepam	$C_{15}H_{11}ClN_2O_2$	287.05818	34	0.378	0.002	0.7
Oxcarbazepine	$C_{15}H_{12}N_2O_2$	253.09715	32	0.339	0.004	-0.3
Paracetamol	$C_8H_9NO_2$	152.07061	33	0.209	0.003	0.3
Phenazone	$C_{11}H_{12}N_2O$	189.10224	27	0.279	0.002	-2.9
Picoxystrobin	$C_{18}H_{16}F_3NO_4$	368.11042	38	0.510	0.005	-0.9
Pipamperone	$C_{21}H_{30}FN_3O_2$	376.23948	59	0.254	0.003	0.5
Piperacillin	$C_{23}H_{27}N_5O_7S$	518.17040	44	0.346	0.002	0.5
Prednisolone	$C_{21}H_{28}O_5$	361.20095	38	0.340	0.005	0.0
Propranolol	$C_{16}H_{21}NO_2$	260.16451	42	0.296	0.002	5
Propyphenazone	$C_{14}H_{18}N_2O$	231.14919	29	0.394	0.002	0.9
Quinoxyfen	$C_{15}H_8Cl_2FNO$	308.00397	70	0.559	0.003	-0.5
Ramipril	$C_{23}H_{32}N_2O_5$	417.23840	34	0.340	0.005	-1.2
Ranitidine	$C_{13}H_{22}N_4O_3S$	315.14854	28	0.192	0.005	-0.2
Ritalinic acid	$C_{13}H_{17}NO_2$	220.13321	15 / 23	0.245	0.005	1.8
Roxithromycin	$C_{41}H_{76}N_2O_{15}$	837.53185	36	0.358	0.01	-0.9
Sertraline	$C_{17}H_{17}Cl_2N$	306.08108	34	0.344	0.003	-0.7
Simvastatin	$C_{25}H_{38}O_5$	419.27920	38	0.549	0.003	0.1
Sotalol	$C_{12}H_{20}N_2O_3S$	273.12674	15 / 25	0.190	0.010	1.0
Stachybotrylactam	$C_{23}H_{31}NO_4$	386.23259	38	0.432	0.004	1.7
Sulfadiazine	$C_{10}H_{10}N_4O_2S$	251.05972	32	0.230	0.004	0.8

Analyte	Molecular formula of [M]	Monoisotopic mass* of $[M+H]^+$	---------- Standard mixture ----------			
			D1 max (fraction no.)	D2 retention time (min)	D2 retention time range (± x min)	Δ *m/z* (ppm)
Sulfadimethoxine	$C_{12}H_{14}N_4O_4S$	311.08085	60	0.349	0.005	3.5
Sulfadimidine	$C_{12}H_{14}N_4O_2S$	279.09102	35	0.276	0.002	-0.8
Sulfamethizole	$C_9H_{10}N_4O_2S_2$	271.03180	35	0.266	0.002	2.5
Sulfamethoxazole	$C_{10}H_{11}N_3O_3S$	254.05939	34	0.301	0.003	-0.5
Sulfapyridine	$C_{11}H_{11}N_3O_2S$	250.06448	33	0.246	0.003	0.6
Tamoxifen	$C_{26}H_{29}NO$	372.23219	34	0.399	0.002	3.2
Terbutaline	$C_{12}H_{19}NO_3$	226.14377	15 / 22	0.188	0.005	-0.6
Terbutryn	$C_{10}H_{19}N_5S$	242.14339	41	0.413	0.003	1.0
Tramadol	$C_{16}H_{25}NO_2$	264.19581	27	0.260	0.001	2.6
Trimethoprim	$C_{14}H_{18}N_4O_3$	291.14517	29	0.230	0.002	2.3
Venlafaxine	$C_{17}H_{27}NO_2$	278.21146	25	0.285	0.002	0.2
Warfarin	$C_{19}H_{16}O_4$	309.11214	44	0.440	0.003	-0.3
Xylometazoline	$C_{16}H_{24}N_2$	245.20123	27	0.323	0.003	0.7
Zuclopenthixol	$C_{22}H_{25}ClN_2OS$	401.14489	56	0.355	0.010	0.4

* The monoisotopic mass was calculated by using the integrated calculator of the PeakView software (AB Sciex).

SI-Table 5-3. Detailed result list of the suspected screening in the LC×LC separated wastewater sample (data basis of Figure 5-2d) including retention time deviations to the standard mixture and including comparative concentration data acquired by conventional LC-MS/MS**.

Analyte	Molecular formula of [M]	Monoisotopic mass of $[M+H]^+$	---------- Wastewater sample ----------				Deviation to standard		LC-MS/MS
			D1 max (fraction no.)	D2 RT (min)	Δ *m/z* (ppm)	IDA-MS/MS data♦	ΔD1 max (fractions)	ΔD2 RT (min)	Conc. (ng mL^{-1})
5,6-Dimethyl-1*H*-benzotriazole	$C_8H_9N_3$	148.08692	46	0.330	0.6	F: 77, 91, 93	-4	0.002	< 0.01
5-Methyl-1*H*-benzotriazole	$C_7H_7N_3$	134.07127	36	0.301	-0.5	F: 77, 79	-1	0.001	2.1*
Acetylsulfadiazine	$C_{12}H_{12}N_4O_3S$	293.07029	Not found						0.23
Acetylsulfadimidine	$C_{14}H_{16}N_4O_3S$	321.10159	Not found						< 0.01
Acetylsulfamerazine	$C_{13}H_{14}N_4O_3S$	307.08594	43	0.266	-0.5	NA	-4	0.003	< 0.01
Acetylsulfamethoxazole	$C_{12}H_{13}N_3O_4S$	296.06995	43	0.316	-0.8	NA	-4	0.004	5.9
Allopurinol	$C_5H_4N_4O$	137.04579	Not found						NA
Ampicillin	$C_{16}H_{19}N_3O_4S$	350.11690	Not found						NA
Atenolol	$C_{14}H_{22}N_2O_3$	267.17032	25	0.190	1.5	NA	0	0.000	0.58*
Atorvastatin	$C_{33}H_{35}FN_2O_5$	559.26028	Not found						NA
Azithromycin	$C_{38}H_{72}N_2O_{12}$	749.51580	Not found						< 0.02
Benzotriazole	$C_6H_5N_3$	120.05562	30	0.262	1.2	NA	-2	0.003	11
Bezafibrate	$C_{19}H_{20}ClNO_4$	362.11536	64	0.439	0.7	NA	9	0.002	2.9*
Bisoprolol	$C_{18}H_{31}NO_4$	326.23259	37	0.294	0.3	86.3%	6	0.002	0.093
Bisoprolol-*d5*	$C_{18}H_{26}D_5NO_4$	331.26397	37	0.294	-0.3	NA	NA	NA	NA
Carbamazepine	$C_{15}H_{12}N_2O$	237.10224	32	0.368	-3.2	90.7%	-2	0.002	0.5*
Carbetamide	$C_{12}H_{16}N_2O_3$	237.12337	34	0.349	-3.4	NA	-3	0.001	NA

Analyte	Molecular formula of [M]	Monoisotopic mass of $[M+H]^+$	---------- Wastewater sample ----------				Deviation to standard		LC-MS/MS
			D1 max (fraction no.)	D2 RT (min)	Δ *m/z* (ppm)	IDA-MS/MS data[♦]	ΔD1 max (fractions)	ΔD2 RT (min)	Conc. (ng mL^{-1})
Cefalexin	$C_{16}H_{17}N_3O_4S$	348.10125			Not found				< 0.02
Chloramphenicol	$C_{11}H_{12}Cl_2N_2O_5$	323.01960			Not found				NA
Chlorbromuron	$C_9H_{10}BrClN_2O_2$	292.96869	68	0.463	-1.6	NA	-7	0.003	NA
Chloridazon	$C_{10}H_8ClN_3O$	222.04287	42	0.302	-1.2	NA	-3	0.004	NA
Chlorprothixene	$C_{18}H_{18}ClNS$	316.09213			Not found				< 0.01
Cilastatin	$C_{16}H_{26}N_2O_5S$	359.16352			Not found				0.046
Citalopram	$C_{20}H_{21}FN_2O$	325.17107	36	0.314	1.4	NA	6	0.005	0.018
Clarithromycin	$C_{38}H_{69}NO_{13}$	748.48417	53	0.358	-0.9	66.8%	6	0.005	0.012
Clenbuterol	$C_{12}H_{18}Cl_2N_2O$	277.08690			Not found				< 0.05*
Climbazole	$C_{15}H_{17}ClN_2O_2$	293.10513	36	0.354	0.3	NA	1	0.003	0.01
Clindamycin	$C_{18}H_{33}ClN_2O_5S$	425.18715	27	0.282	-0.1	NA	0	0.000	0.017
Clozapine	$C_{18}H_{19}ClN_4$	327.13710	30	0.288	-1.4	NA	0	-0.001	0.12*
Cyclophosphamide	$C_7H_{15}Cl_2N_2O_2P$	261.03210	27	0.326	0.0	36%; F:140	-2	0.006	< 0.01
Dapsone	$C_{12}H_{12}N_2O_2S$	249.06923			Not found				NA
Dehydrato-Erythromycin	$C_{37}H_{65}NO_{12}$	716.45795	49	0.343	-0.6	NA	7	0.001	< 0.01
Diacetoxyscirpenol	$C_{19}H_{26}O_7$	367.17513			Not found				NA
Diatrizoic acid	$C_{11}H_9I_3N_2O_4$	614.77694			Not found				11*
Diclofenac	$C_{14}H_{11}Cl_2NO_2$	296.02396	62	0.472	1.0	92.3%	-8	0.003	2.2*
Dimpylate	$C_{12}H_{21}N_2O_3PS$	305.10833			Not found				NA
Diuron	$C_9H_{10}Cl_2N_2O$	233.02429	70	0.411	4.7	NA	-4	0.003	< 0.01*
Enalapril	$C_{20}H_{28}N_2O_5$	377.20710	31	0.308	0.3	NA	-1	0.001	NA
Fenofibrate	$C_{20}H_{21}O_4Cl$	361.12020	62	0.580	-1.8	NA	-9	0.003	NA
Fenofibric acid	$C_{17}H_{15}ClO_4$	319.07316	55	0.486	-1.1	NA	-8	0.006	NA
Fumonisin B1	$C_{34}H_{59}NO_{15}$	722.39575			Not found				NA
Fumonisin B2	$C_{34}H_{59}NO_{14}$	706.40083			Not found				NA
Gemcitabine	$C_9H_{11}F_2N_3O_4$	264.07904	27	0.160	0.1	72.5%	0	0.018	< 0.02
Gliotoxin	$C_{13}H_{14}N_2O_4S_2$	327.04678			Not found				NA
HT-2 Toxin	$C_{22}H_{32}O_8$	425.21699			Not found				NA
Hydrocortisone	$C_{21}H_{30}O_5$	363.21660			Not found				NA
Ifosfamide	$C_7H_{15}Cl_2N_2O_2P$	261.03210	25	0.321	-3.3	NA	-2	0.002	< 0.01
Iopromide	$C_{18}H_{24}I_3N_3O_8$	791.87705	28	0.216	1.3	NA	-2	0.003	2.3*
Isoproturon	$C_{12}H_{18}N_2O$	207.14919	35	0.411	-0.6	90.9%	-2	0.003	< 0.01*
Isoproturon-*d6*	$C_{12}H_{12}D_6N_2O$	213.18685	35	0.411	-0.5	NA	NA	NA	NA
Ketoprofen	$C_{16}H_{14}O_3$	255.10157	37	0.415	-0.7	NA	-3	-0.001	< 0.1
Lidocaine	$C_{14}H_{22}N_2O$	235.18049	24	0.246	1.8	NA	0	0.004	NA
Linuron	$C_9H_{10}Cl_2N_2O_2$	249.01921	58	0.468	-0.8	NA	-6	0.001	< 0.02*
Losartan	$C_{22}H_{23}ClN_6O$	423.16946	40	0.394	-0.2	82.0%	-6	0.004	NA
Mefenamic acid	$C_{15}H_{15}NO_2$	242.11756	53	0.518	0.7	85.7%	-6	0.002	NA
Megestrol	$C_{24}H_{32}O_4$	385.23734	44	0.500	0.8	73.9%	-4	0.003	NA
Melperone	$C_{16}H_{22}FNO$	264.17582	41	0.287	-0.5	88.6%	8	0.006	0.036*
Metconazole	$C_{17}H_{22}ClN_3O$	320.15242	57	0.509	-2.9	NA	-5	0.004	NA
Metformin	$C_4H_{11}N_5$	130.10872	11 / 17	0.139	0.2	47.4%	1 / 2	-0.001	NA
Metobromuron	$C_9H_{11}BrN_2O_2$	259.00767	42	0.423	-0.4	NA	-5	0.004	NA
Metoprolol	$C_{15}H_{25}NO_3$	268.19072	29	0.263	-1.0	79.2%	1	0.003	3.7
Metoprolol-*d7*	$C_{15}H_{18}D_7NO_3$	275.23466	29	0.263	0.9	NA	NA	NA	NA
Metronidazole	$C_6H_9N_3O_3$	172.07167	28	0.215	-0.9	66.2%	-1	0.001	0.029

Analyte	Molecular formula of [M]	Monoisotopic mass of $[M+H]^+$	---------- Wastewater sample ----------				Deviation to standard		LC-MS/MS
			D1 max (fraction no.)	D2 RT (min)	Δ *m/z* (ppm)	IDA-MS/MS data♦	ΔD1 max (fractions)	ΔD2 RT (min)	Conc. (ng mL^{-1})
Mianserin	$C_{18}H_{20}N_2$	265.16993			Not found				NA
Mirtazapine	$C_{17}H_{19}N_3$	266.16517			Not found				NA
Monuron	$C_9H_{11}ClN_2O$	199.06327	42	0.364	-1.3	46.8%	-4	0.004	NA
Nafcillin	$C_{21}H_{22}N_2O_5S$	415.13222			Not found				NA
Naproxen	$C_{14}H_{14}O_3$	231.10157			Not found				1.2*
Oxazepam	$C_{15}H_{11}ClN_2O_2$	287.05818	32	0.381	0.8	82.0%	-2	0.003	0.1
Oxcarbazepine	$C_{15}H_{12}N_2O_2$	253.09715			Not found				NA
Paracetamol	$C_8H_9NO_2$	152.07061	30	0.209	0.2	82.2%	-3	0.000	21
Phenazone	$C_{11}H_{12}N_2O$	189.10224	25	0.280	0.5	NA	-2	0.001	0.01
Picoxystrobin	$C_{18}H_{16}F_3NO_4$	368.11042			Not found				NA
Pipamperone	$C_{21}H_{30}FN_3O_2$	376.23948			Not found				< 0.01*
Piperacillin	$C_{23}H_{27}N_5O_7S$	518.17040			Not found				NA
Prednisolone	$C_{21}H_{28}O_5$	361.20095	37	0.344	0.8	NA	-1	0.004	NA
Propranolol	$C_{16}H_{21}NO_2$	260.16451	49	0.298	-0.7	79.8%	7	0.002	< 0.05
Propyphenazone	$C_{14}H_{18}N_2O$	231.14919	27	0.396	-2.9	NA	-2	0.002	< 0.01
Quinoxyfen	$C_{15}H_8Cl_2FNO$	308.00397	71	0.559	-3.0	NA	1	0.000	NA
Ramipril	$C_{23}H_{32}N_2O_5$	417.23840	35	0.340	4.9	NA	1	0.000	NA
Ranitidine	$C_{13}H_{22}N_4O_3S$	315.14854	28	0.194	3.3	NA	0	0.002	NA
Ritalinic acid	$C_{13}H_{17}NO_2$	220.13321	18 / 21	0.245	2.3	NA	3 / -2	0.000	0.063
Roxithromycin	$C_{41}H_{76}N_2O_{15}$	837.53185	41	0.359	-0.8	NA	5	0.001	< 0.01
Sertraline	$C_{17}H_{17}Cl_2N$	306.08108	40	0.351	-0.8	NA	6	0.007	NA
Simvastatin	$C_{25}H_{38}O_5$	419.27920			Not found				< 0.02
Sotalol	$C_{12}H_{20}N_2O_3S$	273.12674	24	0.190	-0.9	87.1%	-1	0.000	0.39*
Stachybotrylactam	$C_{23}H_{31}NO_4$	386.23259			Not found				NA
Sulfadiazine	$C_{10}H_{10}N_4O_2S$	251.05972			Not found				0.26
Sulfadimethoxine	$C_{12}H_{14}N_4O_4S$	311.08085	55	0.354	1.3	77.3%	-5	0.005	< 0.01
Sulfadimidine	$C_{12}H_{14}N_4O_2S$	279.09102			Not found				0.029
Sulfamethizole	$C_9H_{10}N_4O_2S_2$	271.03180			Not found				NA
Sulfamethoxazole	$C_{10}H_{11}N_3O_3S$	254.05939	33	0.303	0.5	NA	-1	0.002	1
Sulfapyridine	$C_{11}H_{11}N_3O_2S$	250.06448			Not found				0.13
Tamoxifen	$C_{26}H_{29}NO$	372.23219	38	0.403	1.6	NA	4	0.004	< 0.01
Terbutaline	$C_{12}H_{19}NO_3$	226.14377	17 / 20	0.188	-0.3	NA	2 / -2	0.000	NA
Terbutryn	$C_{10}H_{19}N_5S$	242.14339	41	0.416	-0.8	94.2%	0	0.003	< 0.01*
Tramadol	$C_{16}H_{25}NO_2$	264.19581	27	0.264	0.0	NA	0	0.004	0.049
Trimethoprim	$C_{14}H_{18}N_4O_3$	291.14517	38	0.232	0.8	89.5%	9	0.002	NA
Venlafaxine	$C_{17}H_{27}NO_2$	278.21146	25	0.288	-1.2	48.9%	0	0.003	0.14
Warfarin	$C_{19}H_{16}O_4$	309.11214	40	0.444	-0.6	73.8%	-4	0.004	NA
Xylometazoline	$C_{16}H_{24}N_2$	245.20123	32	0.325	-0.7	77.0%	5	0.002	NA
Zuclopenthixol	$C_{22}H_{25}ClN_2OS$	401.14489	62	0.362	-1.3	NA	6	0.007	< 0.05*

NA = not available, RT = retention time

♦In this column, information obtained by IDA-MS/MS fragmentation of the $[M+H]^+$ ion as a precursor was listed if available. A prerequisite, however, was that this precursor was among the four most intense ions at the corresponding detection time. A percent value in this column is the purity of gained library hit for the product ion spectrum. The letter F means that unique

fragments were found in the product ion spectrum allowing the identification of the compound.

*A different solid-phase extraction method was used to obtain an optimum of analyte recovery for the LC-MS/MS quantification.

**LC-MS/MS analysis was performed by IUTA and Ruhrverband within the project "Elimination of pharmaceutical residues in municipal wastewater treatment plants". We want to thank "The Ministry for Climate Protection, Agriculture, Nature Conservation and Consumer Protection of North Rhine-Westphalia (MKULNV)" for their financial support and all project partners for the excellent cooperation. Further project information could be found at http://www.micropollutants.net/index.php/en/projects/project-no-6.

Suspected screening criteria:

The following criteria were needed to be met by a target in the wastewater sample to create a screening hit:

- Δ *m/z* of the $[M+H]^+$ ion < 5 ppm
- Absolute D2 retention time deviation to standard < 0.01 min (in case of retention times below 10 s a deviation < 0.02 min was tolerated).
- Absolute D1 fraction deviation < 10 (compare Section 5.3.4.1, deviations up to 9 fractions could be confirmed by MS/MS fragmentation data).

So, for all substances, at least the molecular formula was confirmed by the absolute mass. In cases where IDA-MS/MS fragmentation data or an internal standard was available, the analytes could be unambiguously identified as the target substances. For a missing MS/MS fragmentation and a D1 fraction deviation < 4, the probability of a false positive hit can be considered very small.

Chapter 6 General conclusions and outlook

The studies of this thesis have resulted in the first multidimensional separation system on the basis of online nanoLC×capillaryLC and hybrid high-resolution mass spectrometry. This system features the advantages of splitless MS hyphenation and very low solvent consumption compared to systems with conventionally sized second LC dimensions. Moreover, it represents a variable development platform for the qualitative screening analysis of complex samples. Its capabilities have been demonstrated using a suspected screening of 99 contaminants in a wastewater sample. For this purpose, the miniaturized online LC×LC was operated in dual gradient RP×RP mode employing Hypercarb and core-shell C18 in the first and second dimension, respectively. This combination provided 60% surface coverage (convex hull) for the separation of the 99 standards without further orthogonality optimizations. A large volume injection and an overall splitless configuration of the capillary system were used to counteract the inherent sensitivity disadvantage of two-dimensional LC in comparison to one-dimensional LC. Accordingly, 65 of the analytes could be found in the wastewater sample. A modulation time of one minute was achieved by combining fast LC approaches in D2. In this regard, a superficially porous sub-3-µm stationary phase was operated at elevated temperature (60 °C) and high pressure. In the context of the column stability study of Chapter 3, it was concluded that the temperature stability of core-shell particles is not increased by the solid core. Thus, it will not be possible to apply significantly higher temperatures to the employed superficially porous stationary phase. As is apparent from the same study, there are different fully porous stationary phases that might be used in an alternative high-temperature second dimension. According to the comparative retention factor analysis approach, particles on the basis of the ethylene bridged hybrid (BEH) technology suit best for a long-term use at high temperatures. Nonetheless, the high-temperature approach was dismissed for the final implementation of the multidimensional system because of the insufficient temperature stability of the widely used capillaryLC column hardware on the basis of packed PEEK or fused-silica tubing. This decision does not exclude the application of high-temperature LC from future versions of the multidimensional system given that the stability issues of the hardware are solved. Central findings of the solvent effect study (Chapter 2) are that solvent strength effects in a reversed-phase second dimension are still pre-dominant at high oven temperatures and that corresponding additional

peak broadening cannot be eliminated by a further increase in the isothermal oven temperature. These results emphasize the importance of sufficiently small transfer volumes to D2 at any operating temperature and encourage the use of gradients to counteract moderate band broadening in D2. Nonetheless, high temperatures still increase the solvent compatibility by decreasing the viscosity differences which otherwise might lead to viscosity mismatch effects. Moreover, all advantages of HT-LC described in Section 1.3 are still valid.

Finally, however, no disadvantages resulted from the alternative approach that combined a core-shell stationary phase, elevated temperature, and high pressures. Instead, the second dimension delivered very stable retention times and sharp peaks. Moreover, this way, a simplified heating concept could be applied.

Outlook

The multidimensional system in its current state offers options for further developments and improvements. For example, the orthogonality could be fine-tuned by using adapted gradient programming such as shift gradient elution [1]. This way, the effective area of the 2-D chromatogram used by peaks could potentially be further enlarged.

Moreover, the chosen MS data acquisition method that uses the IDA mode of the mass spectrometer generally allows for a (suspected) unknown screening of compounds that lack reference standards as long as an MS/MS experiment has been carried out for the respective precursor ion. Thus, the fragmentation pattern of an unknown can be compared to data provided by mass spectral databases and to simulated “in-silico” fragmentation to obtain candidates for the identification. However, a corresponding software tool such as MetFusion [2-3] has not yet been integrated in the multidimensional system.

Although not necessary for qualitative experiments that were focused on in this thesis, the replacement of the pneumatic D2 pump by an appropriate continuous-flow pump would eliminate the need for the pump refill procedure. This becomes important if a quantification of affected analytes is considered. Moreover, the gradient program could start at 0% B to obtain enhanced peak focusing. A potential replacement pump needs to fulfill the high requirements of a fast gradient mixing, an extended pressure range, and a very small gradient delay volume (compare Section 4.3.5). However, such a device is not yet available from the same manufacturer. Possible candidates including the Dionex RSLCnano HPG pump by Thermo Fisher Scientific have not been tested yet. Either way, the integration is not necessarily trivial as its success is strongly related to a proper synchronization with the modulation valve operation.

The introduction of separate contact heaters, preferably with gradient function, for an independent temperature programming of both columns would be even more important for multiple reasons. A low starting temperature in D1 would facilitate peak focusing of the early eluting analytes. This would also reduce the time in which the analytes are exposed to elevated temperatures. Thus, the method could potentially be extended for very thermolabile analytes such as amoxicillin [4]. During the isocratic hold at high %B in D1, an increased temperature would support the elution of the highly retained analytes to reduce the overall analysis time and to improve peak shape. In this case, a temperature gradient would allow band compression as was demonstrated by Wiese et al. [5]. A general advantage of a temperature gradient in D1 is the possibility to reduce the %B maximum for a decreased solvent strength transfer to D2. However, the mobile phase needs to be cooled down prior to the modulation valve if temperatures above 60 °C are applied in D1. Temperatures above 100 °C should be avoided as they potentially damage the column hardware. An independent temperature programming for both dimensions would also be beneficial if other stationary phase combinations were used that needed a distinct temperature difference between the dimensions.

In this context, future research should focus on the development of suitable high-temperature stable column hardware and respective ovens for the use in nano- and capillaryLC.

In the meanwhile, the main suppliers of core-shell stationary phases have included stationary phases to their catalogs that potentially provide better temperature stability (Halo ES by Advanced Materials Technology [6], Kinetex XB by Phenomenex [7], Ascentis Express ES by Sigma-Aldrich [8], and Poroshell SB by Agilent Technologies [9]). Bulky side-chains (e.g., isopropyl or isobutyl) of the functional ligands are used to sterically protect the surface of the silica particle. Depending on the manufacturer, the materials are specified to be stable at temperatures up to 90 °C. Interesting alternatives could be the BEH-based stationary phases in the 2.5 µm i.d. XP particle format [10] that was recently introduced by Waters to compete with sub-3-µm core-shell particles. These fully porous hybrid particles are expected to withstand even higher temperatures. Moreover, the high loading capacity could help increasing the transfer volume to D2.

Further research effort should also be focused on the large volume injection (LVI) concept. The LVI is necessary for trace analysis in complex samples and often causes severe retention time shifts in approaches with only one LC dimension. The high retention time stability in the

second dimension makes the two-dimensional approach of the multidimensional system especially attractive as retention time can be used as a hard identification criterion even though an LVI is used. As the high retentivity of the PGC phase causes extraordinarily strong retention for several late eluting analytes, it should be considered whether a PGC pre-column approach in the first dimension could also allow an LVI at lower overall retention. The analytical column in D1 could then be freely chosen as well from those columns that offer too low retention to perform an LVI.

6.1 References

[1] Li, D.; Schmitz, O. J. *Use of shift gradient in the second dimension to improve the separation space in comprehensive two-dimensional liquid chromatography*. Anal. Bioanal. Chem. 2013, ***405***, 6511-6517.

[2] Gerlich, M.; Neumann, S. *MetFusion: integration of compound identification strategies*. J. Mass Spectrom. 2013, ***48***, 291-298.

[3] Stanstrup, J.; Gerlich, M.; Dragsted, L. O.; Neumann, S. *Metabolite profiling and beyond: approaches for the rapid processing and annotation of human blood serum mass spectrometry data*. Anal. Bioanal. Chem. 2013, ***405***, 5037-5048.

[4] Teutenberg, T. *Potential of high temperature liquid chromatography for the improvement of separation efficiency—A review*. Anal. Chim. Acta 2009, ***643***, 1-12.

[5] Wiese, S.; Teutenberg, T.; Schmidt, T. C. *A general strategy for performing temperature-programming in high performance liquid chromatography-Prediction of segmented temperature gradients*. J. Chromatogr. A 2011, ***1218***, 6898-6906.

[6] Advanced Materials Technology *HALO - HYPER-FAST & SUPER-RUGGED UHPLC & HPLC COLUMNS (Fall 2013 product catalog)*. Online resource: http://www.mz-at.de/resources/brochures/HALO_Fall2013_CatalogA4.pdf (last accessed: March 3rd, 2014): Wilmington, DE, USA, 2013.

[7] Phenomenex Inc. *Kinetex Phase Information*. Online resource: http://www.phenomenex.com/Kinetex/Selectivities/XB-C18 (last accessed: March 3rd, 2014): Torrance, CA, USA, 2014.

[8] Sigma-Aldrich Co. LLC / Supelco *Ascentis Express Products*. Online resource: http://www.sigmaaldrich.com/analytical-chromatography/hplc/columns/ascentis-express.html (last accessed: March 3rd, 2014): St. Louis, MO, USA, 2014.

[9] Agilent Technologies Inc. *Agilent Poroshell 120 SB-C18 Threaded Column – Data sheet*. Online resource: http://prdwww.lvld.agilent.com/Library/datasheets/Public/820302-002.pdf (last accessed: March 3rd, 2014): Santa Clara, CA, USA, 2010.

[10] Waters Corporation *[xp columns] - eXtended performance (product brochure 720004195EN)*. Online resource: http://www.waters.com/webassets/cms/library/docs/720004195en.pdf (last accessed: March 3rd, 2014): Milford, MA, USA, 2013.

Chapter 7 Appendix

7.1 List of abbreviations and symbols

% B	organic solvent concentration in the mobile phase in percent by volume
$\Delta\, i.d.$	relative difference of column inner diameters
ΔP	pressure drop
°C	degree Celsius
1-D	one-dimensional
2-D	two-dimensional
3-D	three-dimensional
abs.	absolute
ace	acenaphthene
ACN	acetonitrile
ami	amitriptyline
APCI	atmospheric pressure chemical ionization
ASCII	American Standard Code for Information Interchange
BEH	ethylene bridged hybrid
C18 or C-18	octadecyl silane
CA	California
capLC	capillary liquid chromatography
CC	column chromatography
CCD	charge-coupled device (sensor type)
CSH	charged surface hybrid
D1	first dimension
D2	second dimension
Da	Dalton
DAD	diode array detector
d_c	inner diameter of the column
${}_1d_c$	inner diameter of the first dimension column
${}_2d_c$	inner diameter of the second dimension column
d_{cap}	inner diameter of the tubing/capillary
DE	Delaware
D_m	diffusion coefficient of a solute in the mobile phase
DOI	digital object identifier
d_p	particle diameter of the stationary phase
ESI	electrospray ionization
eV	electron volt
F	volumetric flow rate
FA	formic acid
GC	gas chromatography
GC×GC	comprehensive two-dimensional gas chromatography
H	plate height
HILIC	hydrophilic interaction chromatography

HPCE	high-performance capillary electrophoresis
HPLC	high-performance liquid chromatography
HRMS	high-resolution mass spectrometry
HT-capLC	high-temperature capillary liquid chromatography
HT-HPLC	high-temperature high-performance liquid chromatography
HT-LC	high-temperature liquid chromatography
Hz	hertz
i.d.	inner diameter
IBM	International Business Machines Corporation
IDA	Information-dependent acquisition
IEC	ion exchange chromatography
inorg.	inorganic
IPC	ion-pairing chromatography
k	retention factor
k_d	desorption rate constant
LC	liquid chromatography
l_c	column length
LC×LC	comprehensive two-dimensional liquid chromatography
l_{cap}	length of the tubing/capillary
LC-MS or LC/MS	liquid chromatography - mass spectrometry
LVI	large volume injection
m/z	mass-to-charge ratio
MA	Massachusetts
MeOH	methanol
microLC	micro liquid chromatography
MN	Minnesota
MS	mass spectrometry
MS/MS	tandem mass spectrometry
M-S-F	Murphy-Schure-Foley
MudPIT	multidimensional protein identification technology
n_1	peak capacity of the first dimension
n_2	peak capacity of the second dimension
nanoESI	nano electrospray ionization
nanoLC	nano liquid chromatography
n_{c2D}	peak capacity of a comprehensive two-dimensional system
n_{hc}	peak capacity of a heart cutting two-dimensional system
NP	normal-phase (chromatography)
o.d.	outer diameter
OR	Oregon
org.	organic
p.a.	pro analysi
PBD	polybutadiene
PEEK	polyether ether ketone
PEG	polyethylene glycol
PGC	porous graphitic carbon
pH	"potentia Hydrogenii" – negative decimal logarithm of the hydrogen ion activity
pol	propranolol
pre-VF	pre-viscous fingering
psi	pound-force per square inch
puriss.	purissimum

QqTOF	quadrupole/time-of-flight (special type of hybrid high-resolution mass spectrometer)
RP	reversed-phase (chromatography)
RT	room temperature
SAX	strong anion exchange (chromatography)
SCX	strong cation exchange (chromatography)
SEC	size exclusion chromatography
SE-mix	solvent effect test mix
SFC	supercritical fluid chromatography
SI	supporting information / supplementary information
SP	service pack
SPE	solid-phase extraction
t_{GD}	gradient delay time
TIC	total ion current
TLC	thin layer chromatography
TOF	time-of-flight
u	average linear mobile phase velocity
UHPLC	ultrahigh-performance liquid chromatography
USB	universal serial bus
UV	ultraviolet
V	volume
V_GD or V_{GD}	gradient delay volume
VF	viscous fingering
WA	Washington
XIC	extracted ion chromatogram
z	number of transferred bands
ε_T	total porosity of the column packing
η	viscosity (of the mobile phase)
σ^2	variance (of a peak)
σ^2_{cap}	variance contribution of the capillaries/tubing
σ^2_{col}	variance contribution of the column
σ^2_{con}	variance contribution arising from void volumes at tubing connections
σ^2_{det}	variance contribution of the detector
σ^2_{ec}	extra-column variance contribution
σ^2_{fil}	variance contribution of optional filters or unions
σ^2_{inj}	variance contribution of the injector
σ^2_T	total variance of an observed peak
σ^2_{tc}	variance contribution caused by the acquisition time constant
φ_D	flow resistance factor based on the Darcy law

7.2 List of figures and SI-figures

7.3 List of tables and SI-tables

7.4 Publications

Articles in peer-reviewed journals

Haun, J.; Teutenberg, T.; Schmidt, T. C. *Influence of temperature on peak shape and solvent compatibility: Implications for two-dimensional liquid chromatography*. Journal of Separation Science 2012, ***35*** (14), 1723-1730.

Haun, J.; Oeste, K.; Teutenberg, T.; Schmidt, T. C. *Long-term high-temperature and pH stability assessment of modern commercially available stationary phases by using retention factor analysis*. Journal of Chromatography, Part A 2012, ***1263***, 99-107.

Haun, J.; Leonhardt, J.; Portner, C.; Hetzel, T.; Tuerk, J.; Teutenberg, T.; Schmidt, T. C. *Online and Splitless NanoLC × CapillaryLC with Quadrupole/Time-of-Flight Mass Spectrometric Detection for Comprehensive Screening Analysis of Complex Samples*. Analytical Chemistry 2013, ***85*** (21), 10083-10090.

Other articles

Teutenberg, T.; Haun, J.; Leonhardt, J.; Portner, C. *Potenziale und Anwendung der umfassenden zweidimensionalen Flüssigkeitschromatografie*. Analytik News, publication date: 03/02/2012. URL: http://www.analytik-news.de/Fachartikel/2012/10.html.

Teutenberg, T.; Leonhardt, J.; Haun, J.; Wiese, S.; Wenkel, N. *Mikro-LC - Nur das ewige Talent?* GIT Labor-Fachzeitschrift 2012, Issue 04/2012, 246-248.

Teutenberg, T.; Leonhardt, J.; Haun, J.; Portner, C. *Die zweite Dimension – Neue Entwicklungen in der 2D-Flüssigkeitschromatographie*. LaborPraxis 2012, Issue 10/2012. URL: http://www.laborpraxis.vogel.de/analytik/chromatographie/hplc/articles/382538

Oral presentations

Haun, J.; Leonhardt, J.; Teutenberg, T.; Wenkel, N. *Kapillar-UHPLC – Chancen, Vorteile und Anwendungsbeispiele. Beispielapplikationen mit UV-, ELS- und MS-Detektion, Zukunftsperspektiven*. Chromatographie automatisieren, Praxisseminar der Fa. Axel Semrau GmbH & Co. KG, Munich and Karlsruhe, Germany, 10/26/2011 and 10/27/2011.

Haun, J.; Teutenberg, T.; Schmidt, T. C. *Development of a comprehensive two-dimensional nano-/capillary-LC system with mass-spectrometric detection for screening analysis of complex samples.* 22. Doktorandenseminar des AK Separation Science, Fachgruppe „Analytische Chemie“, Gesellschaft Deutscher Chemiker (GDCh), Hohenroda, Germany, 01/08 – 01/10/2012.

Poster presentations

Haun, J.; Teutenberg, T.; Schmidt, T. C. *Development of a two-dimensional comprehensive HPLC-system for the screening analysis of complex samples*. analytica 2010, Munich, Germany, 03/23 – 03/26/2010.

Haun, J.; Teutenberg, T.; Schmidt, T. C. *Development of a two-dimensional comprehensive HPLC-system for the analysis of complex samples*. 28th International Symposium on Chromatography (ISC 2010), Valencia, Spain, 09/12 – 09/16/2010.

Haun, J.; Teutenberg, T.; Schmidt, T. C. *Entwicklung eines zweidimensionalen HPLC-Verfahrens zur Analyse komplexer Substanzgemische.* ProcessNet-Jahrestagung 2010, Aachen, Germany, 09/21 – 09/23/2010.

Haun, J.; Teutenberg, T.; Schmidt, T. C. *Development of a two-dimensional comprehensive HPLC-system for the screening analysis of complex samples*. Langenauer Wasserforum 2010, Langenau, Germany, 11/08 – 11/09/2010.

Haun, J.; Teutenberg, T.; Schmidt, T. C. *Development of a Novel LCxLC-system for the Analysis of Complex Samples*. ANAKON 2011, Zurich, Switzerland, 03/22 – 03/25/2011.

Haun, J.; Teutenberg, T.; Schmidt, T. C. *High temperature stability of commercially available HPLC columns*. HPLC 2011, Budapest, Hungary, 06/19 – 06/23/2011.

Haun, J.; Teutenberg, T.; Schmidt, T. C. *High temperatures as a tool to increase solvent compatibility in two-dimensional liquid chromatography*. HPLC 2011, Budapest, Hungary, 06/19 – 06/23/2011.

Leonhardt, J.; Teutenberg, T.; Haun, J.; Portner, C.; Wolff, M. *Development of a comprehensive two-dimensional nano-/capillary-LC system with mass-spectrometric detection for the screening analysis of complex samples*. analytica 2012, Munich, Germany, 04/17 – 04/20/2012.

7.5 Curriculum vitae

Der Lebenslauf ist in der Online-Version aus Gründen des Datenschutzes nicht enthalten.

For reasons of data protection, the curriculum vitae is not included in this online document.

Curriculum vitae

(second page / zweite Seite)

Der Lebenslauf ist in der Online-Version aus Gründen des Datenschutzes nicht enthalten.

For reasons of data protection, the curriculum vitae is not included in this online document.

7.6 Erklärung (Declaration)

Hiermit versichere ich, dass ich die vorliegende Arbeit mit dem Titel

“Miniaturized online comprehensive two-dimensional liquid chromatography”

selbst verfasst und keine außer den angegebenen Hilfsmitteln und Quellen benutzt habe, und dass die Arbeit in dieser oder ähnlicher Form noch bei keiner anderen Universität eingereicht wurde.

Essen, 04.03.2014

UNTERSCHRIFT

7.7 Acknowledgements

First and foremost, my deepest gratitude is devoted to my research supervisors Prof. Dr. Torsten C. Schmidt and Dr. Thorsten Teutenberg for their professional guidance, continuous encouragement, valuable support, and fast constructive critiques to my work.

I would like to express my appreciation to all further co-authors, namely Katja Oeste, Juri Leonhardt, Dr. Christoph Portner, Terence Hetzel, and Dr. Jochen Türk, for their excellent collaboration and the helpful discussions.

Moreover, I would like to thank Dr. Steffen Wiese, Marco Wolff and Andrea Börgers for inspiring discussions and helpful expert advice.

Furthermore, my special thanks are devoted to my friends and former colleagues at the Institute of Energy and Environmental Technology who supported my studies.

Most importantly, I wish to thank my parents, brother, and last but not least Tatjana and her family for the constant support and endless encouragement.